SANDIA REPORT
SAND2005-6487
Unlimited Release
Printed September 2006

Method Development and Validation for Measuring the Particle Size Distribution of Pentaerythritol Tetranitrate (PETN) Powders

Sharissa Young

Prepared by
Sandia National Laboratories
Albuquerque, New Mexico 87185 and Livermore, California 94550

Sandia is a multiprogram laboratory operated by Sandia Corporation,
a Lockheed Martin Company, for the United States Department of Energy's
National Nuclear Security Administration under Contract DE-AC04-94AL85000.

Issued by Sandia National Laboratories, operated for the United States Department of Energy by Sandia Corporation.

Available to DOE and DOE contractors from
U.S. Department of Energy
Office of Scientific and Technical Information
P.O. Box 62
Oak Ridge, TN 37831

Telephone: (865) 576-8401
Facsimile: (865) 576-5728
E-Mail: reports@adonis.osti.gov
Online ordering: http://www.osti.gov/bridge

Available to the public from
U.S. Department of Commerce
National Technical Information Service
5285 Port Royal Rd.
Springfield, VA 22161

Telephone: (800) 553-6847
Facsimile: (703) 605-6900
E-Mail: orders@ntis.fedworld.gov
Online order: http://www.ntis.gov/help/ordermethods.asp?loc=7-4-0#online

SAND2005-6487
Unlimited Release
Printed September 2006

METHOD DEVELOPMENT AND VALIDATION FOR MEASURING THE PARTICLE SIZE DISTRIBUTION OF PENTAERYTHRITOL TETRANITRATE (PETN) POWDERS

by
Sharissa Young
Advisor: D. A. Hirschfeld

Submitted in Partial Fulfillment of the Requirement for the Degree of Master of Science in Materials and Metallurgical Engineering

NEW MEXICO INSTITUTE OF MINING AND TECHNOLOGY
SOCORRO, NEW MEXICO
2005

ABSTRACT

Currently, the critical particle properties of pentaerythritol tetranitrate (PETN) that influence deflagration-to-detonation time in exploding bridge wire detonators (EBW) are not known in sufficient detail to allow development of a predictive failure model. The specific surface area (SSA) of many PETN powders has been measured using both permeametry and gas absorption methods and has been found to have a critical effect on EBW detonator performance. The permeametry measure of SSA is a function of particle shape, packed bed pore geometry, and particle size distribution (PSD). Yet there is a general lack of agreement in PSD measurements between laboratories, raising concerns regarding collaboration and complicating efforts to understand changes in EBW performance related to powder properties.

Benchmarking of data between laboratories that routinely perform detailed PSD characterization of powder samples and the determination of the most appropriate method to measure each PETN powder are necessary to discern correlations between performance and powder properties and to collaborate with partnering laboratories. To this end, a comparison was made of the PSD measured by three laboratories using their own standard procedures for light scattering instruments. Three PETN powder samples with different surface areas and particle morphologies were characterized. Differences in bulk PSD data generated by each laboratory were found to result from variations in sonication of the samples during preparation. The effect of this sonication was found to depend on particle morphology of the PETN samples, being deleterious to some PETN samples and advantageous for others in moderation. Discrepancies in the submicron-sized particle characterization data were related to an instrument-specific artifact particular to one laboratory. The type of carrier fluid used by each laboratory to suspend the PETN particles for the light scattering measurement had no consistent effect on the resulting PSD data. Finally, the SSA of the three powders was measured using both permeametry and gas absorption methods, enabling the PSD to be linked to the SSA for these PETN powders. Consistent characterization of other PETN powders can be performed using the appropriate sample-specific preparation method, so that future studies can accurately identify the effect of changes in the PSD on the SSA and ultimately model EBW performance.

ACKNOWLEDGMENTS

The author wishes to thank:

- Sandia National Laboratories/New Mexico (SNL/NM), for funding and providing necessary equipment for this research. Sandia is a multiprogram laboratory operated by Sandia Corporation, a Lockheed Martin Company, for the United States Department of Energy under contract DE-AC04-94AL85000.
- Deidre Hirschfeld, Leanna Minier, and Sandy Klassen for their involvement and professional grooming throughout this process as academic advisor, research advisor, and professional mentor
- Christa Hockensmith, Bhaskar Majumdar, Leanna Minier and Deidre Hirschfeld for their advice and participation on my thesis committee
- Bob Patton for his outstanding work on the Coulter®
- The PETN particle characterization friends at BWXT Pantex: Pat Foster, Arnie Duncan, Melissa Moore, and Destin Leinen; at Lawrence Livermore National Laboratory: Pat Lewis, George Overturf and George Hampton; and in the UK: Janella Mansell
- All of the people who have helped at SNL/NM: Bill Andrzejewski, Stuart Smith, Victor Baca, Dave Huskisson, Bob Parsons and Tom Massis

TABLE OF CONTENTS

Page

LIST OF FIGURES

Figure **Page**

LIST OF TABLES

Table **Page**

CHAPTER 1
INTRODUCTION

Detonation characteristics of pentaerythritol tetranitrate (PETN) powders have been studied and characterized and it is known that the specific surface area (SSA) of PETN powders is related to detonator performance in exploding bridge wire (EBW) detonators [1,2]. The measured SSA and void structure of the packed bed are dependent on primary characteristics of the powders, such as particle size distribution (PSD), degree of reentrant void formation, particle shape, and the density of the powder. Over time, these primary characteristics may change, and it is not clear whether these changes in the primary characteristics affect the surface area and packing density, which in turn will affect the EBW detonator performance.

One of the possible changes is the particle size distribution. PETN powder in the solid state changes at a finite rate through a sublimation process as it ages [3]. Sublimation of the smaller crystals may cause the PSD in the powder to change over time; larger particles grow at the expense of the smaller ones.

A decrease in small particles and the corresponding change in PSD may affect detonation performance. Based on deflagration-to-detonation (DDT) studies using conventional (106 micron diameter) and “ultrafine” (1 micron diameter) PETN, one such study has shown that the fine-particle PETN was much more sensitive to shock initiation than conventional PETN particles [4]. The particle size of PETN in a loosely packed column (<50% of theoretical maximum density) may even control the actual DDT

processes that occur in a detonation device [5]. The particle size is also known to control the rate of gas generation, which in turn determines the pressure pulse that is related to performance [6]. Because performance is strongly influenced by the particle size, it is important to know how the PSD changes over time. To understand the extent of these PSD changes, the original distribution of the particles must be characterized using a method that is repeatable and accurately describes the particles present.

Some work has already been done to characterize PETN powders using light scattering techniques and several efforts are under way to understand the precision and accuracy of these measurements. Multiple laboratories have measured the SSA, PSD, and other particle characteristics for a plethora of PETN powders using a variety of measurement techniques, both before and after packing, to approximate use densities [7,8,9]. However, the existing PSD data from these different laboratories includes discrepancies in both the bulk distribution and in the submicron-sized fraction.

In spite of the recent advances in technology, some difficulties still exist when measuring the particle sizes of PETN powders. Most light scattering instruments rely on the assumption of individual, smooth spherical particles. The effects of surface roughness and high aspect ratios combined with agglomeration and other dispersion problems challenge the ability of light scattering instruments to accurately measure the PSD of PETN powders, especially with inter-laboratory precision. Some sample preparation steps, such as the addition of the powders to a carrier fluid and sonication, which are designed to deagglomerate and disperse the PETN powders in a liquid media, may alter the characteristics of the particles in suspension. The geometry and hardware

limitations of the measurement instrument coupled with data analysis and interpretation software assumptions may also introduce uncertainty in to the PSD measurement.

The goal of this study was to benchmark standard PSD measurements made between laboratories and to develop and validate a reliable method to measure the PSD of PETN powder that will minimize discrepancies between laboratories. For the benchmarking study three independent laboratories, BWXT Pantex, Amarillo, TX (Pantex), Lawrence Livermore National Laboratory, Livermore, CA (LLNL) and Sandia National Laboratories, Albuquerque, NM (SNL) measured the bulk PSDs of three coned and quartered PETN powder split samples: A, B, and C. Pantex analyzed the samples using a Coulter® LS 230 particle size analyzer (Beckman Coulter®, Fullerton, CA), LLNL used a Saturn DigiSizer® 5200 particle size analyzer (Micromeritics® Instrument Corporation, Norcross, GA), and SNL used a Coulter® LS 100Q particle size analyzer. Each laboratory used their respective standard methods for preparation and measurement of the three PETN powder samples.

To understand the differences in results, the effects of variations in the sample preparation techniques at each of the laboratories, including sonication time and type of carrier fluid, were subsequently studied to isolate differences in PSD measurements resulting from variations in the preparation methods. Preparations of each of the three PETN powders were made at SNL using four sonication times that spanned the times used at each of the laboratories. These sonication times were applied to PETN samples prepared in each of the three different carrier fluids used by each laboratory. The resulting twelve sample preparations for each type of PETN were measured using the same light scattering instrument and operator at SNL. Differences in the resulting PSD

data were then linked to physical changes in the PETN particles identified in optical microscopy photographs of the sample preparations.

To evaluate differences in the submicron-size range two particle size standard reference materials were analyzed. The two standards consisted of two percent cross-linked polystyrene spheres of nominal 0.5 and 1.0 micron diameters. These two standards were measured using the LLNL and SNL light scattering instruments to ensure that the instruments were capable of accurate measurement in this size range.

Scanning electron microscopy (SEM) photomicrographs of each of the three powder samples were taken at both Pantex and SNL. These images documented the physical appearance and dimensions of the samples analyzed, in addition to revealing whether submicron-sized particles may be present in the approximate volume percentages identified in the bulk PSD measurement at the one laboratory.

Conflicting or divergent results for the PSD, especially for the submicron-sized fraction may be due to variations in sample preparation and geometric or software programming differences between instrument manufacturers. These sources of variation can be minimized or addressed by eliminating the differences, where possible, and otherwise evaluating the impact to the data.

CHAPTER 2
LITERATURE REVIEW

2.1 PETN Properties

PETN has been an important compound in a variety of applications since it was first synthesized in 1895 for use as a pharmaceutical vasodilator, similar in use to nitroglycerine (NG). PETN is not as effective as NG during a heart attack due to its slower onset, but is ideally suited to the prevention of heart attack when mixed with lactose to inhibit detonation [10].

As a high explosive, it is one of the more important compounds in use [11]. A high explosive detonates readily, while a low explosive burns rapidly but does not detonate (e.g., propellants) [12]. It is the thermally most stable and least reactive of the family of explosive nitrate esters [13,14]. Classified as a secondary high explosive due to its impact sensitivity [6], PETN is used in its pure form as a primary in EBW detonators due to its unique combination of low critical energy fluence and short run distance [11]. High explosives are either primary, which explode or detonate when merely ignited, or secondary, which must be initiated by a detonating device, but PETN exhibits both characteristics, depending on the conditions and configuration [13,15]. It is also the primary active ingredient in a number of widely used commercial plastic bonded explosive products, including Detasheet® and DetaFlex® (DuPont, Willmington, DE), Primasheet® (Ensign-Bickford Aerospace & Defense Company, Simsbury, CT) and Primacord® (The Ensign-Bickford Company, Spanish Fork, UT), and is mixed with

trinitrotoluene (TNT) to form pentolite, which can be easily cast into desired shapes [6,11].

The energetic properties of PETN make it a valuable compound for use in explosive products. PETN performs exceptionally well in "compound detonators due to sensitivity and high brisance," referring to the shock that is produced when it explodes [13]. PETN is a secondary explosive that is relatively insensitive to friction [13], but is quite shock sensitive [11]. It is an under oxidized explosive with a relatively high detonation velocity of 8.26 km/second and a Chapman-Juget pressure (P_{CJ}) of approximately 33.5 GPa at the nominal theoretical maximum density (TMD) of 1.76 g/cc [16,15]. During the 1980's, T. L. Eremenko developed a method to calculate an approximate TMD based on the hydrogen content and structural group of the explosive [11]. TMD is commonly used in explosive literature to report detonation velocity and other parameters. Detonation velocities for common explosives at their TMD typically range from 7 km/sec for TNT to 9.15 for octahydrotetranitrotetrazocine (HMX) [11].

2.1.1 Crystal Structure

The chemical formula of PETN is $C_5H_8N_4O_{12}$ and is also known by the synonym 2,2-bis[(nitroxy)methyl]-1,3-propandiol dinitrate [15]. It has the chemical structure given in Figure 2.1.1-1 [11,13,15]. Two polymorphs of PETN are known to occur: PETN I and II. Both polymorphs have primitive Bravais lattices, but PETN I forms as tetragonal space group $P42_1/c$ and PETN II as orthorhombic space group Pcnb [3,14,15].

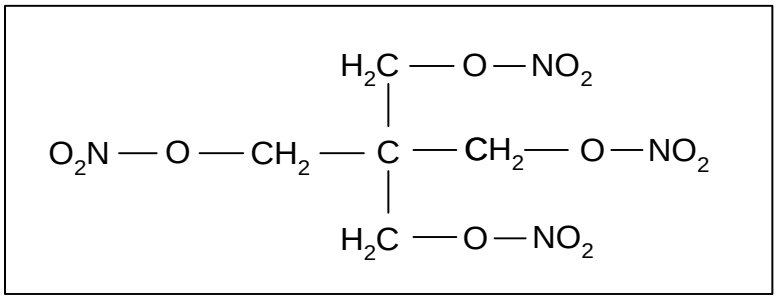

Figure 2.1.2-1 PETN Chemical Structure [6, 12]

During fabrication, the crystallization method controls the crystal habit in which PETN forms. PETN I has been observed to form various crystal habits, including tetragonal crystals, nearly hollow prismatic or hour-glass crystals with reentrant voids, equant crystals, and irregular plates [3]. The science of mineralogy has long been concerned with descriptions of crystal shapes and a glossary of descriptive terminology is in common use. Prismatic is a term that describes crystals with a high length to width aspect ratio, but which are thicker than needles (acicular) or fibers (fibrous). Equant refers to crystals that can be rounded or angular, but which have approximately equal dimensions of length, width and height. Blocky crystals are slightly elongated compared to equant, but have a lower length to width ratio than prismatic [17].

2.1.2 PETN Thermodynamic and Physical Properties

The thermodynamic properties of PETN also make it a good candidate for use in many applications. PETN normally used for EBW detonators is in the form of a white fluffy powder having poor flow characteristics, making it difficult to handle. PETN is a solid at room temperature, with a melting point of 140° C and has an endothermic heat of formation (ΔH_f) of –128.7 kcal/mol. It is has a vapor pressure of 8×10^{-5} mm Hg at

100°C, so it has a reasonably long shelf life [15]. The refractive index (RI) of PETN is listed as 1.558 [23], but recent work at Pantex has identified it as 1.555 [18].

For aging studies, however, it is important to know that PETN becomes relatively volatile above 100°C [13, 15]. Thermal decomposition is thought to begin with a de-nitrification reaction during which the O-NO_2 bond is broken in the nitrate functional group [19]. This is the reverse of the manufacturing process of the compound, which involves nitrification of pentaerythrite, a synonym for pentaerythritol [13].

The solubility of PETN is an important parameter for this study, because the samples will need to be dispersed in various liquids for PSD analysis. The solubility of PETN in water has been published as 1.5 –2.1 mg/L [20,21]. PETN was observed to be slightly soluble in alcohol and ether, and completely soluble in acetone [13,20]. The solubility of PETN in isopropyl alcohol was given as 0.02 grams per 100 mL of solvent [22]. At 20° C the solubility of PETN in ethanol is listed as 0.125 grams PETN per 100 grams of solvent [23].

2.2 Split Sampling Methods

For comparison studies, it is imperative that the powders measured by each laboratory are identical. Poor flow characteristics of PETN powders complicate efforts to obtain a representative split sample. Many strategies have been proposed and studied to subdivide a bulk powder into identical split samples. Although the use of a riffler for sample splitting is the most reliable, as evidenced by the lowest relative standard deviation (SD), it is not suitable for powders that exhibit poor flow characteristics [24].

For powders with poor flow characteristics, coning and quartering is the most applicable procedure, producing a 6.81% relative SD in reliability tests [24]. Coning and quartering is easy to practice in any setting, results in little sample waste, requires no special equipment to perform, and is applicable to a wide variety of materials. The American Society for Testing and Materials (ASTM), for example, includes procedures for sampling ceramic clay (ASTM C322), carbon black (ASTM D1900), aggregates (ASTM C 702-98), metal powders (ASTM B215-96), field environmental media (ASTMD6051-96 [2001]), and laboratory waste management media (D6323-98 [2003]) [25, 26, 27, 28, 29, 30]. The International Organization for Standardization (ISO) is also drafting a standard method titled: *Sample Splitting of Powders for Particle Size Characterization* (ISO/WD 14888). This document is in the final committee stages and is expected to be published soon [31].

2.3 Particle Characterization Methods

Characterization of powders is extremely important to understanding the properties of materials and encompasses many aspects of particle properties and interactions [32]. If a powder has a wide variation in particle size, is composed of non-spherical particles, or has a large fraction of submicron particles, the measurement of particle size becomes even more difficult. However, advances in technology, especially in the areas of electronics miniaturization and signal processing software development, have permitted both individual and bulk property characterization to become more refined [24, 33]. There are still some challenges in performing PSD measurements

because assumptions and approximations inherent in the measurement methods are not always applicable to the sample [24].

2.3.1 Surface Area Measurement Methods

The SSA of particles has a significant impact on the physical properties of powders and has been the focus of much attention from such diverse communities as the pharmaceutical, paint, toner and geologic professions. Because of the difficulties in directly measuring the surface area of small particles, several methods to indirectly estimate the surface area have come into popular use. These includes permeametry using the Fisher sub-sieve sizer (FSSS) and gas adsorption using the Brunauer, Emmett and Teller (BET) methods.

2.3.1.1 FSSS Method

The FSSS method is essentially gas flow permeametry. It requires a tube of specified dimensions to be loaded with sample powder, which is then compacted to a specified density (porosity). Alternatively, a known mass of powder can be compressed to a given dimension to achieve a standard compaction density. An inert gas, or more typically, air is then flowed through the packed bed and the pressure drop across the sample is related to the SSA of the powder sample. The gas flows around the particles, but is not absorbed into the surface cavities, which defines it as an envelope method rather than a total surface area determined by adsorption. In the simplest form, SSA, or S_o is related to particle diameter through the equation:

$$S_o = \frac{6 \times 10^4}{d_m \ \rho_{TMD}} \qquad \text{Equation 1}$$

where d_m is proportional to the gas pressure difference and ρ_{TMD} is the theoretical maximum density. The gas pressure drop is obtained from gauges on the instrument. This calculation is based on an assumption of monodisperse spheres [34,35].

2.3.1.2 BET Method

A different surface area measurement technique was proposed in 1938 by Brunauer, Emmett and Teller [36]. This BET method relies on the adsorption of a monolayer of nitrogen or less frequently, krypton or argon gas molecules or atoms on the surfaces of the particles at liquid nitrogen temperatures rather than on flow around particles. A known amount of sample powder is placed in a sample tube. The flow rate of gas applied to and exiting the sample tube is carefully measured and the difference in surface attraction at liquid nitrogen compared to room temperatures is converted into the number of gas molecules or atoms remaining in the sample tube adhered to the sample surfaces. The gas molecules or atoms adhere not only to exterior particle surfaces, but also to particle voids that are open to the surface, such as the reentrant voids present in some PETN particles. Knowledge of the gas molecule or atomic diameter is transformed into a calculation of the surface area, assuming a monolayer of gas. An estimation of the pore volumes can be made when higher partial pressures are used to adsorb gas molecules or atoms to completely fill in reentrant void features, rather than simply creating a monolayer [37]. Whereas this may be useful for studying the characteristics of

packed beds, if higher partial pressures are inadvertently used, the surface area of a sample may be over reported.

2.3.1.3 Comparison of Surface Area Measurement Methods

One drawback of permeametry is that delicate or prismatic particles, such as those common in PETN may be broken or damaged during the packing, which may alter the surface area of the powder and PSD. Logic dictates that the SSA will increase if breakage of the crystals occurs. Some researchers have noted such an increase in SSA by performing a BET surface area measurement on a PETN powder sample before and after the sample was compacted into a FSSS measurement tube [38].

This difference between the FSSS and BET measurements is due to the fact that the FSSS technique actually measures resistance to flow or permeability, which is related to the compact bed pore structure, reentrant void characteristics as well as the powder surface area. Also, the surface roughness of the particles has an effect on the flow of gas around each particle. In this way, the FSSS measurement gives a measure of specific surface area, but the reported surface area is a function of PSD, surface roughness, and other related parameters whereas the BET measurement includes surface area created by all of these characteristics and the reentrant voids on the surface of the each particle [35].

This envelope method is advantageous over the BET gas adsorption method when studying fluid flow through the packed powder or if the average particle size is of interest because it provides a measure of the external surface area and particle size. The experimental apparatus is also simple, inexpensive, and easy to use [39].

2.3.2 Visual Characterization Methods

One of the earliest methods used to determine particle sizes and distribution was optical microscopy. Using this technique, a powder sample was dispersed on a slide, a photograph was taken, and the individual particle dimensions were measured by hand from the image. In order to get statistically significant results, a minimum of 600 particles had to be measured and counted [40]. It was a tedious and time consuming process and was impacted by poor or non-representative dispersion of the particles on the slide and by the fact that it was only a two dimensional analysis [7,41]. The technology was limited to particle sizes visible with the highest magnification optical lens using visible light, so the smaller particles could not be characterized or were missed entirely. Quantitative microscopy software was used with optical microscopes in the 1980's but again, limited by magnification, dispersion and two-dimensionality.

The magnification limits were extended with the use of the SEM. By the early 1970's, advances in computer and electronics technology permitted electron microscopes to be used for particle characterization [42]. The advantage of this technique was that the surface of particles could be examined in detail, including elemental analysis of very small areas of each particle. However, this technique had the same flaws as optical microscopy, (i.e., poor dispersion and two dimensionality impacted the analysis), and in addition enhanced the problem of having too narrow a field of view to get a single photomicrograph that was representative of the entire sample [43].

2.3.3 Light Scattering PSD Measurement

The technology of PSD measurement has advanced along several parallel lines that can be grouped into broad categories and ranges from those methods that are based on visual observation of particles such as microscopy, to those that use more indirect methods of measuring particle sizes, such as light scattering. Within the broad category of light scattering methods, different techniques have improved and diverged from each other as technology has advanced. Variations that are currently in commercial use include the measurement of stationary dispersed particles in a vial or cuvette of fluid, in-line real-time measurement of particle sizes such as those emitted from the outflow of a process or exhaust stack, and laser light scattering measurements on both fractionated and non-fractionated samples that are either stationary or flowing through a liquid carrier medium.

The characterization of fine particles using light scattering principles is based on optical theory developed through a series of discoveries in the nineteenth and early twentieth century. These discoveries culminated in the invention of the first commercial laser light scattering instrument in 1970 [44,45]. Light scattering has emerged in recent decades as one of the more widely used techniques for particle size characterization due to advances in technology that improve the reproducibility of results, simplicity of use, detection range, and speed of analysis [46,47,48,49,50,51]. However, instrument resolution limitations have prevented full characterization of the submicron-sized fraction of powders until very recently [24,52]. It is now possible, using the latest generation of commercial light scattering instruments, to focus the detection and measurement on the submicron-sized fraction of powder.

Scattering has been used to describe any general phenomenon that changes the direction and/or phase of incident waves, and has been detailed in theories by Raman, Compton, Bragg, Rayleigh, Mie, and others to describe different ways in which electromagnetic radiation interact with matter [53]. The intensity of light scattered by interaction with matter varies due to phase changes that create areas of constructive and destructive interference spread over an angular distribution [54,55]. Joseph Von Fraunhoffer recognized such a diffraction pattern in the early 1800's.

Two researchers, Edward Lorenz, in 1890 and Gustov Mie in 1908 independently recognized this Fraunhoffer diffraction to be a special case of a more complicated and comprehensive theory based on James Clerk Maxwell's equations describing electromagnetic radiation [24,54]. Fraunhoffer diffraction best describes scattering that occurs when particles are much larger than the wavelength of the light source used. In this case, incident light is scattered predominantly at low angles, i.e., mostly in the forward direction (Figure 2.3.3-1). The Lorenz-Mie (Mie) theory recognizes that for particles slightly smaller than the wavelength of light used, the light is scattered through a range of angles, but low angle scattering still predominates (Figure 2.3.3-2) [24,53,40].

The equations developed by Lorenz and Mie relate the light scattering angle and intensity of the diffraction pattern to the particle size, assuming smooth, spherical particles. For particles near the wavelength of incident light, the general rule under Mie theory is that the smaller the particle, the higher the angle of refraction and the broader the range of angles that scattering occurs over [24]. The intensities of light at each scattering angles can be measured and correlated to particle size [56].

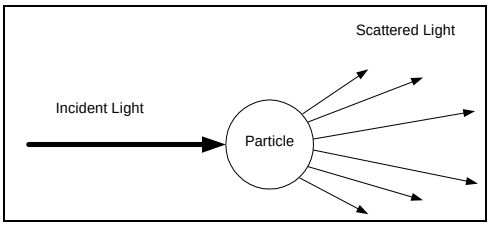

Figure 2.3.3-1
Fruanhoffer Scattering [39, 53]

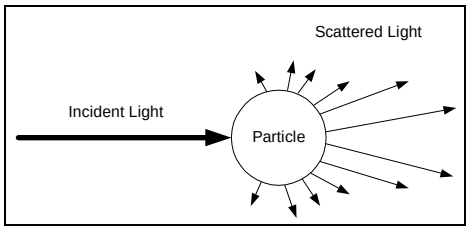

Figure 2.3.3-2
Mie Scattering [39, 53]

The advantage of using the Frauhoffer approximation is the simplicity of the calculations and the fact that the measurement is independent of material properties such as RI. The disadvantage, however, is that it is not applicable for particles of the same or smaller diameter as the wavelength of the light used [33]. The more comprehensive Mie theory equations require the RI of the material to solve for the particle size.

Due to these advantages and disadvantages, various instruments use the different theories to calculate particle sizes based on the range of measurement desired. Instruments that are designed to cover a wide range of particle sizes, such as the Coutler® LS 100Q and LS 230 and the Micromeritics® Saturn DigiSizer® 5200 use the Mie theory equations, which provides solutions for particles smaller and larger than the wavelength of the laser. In instruments with this wide analytical range, the special case of the Mie theory described by Fraunhoffer is typically applied to the particles larger than the wavelength of the installed laser and the more comprehensive Mie equations can be applied when smaller particles in this range are of interest. In some cases, multiple light sources with smaller and larger wavelengths have been installed to enhance the analytical range of the instrument.

In submicron particle size measurements the RI becomes important. The RI is a measure of changes in the velocity, wavelength and amplitude of light as it interacts with

matter, as compared to free space (vacuum). There is a real and an imaginary component to the RI, where the imaginary portion is related to the transparency or color of the material. For materials with large real values, the complex portion of the RI does not have a great influence on the size measurement [56]. However, other research has shown that for SiO_2 particles with a measured diameter between 0.4 and 1.3 microns, a change in the imaginary component of the RI resulted in an approximate 50% decrease in the measured particle size. The imaginary portion of the RI is also affected by surface roughness and density differences within the particle [24].

Scattering equations are all based on the assumption of spherical particles, yet PETN is seldom present in this crystal habit. Mathematical solutions for cylindrical particles using the Mie equations exist, but the use of these solutions in instrument data analysis software is not a standard practice [24]. A pre-existing knowledge of the general shape of the particles is necessary to interpret information that can be related to non-spherical morphologies [57].

2.3.4 PSD Validation

PSD measurement is not a straightforward endeavor, despite efforts of instrument manufacturers to simplify the analysis and data processing tasks [58,59,60]. Material properties, such as particle shape and degree of birefringence may affect the measurement. In addition, instrument and software manufacturer computer codes and data processing algorithms are often proprietary, so it is difficult to distinguish geometric differences or hardware sensitivities from differences caused by proprietary codes between instruments manufactured by different companies [59].

Given the difficulty in assessing the accuracy of PSD data generated using different methods and/or different instruments, a variety of approaches have been used. In every case, the results vary within each study and the attempts to resolve the data have fallen into several categories. Some researchers have made statistical evaluations of the data to determine which data sets match more closely, some have applied various inversion and deconvolution techniques to the raw intensity and angular data, and others have identified biases of each instrument and suggested that the instruments be selected based on the material and data end uses.

Several studies examined the preparation methods and found that these steps could significantly affect the results of the PSD analysis [61]. Agglomeration of particles in the liquid media was a common problem, and sonication and pH control were both used to minimize this condition. However, sonication time was found to have an inverse relationship to the measured PSD. The minimum sonication time necessary to deagglomerate the particles without causing particle breakage was recommended [60]. Agglomeration was identified by the presence of peaks in the large size region when no particles of that size were seen in image analysis data [62]. The use of a liquid media that will not dissolve the particles was also recommended to avoid questions regarding the solution equilibrium in a saturated solution. The use of a saturated solution was suggested as a last resort, citing storage and preparation difficulties in addition to sample dissolution potential [62].

Instrument and material biases that have been noted are related to preferred orientation and consistent trends particular to individual instruments. For instruments that use a flow through cell for light scattering measurements, such as the Coulter® and

Micromeritics®, preferential alignment of rod-shaped and platy particles in the direction of flow was noted and caused a tendency to measure only one dimension of the particle rather than a random orientation (usually the end-on dimension, based on instrument geometry) [63].

Several researchers have found that a particular instrument consistently over or under estimated some of the sample particles. Most researchers found that all of the light scattering instruments used were able to predict the average or mean particle size reasonably well and that most instruments measured the PSD of mono-dispersed samples better than poly-dispersed. But all other conclusions about instrument performance were similar in that no other overall statements could be made. One researcher found that one brand of instrument consistently predicted a much lower poly-dispersity, while one overestimated the size of particles that were approximately 55 nm, compared to other instruments. The Wyatt® MiniDAWN® light scattering detector was found to overestimate 150 nm particles by as much as 30 nm [64]. The conclusion of most researchers regarding instrument biases is that they exist and that the measurement of PSD is not independent of the instrument or the sample material [59,65]

The material properties, including the sharpness of the particle edges, the color of the particles and the presence of a large amount of small particles (e.g., <10 micron) influence the tendency of "ghosting". "Ghosts" are defined as an artifact of the measurement system that occurs when high angle reflections are generated from larger particles. The high angles are interpreted by the instrument software to represent small particles when, in fact, they are spurious signals created by the larger particles. Most frequently seen when using Fraunhoffer theory to measure particle sizes, some

researchers find that “ghosting” also occurs occasionally when using the Mie theory model.

Due to the desire to measure a large range of particle sizes with a single instrument, many manufacturers equip their instrument software to solve the comprehensive Mie theory equations. In some cases, the simple solution of the Frauhoffer equations are applied to larger particles, and the comprehensive Mie theory solutions are used for the smaller particles. Either way, the accuracy of the data corresponding to smaller particles should be verified by independent means to detect the presence of “ghosts” and other artifacts of the measurement instrument [43, 59].

Also related to the material properties, the degree of transparency affects the complex portion of the RI. Darker and more strongly colored materials have a larger complex value for the RI, while lighter and more transparent materials have a small or null complex RI value. These complex RI values are not readily available in the literature and so are often set to zero. One suggestion to facilitate the comparison of data from one laboratory to another is to enter the complex RI values used by each lab to evaluate the impact of this complex value on the data [65].

Other methods used to compare data from one laboratory or methods to another involved the use of statistical analysis. A variety of methods were used and ran the gamut from working with the raw intensity and angular data to devising new deconvolution methods to assuming one true result that was used to measure the other data against [66,67]. The Bootstrap statistical analysis method was also used, both before and after eliminating outliers. The SD of the mean diameters was then used as a metric

[43]. SD can also be applied to replicate measurements to quantify the reproducibility, or precision of the measurement.

Ruggedness was also defined as a measure of precision and validity for a batch of 58 pharmaceutical PSD measurement methods that were developed. A method was defined as acceptable under this scheme if the relative percent deviation was within 20% for the measured median diameters (d_{50} values) [62]. One researcher suggested to the ISO committee responsible for developing standards that three criteria for comparison could be used: a) the maximum difference in the cumulative distributions, b) the relative sigma of the differences in median diameter and c) a quartile graph of the relative differences [68].

Statistical tools often used in engineering include factorial designed experiments (DOE). DOE analysis yields information regarding which factors have an effect of the response variable, within selected confidence limits. A main effects plot provides a visual representation of the data where the steepness of the line is correlated to the strength of the effect of the factor on the response. Of particular interest in the factorial fit calculation results are the probability value (P-value) for each factor as well as for the combination of factors. A selected alpha value represents the confidence level at which the correlation of the factor to the response is to be tested. A resulting P-value less than the chosen alpha value indicates that the factor is significant within the corresponding level of confidence. A normality plot of the standardized effects presents these numerical values in an intuitively obvious graphical format [69, 70].

To arrive at a conclusion regarding whether the particle size measured at each lab were the same with a given confidence level, a two-sampled t-test can be used to test for

variance between means. This statistical test can also be applied to duplicate measurements made at the same lab as an indication of reproducibility, which is a measure of precision, but not accuracy [59, 69, 70].

Another method used to quantify precision is the relative percent difference (RPD), which is the difference between two values divided by the average of the values multiplied by 100. The RPD can also be used to communicate how different one data point or set is from another, once statistical difference has been established. Originating in the medical community, this statistical tool was adapted by the environmental industry as the science of risk assessment emerged to allow comparison of differences between one pair of data to differences between another pair of data. For example, the RPD between the numbers 1 and 2 is the same as the RPD between 50 and 100. Another way to express this relationship is that the number one is as far away from 2 as 50 is from 100, on a relative scale [71, 72, 73].

The absolute difference, however, may also be important because the relative values mask the magnitude of the data. The absolute difference, which is simply the difference between values, may be used to describe the differences between data. Several researchers assumed image analysis data to be an absolute measure and determined whether the other methods reported the proportion of each population was within 5% of the SEM values [64].

Other researchers, however, refuted the use of image analysis as an absolute measure. Citing the potential to bias to the image during sample preparation (e.g., breakage of particles, air bubble formation), image distortion, and field of view issues, the use of image analysis as a reliable “absolute” standard was discussed. The

advantages of using the higher resolution field emission SEM for examination of colloidal and other very fine particles compared to the representativeness of a small field of view were presented. It was also noted that the images analysis methods measure different physical properties than light scattering methods, thus it may not be valid to use images as an absolute standard against which to compare light scattering data [43, 60, 64].

CHAPTER 3
EXPERIMENTAL PROCEDURE

3.1 Sample Selection

Three PETN powders were used for this study and were selected on the basis of their availability, specific surface areas, and morphologies so that the method developed in this study can be shown to be effective for a variety of PETN powders. Table 3.1-1 identifies the characteristics of PETN powder samples A, B, and C. Powders A and B are known to have similar morphologies that are distinct from sample C, and all three of the powders are known to have different specific surface areas.

Table 3.1- 1 PETN Sample Powders

PETN Sample	Specific Surface Area (cm^2/g)	Dominant Particle Morphology
A	Medium	Hollow prismatic
B	Low	Hollow prismatic to tabular
C	High	Subhedral equant

cm^2/g = square centimeters per gram.

3.2 Split Sampling

Each of the three PETN samples was coned and quartered according to ASTM Method D D6323-98 (2003) [27]. Based on the original amount of sample material

present, the material was coned and quartered a variable number of times to achieve quarters that were approximately equal to the sample quantity needed for each laboratory. A flow chart for splitting each of the three powders is presented in Figures 3.2-1 through 3.2-3. Additional sample volume was obtained from the remainder containers, as needed.

3.3 Specific Surface Area Measurements

The SSA of each of the PETN samples was measured at Pantex using both the permeametry (FSSS) and the dynamic flow BET techniques. The BET surface area of the three PETN powders was measured before and after forming the packed bed in the FSSS tube at 0.400 density to determine if the measured surface area and/or PSD was affected by the packing.

3.4 Sample Preparation

Measurement of the PSD using the Coulter® and Micromeritics® systems require that the PETN particles be suspended in a liquid media at the correct concentration and the RI of each sample preparation must be known for accurate deconvolution of the light scattering data. Each of the three laboratories participating in this study, LLNL, Pantex and SNL, used their standard preparation procedures to obtain particle size data from the light scattering instruments. Subsequently, SNL prepared all three samples using the standard liquid media and sonication time procedures employed by the other two labs, and measured the PSD again.

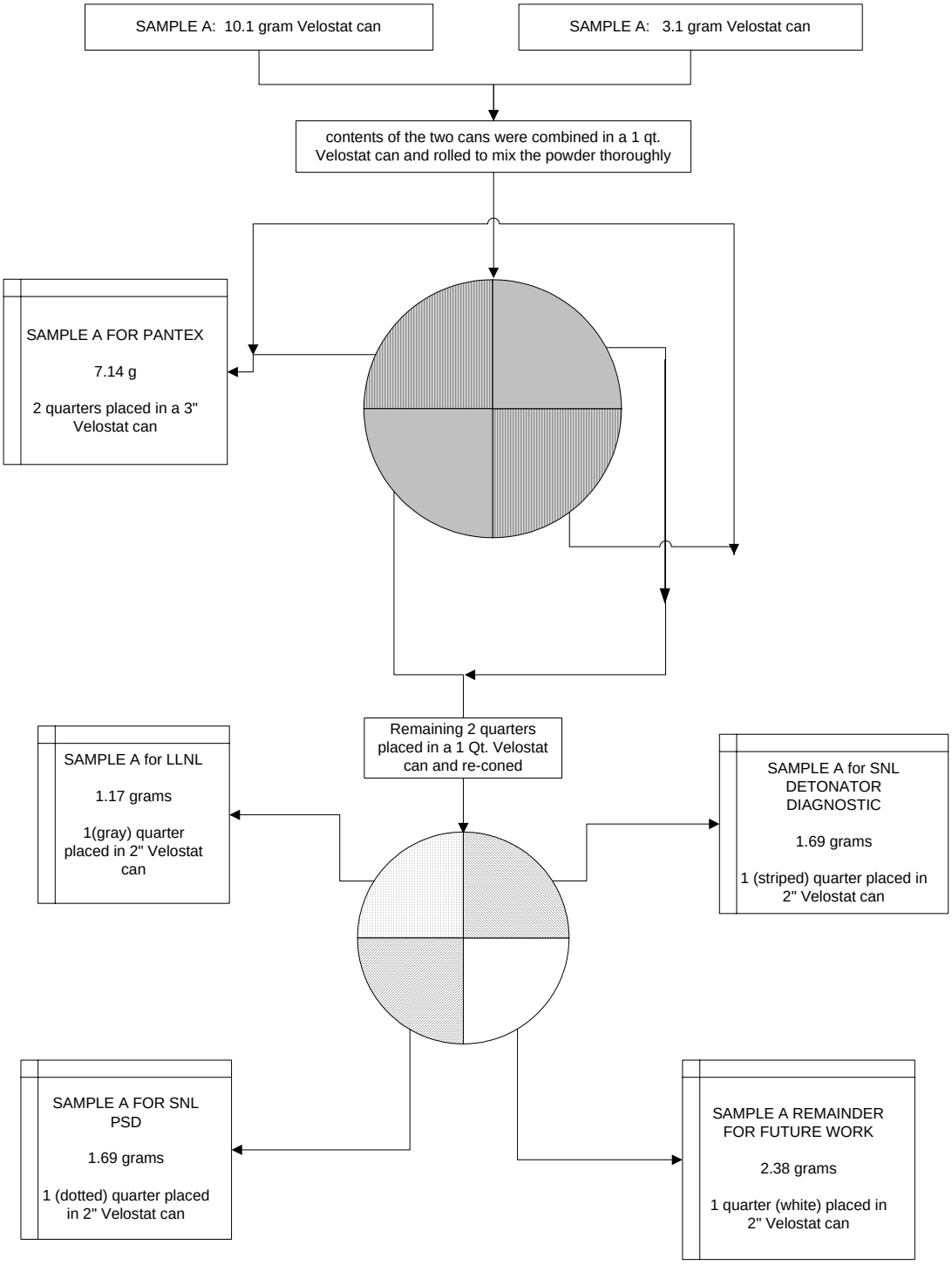

Figure 3.2-1 Splitting History for Sample A

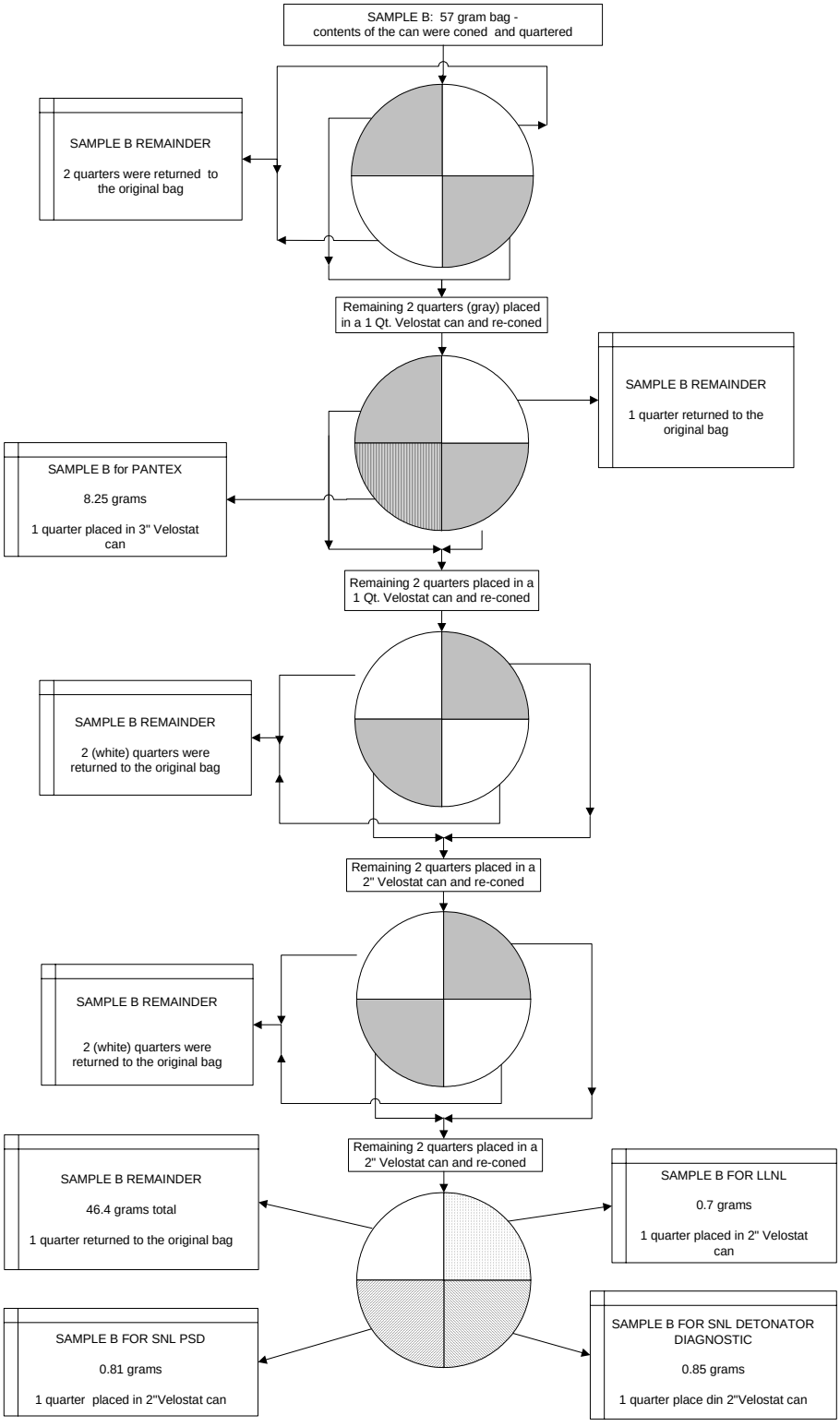

Figure 3.2-2 Splitting History for Sample B

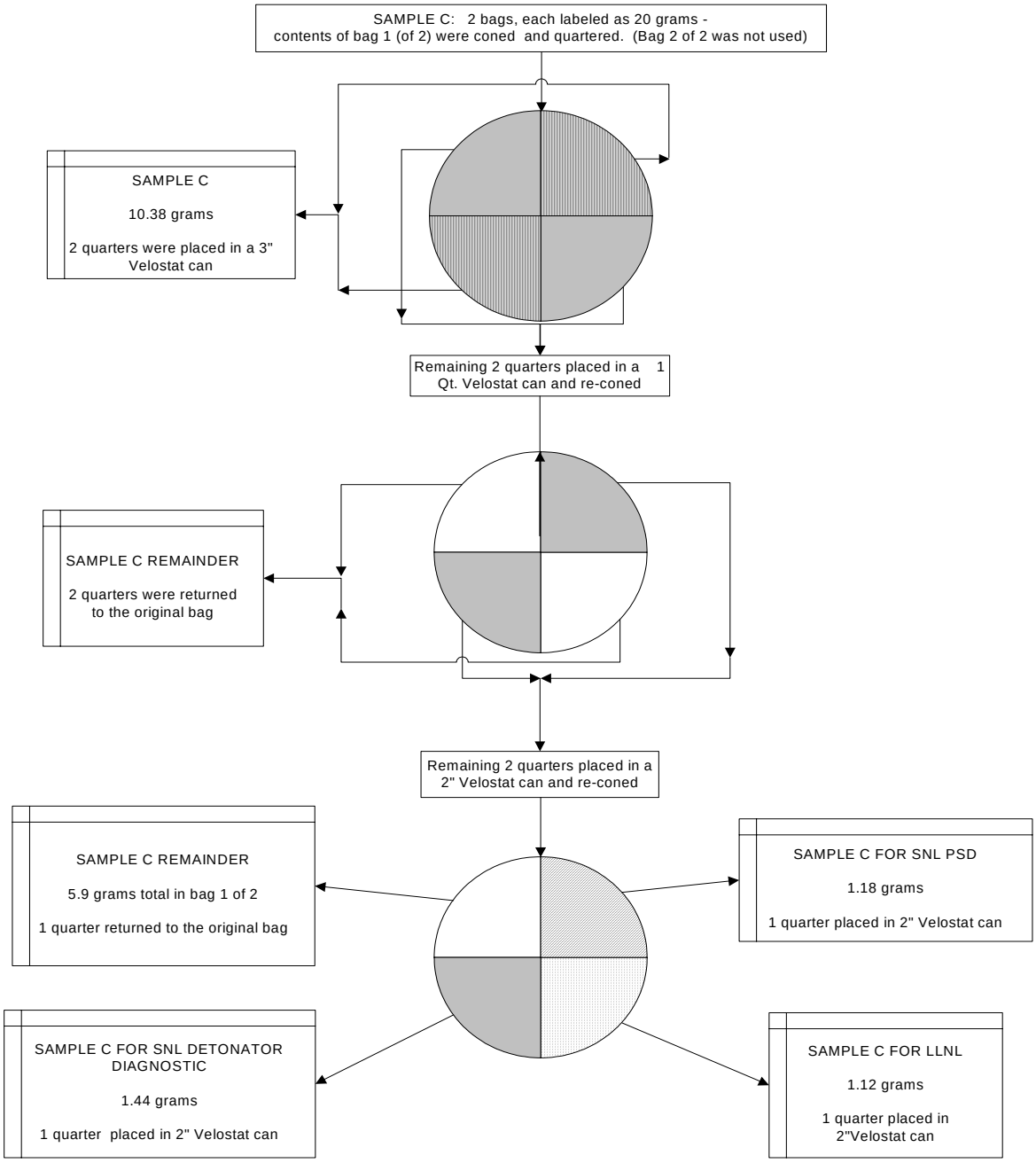

Figure 3.2-3 Splitting History for Sample C

3.4.1 Liquid Media Preparation

The standard liquid media used as carrier fluids to suspend the PETN powder samples for PSD measurement at the three laboratories are given in Table 3.4.1-1. Subsequently, at SNL each of the three PETN samples were prepared in each of the three carrier fluids to isolate any effects that carrier fluid may have on the PSD measurement.

All water used in this study at SNL was deinonized (DI) water, supplied by a Culligan®, Northbrook, IL, pretreatment filter followed by a Labconco®, Kansas City MO, water purification system. The in-line conductivity measurement of the water was at least 16 micro-ohms or less. The water introduced into the Coulter® light scattering instrument at SNL also had 0.02% by weight laboratory grade sodium azide powder (Fisher Scientific®, Hampton, NH) added as an anti-bacterial agent. Coulter® Type IA non-ionic dispersant, part number 6600703 was used at both LLNL and SNL to disperse the PETN powder samples in the water. High-pressure liquid chromatography (HPLC) grade isopropyl alcohol (IPA) and ethanol (both Fisher Scientific®), were used to make the saturated solutions of carrier fluid at SNL.

Table 3.4.1- 1 Sample Preparations

Laboratory	Standard Liquid Media
Pantex	PETN-saturated ethanol
SNL	PETN-saturated IPA/DI water (50%/50%)
LLNL	DI water with dispersant and 2% by weight sodium azide

3.4.2 Ultrasonic Dispersion

Each of the three laboratories use different sonication procedures in their standard methods. LLNL placed the suspended sample in a weighted double plastic beaker configuration in a 130-watt bench top ultrasonic bath and sonicated the liquid preparation for 180 seconds. SNL procedure calls for the placement of the suspended sample in a single glass beaker in a 180-watt bench top ultrasonic bath with sonication of the sample for 30 seconds. The subsequent study conducted by SNL included 0, 30, 60 and 180 second sonication times using this bench top ultrasonic bath. The Coulter® instrument at Pantex is equipped with an internal sonication device that can be varied from 30 to 50 watts, but the standard procedure at Pantex calls for no sonication of the suspended samples. Pantex did, however use this internal sonication device for another study of the effects of sonication time on the PSD of energetic material powders.

3.5 Particle Size Distribution Measurement

The PSD of each of the three PETN sample powders were measured at LLNL, Pantex and SNL using the standard procedures for each of the labs. Each of the three labs used the Mie optical model with their light scattering instrument designed to measure the sizes of the entire range of particles present in the PETN powder samples. Table 3.5-1 illustrates principal parameters associated with each method for the labs.

The Coulter® and Micromeritics® instruments at the three laboratories are all equipped with small volume modules. These accessory modules allow a smaller amount of sample to be used to make the PSD measurement. The amount of sample needed is determined by the obscuration of the laser. For proper operation, there must be enough

Table 3.5-1 Major Elements of PSD Methods

	Pantex	LLNL	SNL
Instrument	Coulter® LS 230	Micromeritics® Saturn DigiSizer 5200	Coulter® LS 100Q
Lower Detection Limit	0.04 μm	0.1 μm	0.4 μm
Carrier fluid	Saturated ethanol	Water with dispersant	Saturated 50% IPA/water
Sonication time	None	3 minutes	30 seconds
PETN RI	1.558	1.520 + 0.0316i	1.558

sample particles present in the suspension to cause 8-9% obscuration for the Coulter® and between about 5-20% for the Micromeritics®. For PETN, this can usually be achieved by using on the order of 20 mg of powder, less for finer particle-sized powders than for coarser.

To address sources of uncertainty associated with differences in preparation methods, the sample preparation methods employed by each laboratory were subsequently examined at SNL to identify if differences in the sample preparation steps, sonication time and/or carrier fluid, influenced the PSD data. This subsequent study at SNL sought to minimize the influence of other differences in the measurement by using a single instrument, refractive index and operator. The effects of sonication and carrier fluid on the mean particle size were studied by implementing a DOE using these two parameters as the factors. Levels of these factors were chosen to include the sonication times and carrier fluid combinations used at the other two laboratories.

To this end, twelve sonication time and carrier fluid conditions were applied to each of the three PETN samples in this study. All three samples were suspended in ethanol and four sonication times ranging from 0 to 180 seconds were applied. This captured the Pantex standard operating method, which called for the use of ethanol with

no sonication. In addition, water with 0.02% antibacterial agent (i.e., sodium azide) was used with the same four sonication times, capturing LLNL's standard procedure of using water with 180 seconds of sonication. The SNL standard method calls for the use of 50% IPA and water with 30 seconds of sonication. To complete the factorial design, this carrier fluid was used with all four sonication times also. These twelve combinations of factors, summarized in Table 3.5-2, were applied to each of the three PETN samples. Each of the 36 sample runs were performed in triplicate, yielding 108 individual PSD data files. The test at 30 seconds sonication in 50% IPA is the standard method at SNL and so the initial PSD measurement data were used.

To address questions regarding the ability of the SNL Coulter® and LLNL Micromeritics® instruments to accurately identify the presence of submicron-sized particles, two standard reference materials were analyzed. Cross-linked polystyrene spheres with mean particle sizes of 0.48 and 1.23 microns (μm), respectively were

Table 3.5-2 Factors and Levels for Preparation Method Study

	Sonication Time			
Carrier Fluid	0 seconds, water + dispersant	30 seconds, water + dispersant	60 seconds, water + dispersant	180 seconds, water + dispersant
	0 seconds, 50% water/IPA	30 seconds, 50% water/IPA	60 seconds, 50% water/IPA	180 seconds, 5 0% water/IPA
	0 seconds, ethanol	30 seconds, ethanol	60 seconds, ethanol	180 seconds, ethanol

prepared and analyzed using the two instruments. Measurement of these ideal spheres indicated whether the instrument is capable of measuring particles in these size ranges near the lower detection limits.

3.5.1 LLNL PSD Measurement

At LLNL, a Micromeritics® Saturn DigiSizer 5200 analyzer® was used. Approximately 8 mg of each PETN sample was weighed and 10 drops of Coulter® brand Type IA non-ionic surfactant was placed directly on the powder. Approximately 2 milli-liters (ml) of water was added, then the preparation was placed in a small polymer vial inside a larger beaker weighted down with a custom-fabricated ram, and both of the containers were placed in an ultrasonic bath for 3 minutes to disaggregate the particles.

The sample preparations were then mixed thoroughly and aspirated into a syringe or pipette for injection into the PSA instrument. Based on manufacturer recommendations, the real value for the RI for the analysis was set to 1.520, and the imaginary part of the RI was set to 0.0136, signifying that the PETN particles were not transparent. A small volume cell was installed in the instrument for these PSD measurements [74].

3.5.2 Pantex PSD Measurement

At Pantex, a Coulter® LS 230 light scattering instrument was used to measure the PSD. A prepared solution of PETN saturated ethanol was made in liter quantities by adding PETN from other sources to HPLC grade ethanol until visible particulates were present. The solution was filtered into a flask through a Whatman® #5 filter using a Buchner funnel apparatus. This solution was stored until needed for sample analysis.

A small amount of sample powder, enough to make a highly concentrated liquid, was added to approximately 2 ml of the saturated ethanol solution. This sample suspension was mixed using a wrist action shaker then aspirated into a pipette for introduction into the Coulter® LS 230 particle size analyzer. The RI used by Pantex for pure ethanol for this analysis was 1.36 and for PETN is 1.558. Only the real value for the RI for the unmixed products (PETN and ethanol) was required for these measurements. The absolute RI of the saturated ethanol sample solution has not been measured [7,75].

3.5.3 SNL PSD Measurement

At SNL, a Coulter® LS 100Q instrument was used to measure the PSD. The standard method called for the use of a prepared solution of 50% IPA/50% DI water saturated with PETN that was made in liter quantities by adding PETN from other sources to the combination of HPLC grade IPA and DI water until visible particulates were present. The solution was filtered into a flask through a Whatman® #5 filter using a Buchner funnel apparatus. This solution was stored until needed for sample analysis.

A small amount of sample, enough to make a highly concentrated liquid, was added to approximately 2 ml of the saturated solution. This sample suspension was sonicated for 30 seconds using a 180 watt bench top ultrasonic bath, then aspirated into a pipette for introduction into the Coulter® LS 100Q particle size analyzer. Using the Mie model, the RI for water was specified as 1.36 and for PETN as 1.558 [23]. Only the real value for the RI was used for these measurements. The absolute RI of the saturated sample solution has not been measured.

For the subsequent study using various carrier fluids and increasing amounts of sonication, a solution of DI water with 0.02% by weight sodium azide as (an anti-bacterial agent) was prepared at SNL. 10 drops of Coulter® type 1A non-ionic dispersant was added to approximately 8 mg of each PETN powder, and was then diluted using 2 mL of the DI water prepared with anti-bacterial agent. This solution was then placed in a beaker and either shaken gently by hand or placed in the bench top 180-watt ultrasonic bath for the specified amount of time.

3.6 Data Validation

The data collected using the foregoing methods were evaluated to complete the goal of benchmarking the PSD data. First, it was determined whether there were differences between the particle size data for each PETN type within each laboratory and between laboratories. The SD was used to quantify the precision associated with each laboratory.

Where differences were found to exist, an evaluation of the cause and magnitude of those differences was made. Differences in the data between laboratories may be due to variations in the sample powder, sample preparation methods, or differences between instruments, instrument settings, and/or operators. From these possible sources of variation, sample preparation was identified as a potential cause for significant data variations, and so it was isolated from the other sources of bias by holding all else constant. This isolation was accomplished by applying the mitigating procedures identified in Table 3.6-1.

Table 3.6-1 Potential Sources of Variation and Mitigating Factors

Potential Source of Variation		**Mitigating Factor or Procedure**
Non-representative sampling techniques		Application of ASTM coning and quartering procedure for split sampling
Use of different sample preparation methods by different laboratories		Prepare split PETN samples according to all sample preparation methods for direct comparison to each lab using the same preparation methods at a single laboratory
Manufacturing differences between instruments	Geometric differences (e.g., number and arrangement of detectors)	Use of a single instrument
	Differences in the electronics (e.g., signal strength or electronic detection capabilities)	
	Software differences (e.g., rounding errors or calculation assumptions)	
Operator-dependent methodology		Use of a single operator to prepare and analyze samples
Differences in lower detection limit ranges of instruments		Measurement of a fine particle standard reference material

Sample preparation was then divided into two factors and the impact of these factors on the PSD data were statistically evaluated for significance by analyzing a factorial DOE. The factors for this DOE were sonication time, with 4 levels (0, 30, 60 and 180 seconds) and percent alcohol with 3 levels (0, 50 and 100 percents). Although different alcohols were used at both SNL and Pantex (e.g., isopropyl alcohol and ethanol, respectively), the question to be addressed is whether the use of alcohol in the carrier fluid caused dissolution of the PETN particles, resulting in mean particle size differences. Therefore, percent alcohol was a relevant factor.

Various levels of the significant factors were then applied to each of the samples while holding all else constant in an attempt to reproduce the original data measured at

the other laboratories. An analysis of variance between the original and the subsequent data was made to determine if these two values were the same, within a given confidence level. Two-sample t-tests were used to identify if SNL's replication of analytical conditions at Pantex and LLNL resulted in the duplication of the mean particle sizes measured by the other two laboratories within a 95% confidence level.

When this t-test found statistical differences between the measurements, the RPD was calculated and used to quantify how different the measurements were in a relative way. Using this relative value, differences between the means were compared to identify whether one PETN type was consistently difficult to accurately measure between laboratories. The relationship of the difference in the SNL data to the corresponding data produced at the other two laboratories was quantified based on the RPD.

Due to discrepancies between laboratories regarding the presence of very fine PETN particles, validation of submicron-sized measurements was necessary. The ability of the SNL Coulter® instrument to identify small particles of PETN, if present, was established by measuring a sample of a standard reference material. Cross-linked polystyrene spheres with mean particle sizes of 0.48 ± 0.012 and 1.23 ± 0.029 microns, obtained from Spherotech®, Libertyville, IL were used as the standard reference material. The cross-linking of the polystyrene creates a product that is more solvent-resistant and less prone to swelling in alcohols. The manufacturer's information regarding these standard reference materials is provided in Appendix A. In addition, the LLNL Micromeritics® instrument was used to analyze these particle size standards to verify the submicron-sized detection accuracy of this instrument.

An independent method was used at Pantex as a qualitative verification of the PSD using different sonication times. The suspended PETN particles were examined using optical microscopy for several sonication times to ascertain if increasing sonication produced visible changes to the particles in suspension that could be correlated to differences seen in the PSD produced by the Coulter® instrument. The optical microscopy slide preparation technique used at Pantex calls for a cover slip to be gently placed on a clean slide and then a drop of the suspended sample is placed at the edge of the cover slip and allowed to be drawn under it by capillary forces.

CHAPTER 4
RESULTS AND DISCUSSION

4.1 Specific Surface Area Measurements

Previous SSA measurements of the bulk powders using the FSSS method, performed prior to this study were used in the sample selection process and were 4520, 3600, and 5670 cm^2/g for samples A, B, and C, respectively [8]. SSA measurements of each of the three coned and quartered PETN samples used in this study were made by Pantex in April 2005. Pantex performed both the FSSS and dynamic flow BET measurements to determine the SSA of the samples for this study. The results of these recent SSA measurements are given in Table 4.1-1. The FSSS measurements made for this study are within ten percent of historical values.

In addition, Pantex performed the dynamic flow BET method measurement on each of the powder samples again after the samples had been placed in the FSSS tube and

Table 4.1-1 Specific Surface Area Measurements

	FSSS SSA (cm^2/gram)	BET SSA (m^2/gram)
Sample A	4514 ± 91	1.78 ± 0.16
Sample B	3265 ± 175	1.11 ± 0.07
Sample C	5878 ± 29	1.24 ± 0.07

compacted to 0.400 porosity. PETN powder is compacted to 50% of the theoretical maximum density in many EBW devices. Therefore, pressing into the FSSS tube approximates the EBW pressing. Because prismatic PETN crystals are delicate, due to the high aspect ratio and low strength, it was suspected that pressing the powder into the EBW detonator would change the specific surface area significantly, such that a PETN with a prismatic crystal habit and lower initial surface area would develop a higher specific surface area after pressing into a detonator. The opposite trend was seen in this study. The data for these subsequent BET measurements are given in Table 4.1-2. Because there was only enough powder in each FSSS tube to perform a single BET measurement, no error term is associated with the BET measurement after compaction.

Table 4.1-2 BET Specific Surface Area Before and After Compaction

	BET Specific Surface Area Before Compaction (m^2/gram)	BET Specific Surface Area After Compaction[1] (m^2/gram)
Sample A	1.78 ± 0.16	1.04
Sample B	1.11 ± 0.07	0.86
Sample C	1.24 ± 0.07	1.21

[1] Samples were compacted to 0.400 porosity in the FSSS device

4.2 Particle Morphology

The shapes of the PETN particles for the three samples were characterized using SEM photomicrographs at 500X and 2000X magnifications. Samples A and B appear as prismatic crystals with re-entrant voids, whereas Sample C generally appeared as subhedral equant crystals with an overall average length to width ratio of approximately unity (Figures 4.2-1 through 4.2-3).

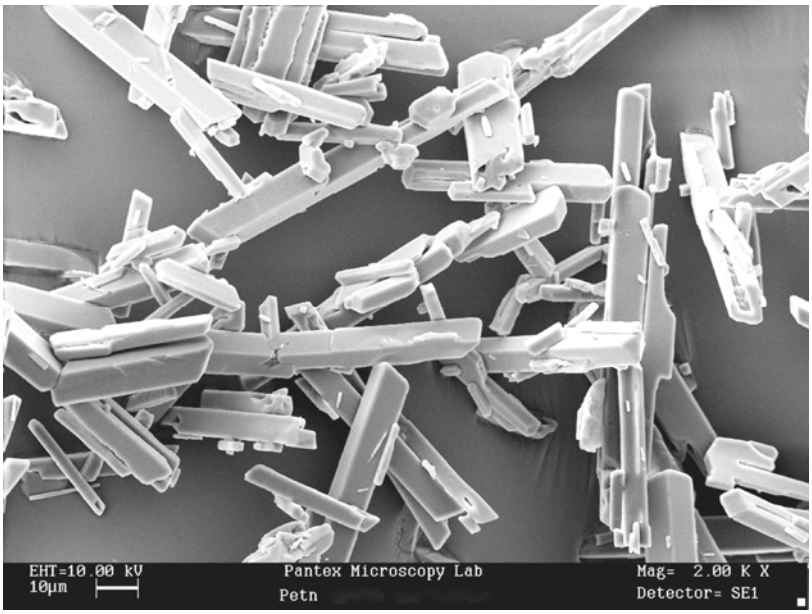

Figure 4.2-1 SEM Photomicrograph of Prismatic Sample A

Figure 4.2-2 SEM Photomicrograph of Prismatic Sample B

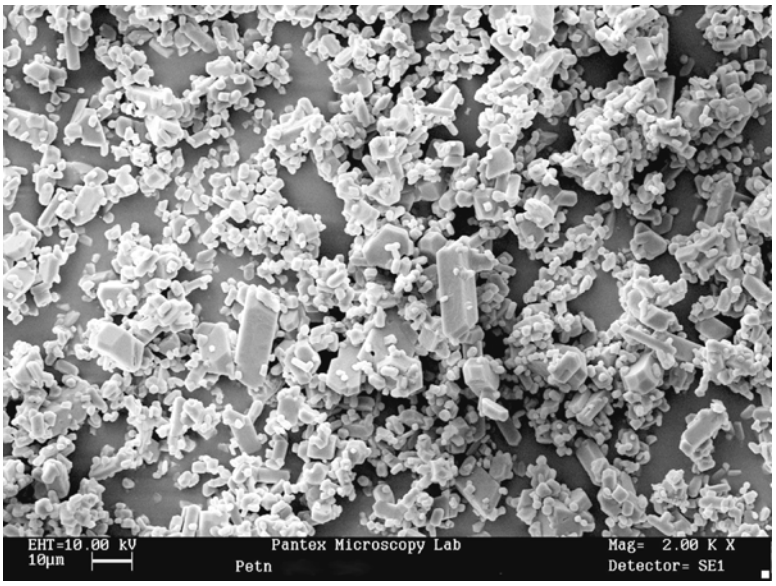

Figure 4.2-3 SEM Photomicrograph of Subhedral Equant Sample C

As seen in the micrographs, the general size of the PETN crystals ranges predominantly from the largest in Sample B to the smallest in Sample C. A distribution of particle sizes is clearly evident in Sample C, with many particles being on the order of a few microns, but with a few particle sizes on the order of 10 microns long and larger.

4.3 Particle Size Distribution Measurements

4.3.1 Initial Laboratory PSD Measurements

Each of the three laboratories measured the PSD of each sample using their respective standard light scattering method. The entire sample was introduced into the light scattering instrument flow using the small volume module and the particle sizes present during each counting interval were recorded for that counting interval. The software then sorted the data by size and determined the frequency with which each particle size was counted.

As expected, the PSD curves did not overlay each other, confirming that the three PETN powder samples had very different PSDs from each other. The mean particle sizes of each of the three powders were significantly different from each other at Pantex, which could be predicted based on the micrographs. However, the data for samples A and B at both SNL and LLNL did not show a large difference in mean particle size. In addition, the mean particle size for each sample varied substantially between laboratories. The precision demonstrated by each lab was acceptable, as judged by the SD between duplicate or triplicates runs. The SDs were generally less than ten percent of the measured mean particle sizes, with sample C providing the most variation which may be indicative of sample variability rather than laboratory precision. The mean particle sizes with the SDs measured by each laboratory are given in Table 4.3.1-1. The PSD graphs produced by each laboratory are given in the following sections.

Table 4.3.1-1 Standard Method Particle Size Measurements

PETN Sample	Lab	Mean Particle Size (μm)
Sample A	PANTEX	55.4 ± 1.9
	LLNL	27.1 ± 0.4
	SNL	22.1 ± 1.1
Sample B	Pantex	106.3 ± 1.5
	LLNL	29.5 ± 0.3
	SNL	22.6 ± 0.7
Sample C	Pantex	25.5 ± 1.3
	LLNL	9.1 ± 1.0
	SNL	13.2 ± 1.3

4.3.1.1 Pantex PSD Measurements

Pantex measured the particle size distribution of the three PETN powder samples on three separate aliquots of each of the PETN split samples. Aliquot 2 was measured twice, providing a duplicate measurement as an indication of the reproducibility of the measurement. The PSD data provided by Pantex included a volume percent PSD graph of the results for each sample run, but the only numerical data points included were for standard sieve sizes, rather than the more detailed raw data set. Therefore, digitization of scanned PSD curves provided by Pantex was necessary to input detailed numerical data points into a spreadsheet so that an average of the triplicate analyses for each sample could be calculated and graphed.

The average of the three aliquots for each PETN powder is presented in PSD graphs as cumulative and volume percent particle size distributions. The PSD for sample B appears to be broad and bimodal, whereas the PSD for sample C is much narrower. Figures 4.3.1.1-1 and 4.3.1.1-2 present these PSD graphs. The results also show that the mean particle size for Sample B was much greater than for samples A and C, and that the mean particle size of sample A was significantly larger than for sample C. No submicron-sized particles were measured by Pantex in any of the PETN samples.

4.3.1.2 LLNL PSD Measurements

LLNL measured the particle size distribution of the three PETN powder samples twice on two separate aliquots of each of the sample splits received, providing a duplicate measurement for every sample as an indication of reproducibility. For each PETN sample all four measurements were averaged to produce the mean value for that sample. The

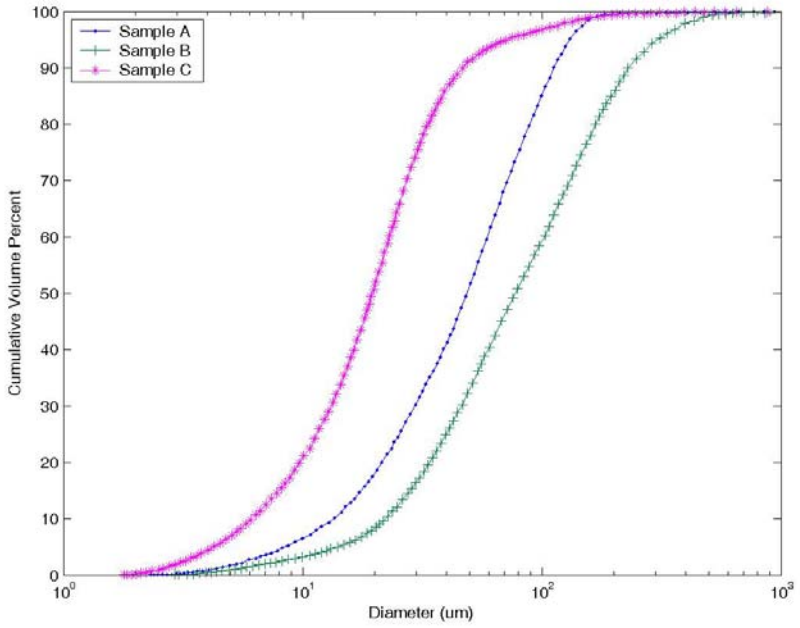

Figure 4.3.1.1-1 Pantex Cumulative Particle Size Distributions

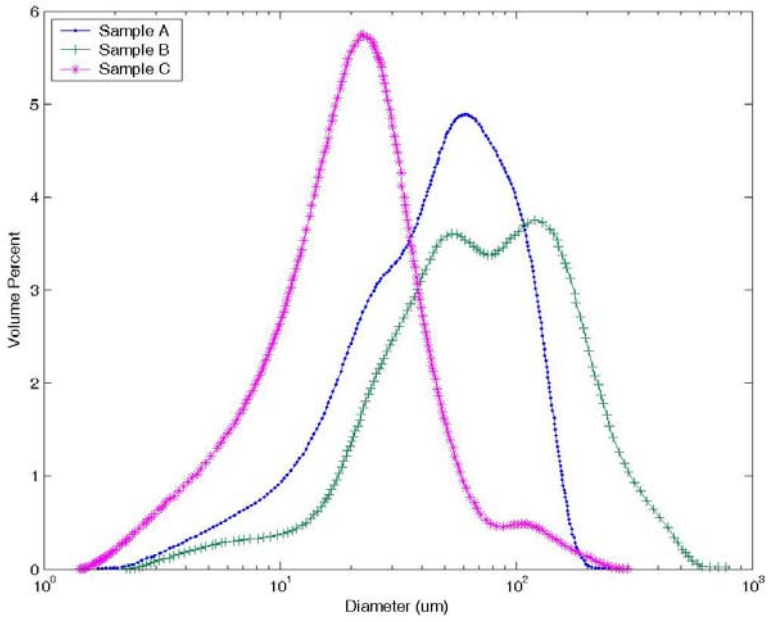

Figure 4.3.1.1-2 Pantex Particle Size Distributions

PSD for samples A and B were very similar. Both samples showed moderately broad bulk distributions and each showed a small but significant narrow peak in the submicron-size range. Sample C had a fairly narrowly defined bulk distribution and a small but very broadly distributed submicron-sized population of particles. These cumulative and volume percent PSD graphs are given in Figures 4.3.1.2-1 and 4.3.1.2-2.

The LLNL data indicates that approximately 1 percent in Sample B to as much as 8 percent in Sample C of the volume of each powder may be comprised of particles in the submicron-sized range. The mean size of these small particles was half a micron in sample C to just under 1 micron in sample B. The percentage of submicron-sized particles for each sample by volume and the mean diameter of submicron-sized particles for each PETN powder was calculated from the raw data provided by LLNL (Appendix B) and are summarized in Table 4.3.1.2-1.

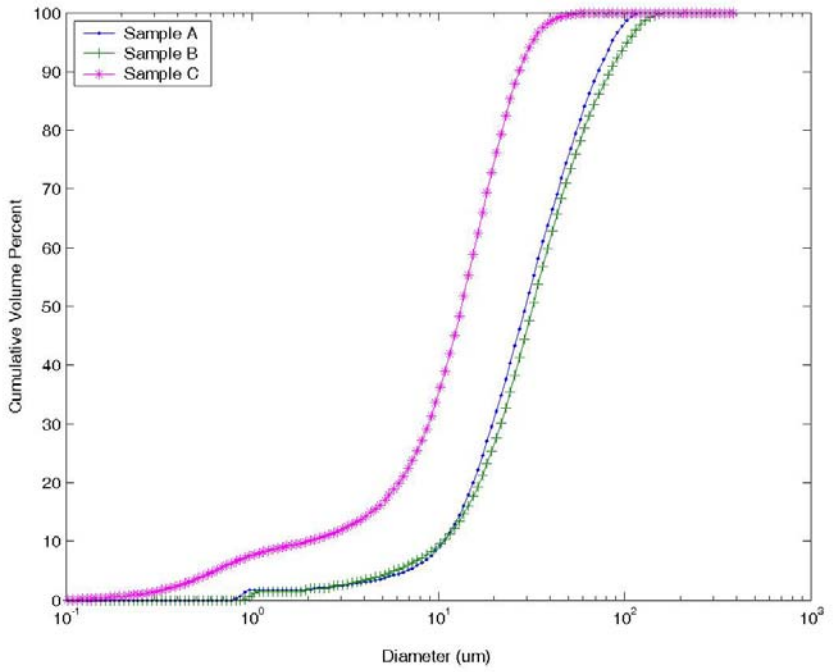

Figure 4.3.1.2-1 LLNL Cumulative Particle Size Distributions

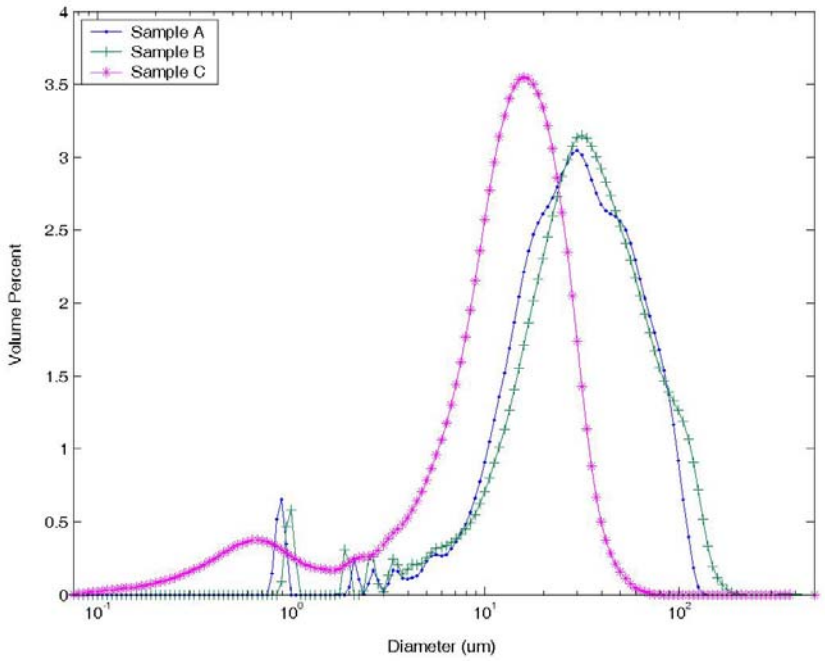

Figure 4. 3.1.2-2 LLNL Particle Size Distributions

Table 4.3.1.2-1 LLNL Submicron-Sized Particle Volume Percent and Diameter

	Sample A	Sample B	Sample C
Volume Percent of Submicron-Sized Particles	1.67	1.14	7.77
Mean Diameter of Submicron-Sized Particles (μm)	0.88	0.97	0.54

4.3.1.3 SNL PSD Measurements

SNL measured the particle size distribution of the three PETN powder samples on three separate aliquots of the sample splits. Both 15 and 35-micron garnet standard reference materials were analyzed before the PETN samples were run to demonstrate that the instrument was in control (Appendix C). The average of the three aliquot

measurements for each PETN powder plotted together as cumulative and volume percent particle size distributions show the distributions for samples A and B to be similar. Sample B had a slightly bimodal distribution due to the presence of a small knee on the smaller particle size side of the distribution curve. Sample C showed a fairly narrow distribution, skewed towards the larger particle sizes. Figures 4.3.1.3-1 and 4.3.1.3-2 display these distributions.

4.3.2 Subsequent SNL PSD Study Results

A subsequent study was conducted at SNL to understand the differences in the initial measurements performed by each laboratory and to assess the role of sonication and carrier fluid in the PSD measurements. Because the particle size results obtained

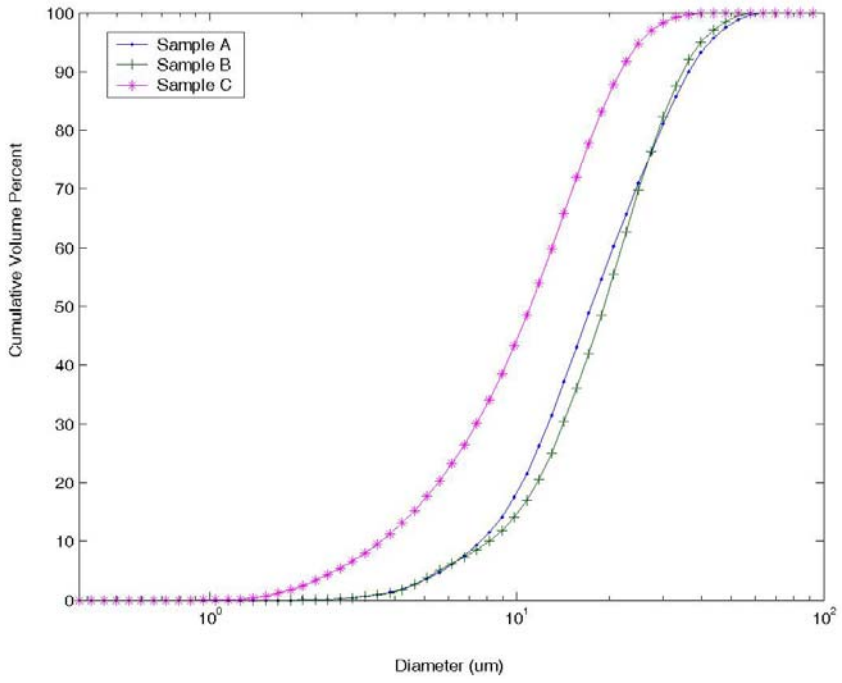

Figure 4.3.1.3-1 SNL Cumulative Particle Size Distributions

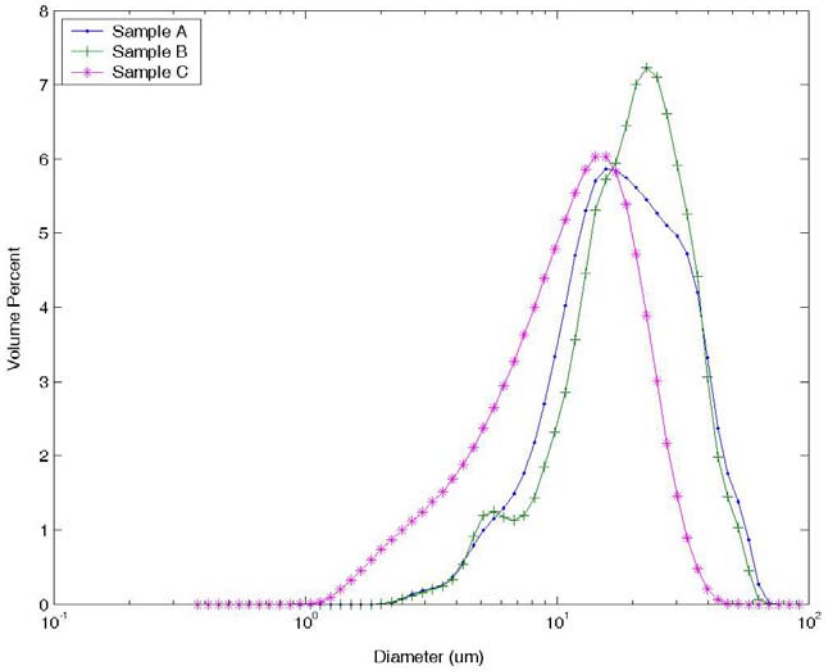

Figure 4.3.1.3-2 SNL Particle Size Distributions

from each laboratory using their own standard methods were dissimilar, the differences in the measurement process were examined. Instrument model and/or manufacturer, refractive index, operator, sonication time, and carrier fluid were found to be the primary differences between labs. This subsequent study at SNL sought to minimize the influence of these differences by using a single instrument and operator and by matching the sonication times and carrier fluids used at the other two laboratories. A single refractive index value was used. At the same time, the effects of sonication and carrier fluid on the mean particle size were studied by implementing the DOE described in Chapter 3 using these two parameters as the factors.

The mean particle size for each sample under each of the 12 sonication time and carrier fluid combinations were calculated, yielding 36 data points. The SDs for each

replicate measurement were generally within about 10 percent of the mean particles sizes measured, indicating adequate precision. A graphical presentation of these data points facilitated understanding of trends that may be present. Lines connecting individual data points provided easily observable relationships between the consistencies of each preparation condition relative to the others. From this, it can easily be seen that the mean particle size of all three PETN samples drops markedly when 30 seconds of sonication is applied to the suspension, regardless of carrier fluid. Although increasing sonication corresponds to decreasing mean particle size, the changes in particle size are not as great in subsequent sonication times as in the initial sonication.

It can also be seen that the type of carrier fluid does not have a consistent effect on mean particle size. For example, the use of water to suspend the PETN particles does not consistently give smaller or larger mean particle size results than the use of ethanol or 50% IPA. If this had been the case, the lines representing different carrier fluids for the same PETN sample would not cross each other on the graph. However, because the lines do cross for each PETN type from the 0 second to the 30 second sonication sample and between other sonication times, it indicates a lack of correlation between carrier fluid and mean particle size (Table 4.3.2-1, Figure 4.3.2-1).

Several of the individual PSD graphs show an unusual multi-modal distribution, similar to sonication study results obtained by Pantex. SNL responded by initiating repairs to the Coulter® internal stirring mechanism impeller. However, samples analyzed after this repair still exhibited this unusual distribution. The volume percent PSD graphs of the results for this subsequent study are given in Appendix D.

Table 4.3.2-1 Mean Particle Sizes Using Various Solvents and Sonication Times

Sample	A											
Carrier fluid	Water				IPA/water				Ethanol			
Sonic time (s)	0	30	60	180	0	30	60	180	0	30	60	180
Mean	68.5	27.0	23.5	20.3	58.8	22.1	18.7	18.2	48.2	18.9	16.8	14.8
SD	5.6	1.2	1.6	0.5	0.4	1.1	0.3	0.7	2.5	0.4	0.0	0.2
Sample	B											
Carrier fluid	Water				IPA/water				Ethanol			
Sonic time (s)	0	30	60	180	0	30	60	180	0	30	60	180
Mean	74.4	27.8	26.3	22.9	83.5	22.6	19.4	17.9	71.8	23.8	22.3	18.8
SD	6.0	0.2	0.8	0.7	1.1	0.7	0.4	0.1	3.5	0.4	0.3	0.7
Sample	C											
Carrier fluid	Water				IPA/water				Ethanol			
Sonic time (s)	0	30	60	180	0	30	60	180	0	30	60	180
Mean	27.6	10.7	9.3	7.4	25.9	13.2	12.0	9.8	22.8	12.2	11.3	10.5
SD	3.0	1.2	0.5	0.2	0.1	1.3	1.4	0.3	0.3	0.2	0.1	0.1

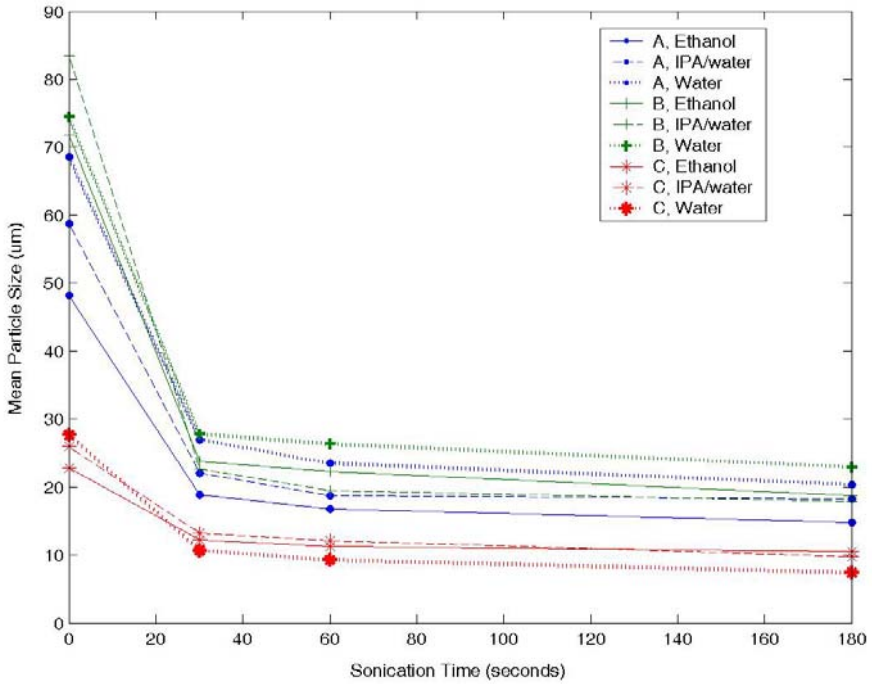

Figure 4.3.2-1 Mean Particle Size For All Fluids and Sonication Times

These graphical observations are supported by analysis of a factorial DOE using Minitab® software, release 14 (Minitab Inc., State College, PA) with mean particle size as the response. The results of this statistical treatment were evaluated using a main effects plot to determine whether each factor had a strong effect on the mean particle size. The main effects plots for all three PETN samples in this study portray very steep lines for the sonication time factor, indicating a strong effect on the mean particle size, while the opposite is true for the percent of alcohol.

Quantitation of the influence of each factor was also performed during the statistical analysis and indicated that the sonication time factor was significant for samples A and C at a 95% confidence level and for sample B at a 94% confidence level. This is based on the fact that the P-value for samples A and C were below 0.05, the alpha value that corresponds to a 95% confidence level and that the P-value for sample B was less than 0.06, which corresponds to a 94% confidence level. This same analysis indicated that neither the percent alcohol nor the combination of the sonication time and percent alcohol had a significant effect on the mean particle size measured (Table 4.3.2-2). See Appendix E for more detailed statistical calculations and information.

4.3.3 Standard Reference Material Measurements

Although a few submicron-sized particles can be seen in some PETN sample micrographs, subjective evaluations of these images have been largely inconclusive due to the difficulty in visually estimating whether the approximate volume percentages of

Table 4.3.2-2 Fractional Factorial Fit Table of P-Values

Sample	Factor	P-Value
A	Sonication Time	0.046
	Percent Alcohol	0.476
	Sonication Time * Percent Alcohol	0.728
B	Sonication Time	0.055
	Percent Alcohol	0.828
	Sonication Time * Percent Alcohol	0.981
C	Sonication Time	0.032
	Percent Alcohol	0.796
	Sonication Time * Percent Alcohol	0.612

small particles indicated by the LLNL light scattering data can be seen in the micro-graphs. Therefore, two standard reference materials were measured at SNL and LLNL.

It is apparent from the resulting data that the SNL Coulter® instrument was able to reasonably measure the ideal spherical particles present in the <2 micron range, albeit slightly low for the 1.23 micron standard, whereas the Micromeritics® instrument encountered some difficulty with accurate measurement of the standard reference materials. Two peaks were measured at LLNL for the 1.23 micron material, one at approximately 1.2 microns and another peak approximately 0.75 microns. Only one peak was measured for the 0.48 micron standard at LLNL and it was centered around 0.12 microns, much smaller than the particle size of the reference material (Figures 4.3.3-1 through 4.3.3-4). It become obvious from this data that the LLNL measurements for all materials in these small particle sizes should be considered suspect until such as time as the instrument demonstrates the capability to accurately measure particles in this size range. It is not clear from this data whether the instrument is prone to detecting “ghosts” or if there is another instrument-specific issue that must be addressed by the manufacturer’s representative.

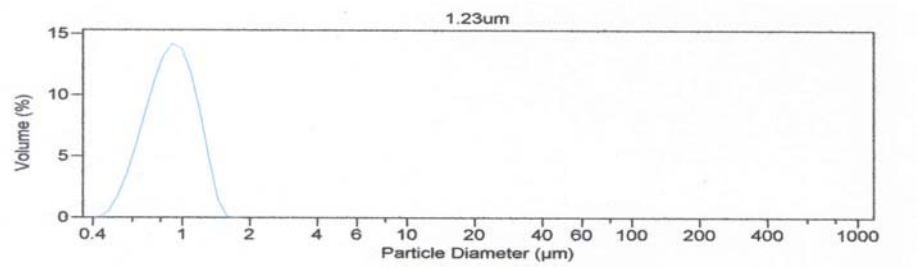

Figure 4.3.3-1 SNL Measurement of 1.23 µm Standard

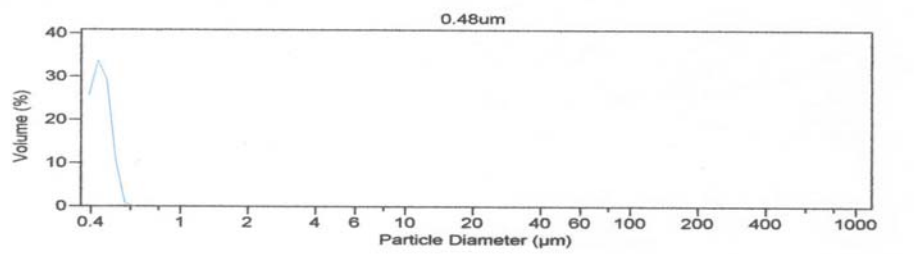

Figure 4.3.3-2 SNL Measurement of 0.48 µm Standard

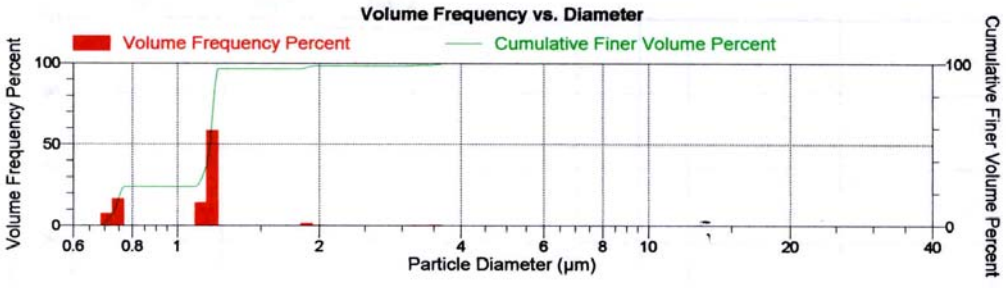

Figure 4.3.3-3 LLNL Measurement of 1.23 µm Standard

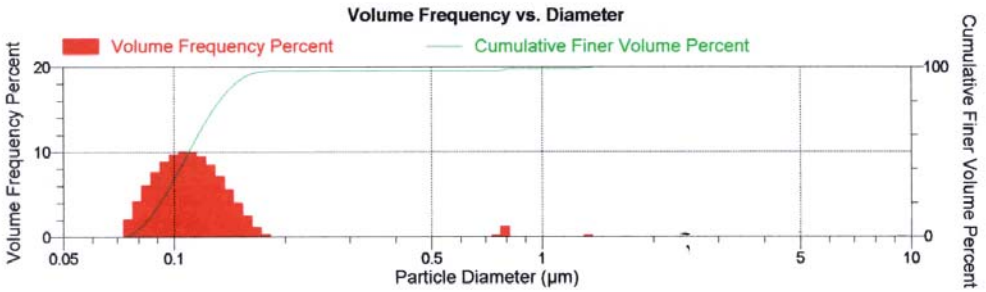

Figure 4.3.3-4 LLNL Measurement of 0.48 µm Standard

What is not obvious from the mean particle size data is whether the presence of submicron-sized particles depends on the carrier fluid used. The hypothesis that the use of alcohol as a carrier fluid dissolved submicron-sized particles was able to be evaluated from the results of this study. Because the SNL instrument was able to detect and measure the 0.48 μm and 1.23 μm standard reference materials with reasonable accuracy, submicron-sized PETN should have been detected and measured, if present, when water was used as the carrier fluid, but no submicron-sized particles were measured in these samples. This leads to the rejection of this hypothesis.

However, with increasing sonication time the mean particle size decreases and if this trend were extrapolated, logic dictates that submicron-sized particles should be created if sonication were continued for a sufficient duration. The question then becomes one of whether LLNL sonication at 180 seconds was of a sufficient duration to create submicron-sized particles. To answer this, it is of interest that the SNL data bracketed the mean particle sizes measured at LLNL, and in fact included sonication times that produced even smaller mean particle sizes, but no submicron-sized particles were measured at SNL even at the longest sonication times using any of the three carrier fluids.

Because the submicron-sized particles in the LLNL data do not seem to be created by the sonication process and are not preserved from the original powder by the use of water instead of alcohols as a carrier fluid in PSD measurements, this leaves the instrument-specific parameters as a variable in the LLNL PETN data that have not been specifically investigated. This is consistent with the data obtained by measuring the standard reference materials.

4.4 Data Validation

The general disagreement between the initial bulk PSDs measured at each laboratory for these samples was not entirely unexpected because previous measurements have shown some discrepancies. However, the degree of differences and the sources of the discrepancy in the PSD measurements have not been previously recognized and it is the goal of this study to benchmark the measurements and understand the differences.

4.4.1 Comparison of Initial Laboratory PSD Measurements

To compare these data for each PETN type, the results from each laboratory for samples A, B, and C were graphed together. This graphical comparison of the entire distribution data set shows that there is somewhat poor correlation between PSD measurements from one laboratory to another using their respective standard methods. It became obvious that the LLNL submicron-sized particles were not detected by either of the other laboratories. In addition, it is clear that the SNL data show a much greater volume percent of the principle particle sizes for samples A and B, as compared to the other two laboratories; the SNL volume percent peak for these two samples is much taller than the other two laboratories and since the area under each peak adds up to 100%, the distribution measured by SNL must be much narrower than the other two laboratories. Although both SNL and Pantex measured a somewhat bi-modal distribution for sample B, it is clear that these distribution curves do not overlay well. The distributions for sample C from each laboratory overlay much better, for the majority of the distribution, than the other two samples (Figures 4.4.1-1 through 4.4.1-6).

The mean particle sizes for each PETN sample measured by each laboratory were clearly very different from each other and so a two-sample t-test was not performed on these data to determine if they were the same. Rather, beginning with the fact of their difference, the magnitude of the differences were compared by calculating the RPD between the mean particle sizes measured at SNL versus the other laboratories. This calculation indicated that the differences between the means measured at each laboratory were large; the closest being only within 20 RPD and the most dissimilar was found to be 78 RPD.

The PSD measurement for the three PETN powder samples in the submicron range also showed poor agreement between laboratories. The results from Pantex and SNL suggest that virtually no submicron-sized particles exist in any of the three PETN powders. Although LLNL recorded submicron-sized particles in every sample, these

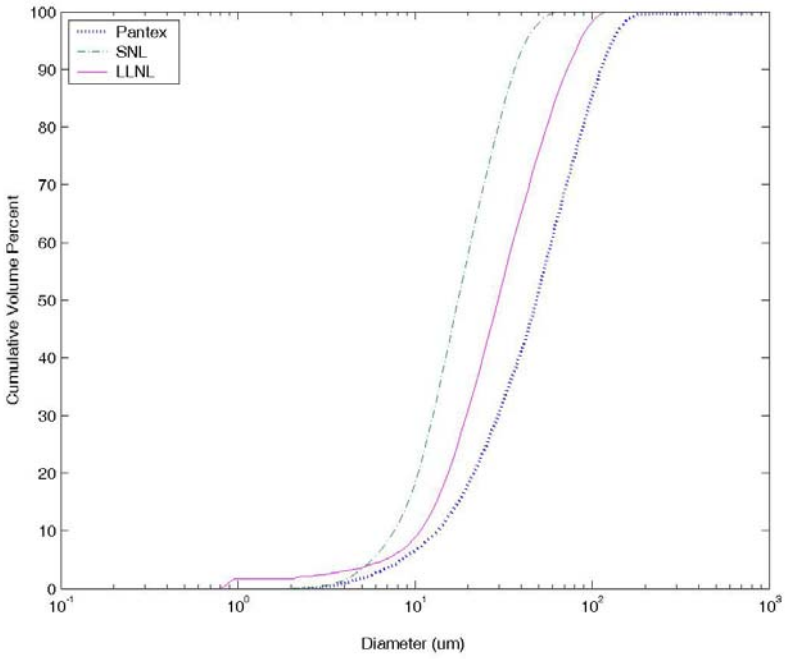

Figure 4.4.1-1 Sample A Cumulative PSD for Pantex, SNL, and LLNL

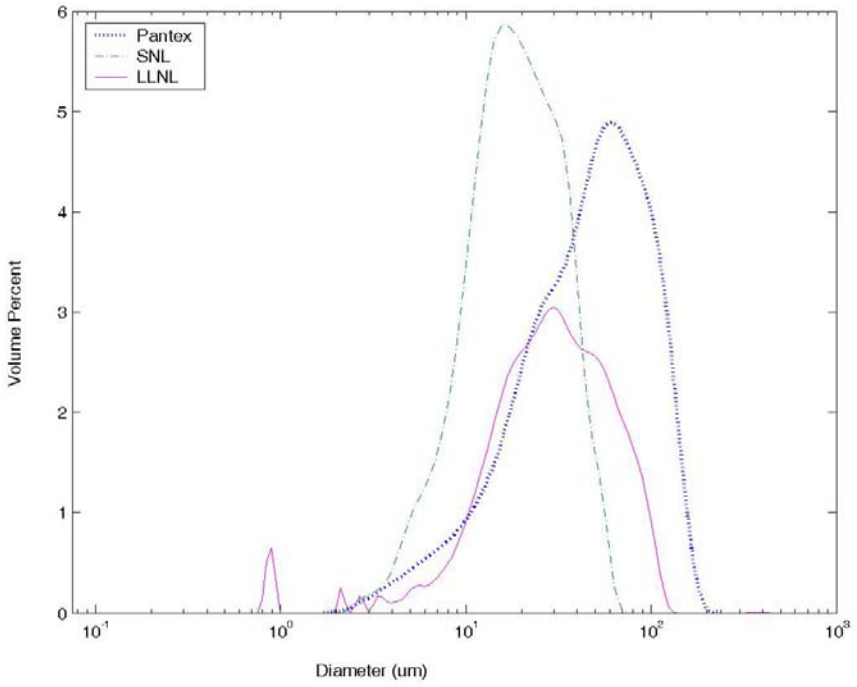

Figure 4.4.1-2 Sample A PSD for Pantex, SNL, and LLNL

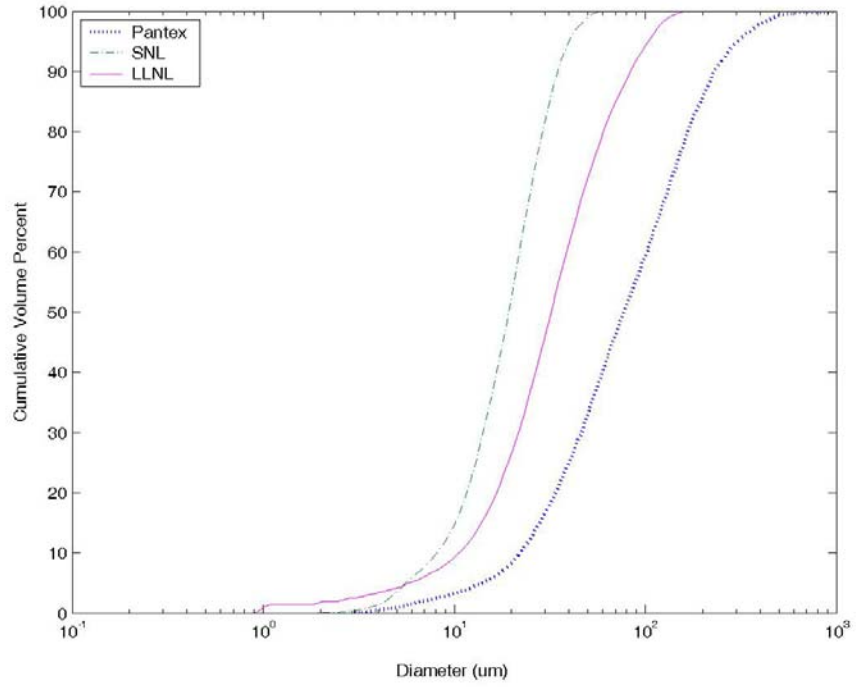

Figure 4.4.1-3 Sample B Cumulative PSD for Pantex, SNL, and LLNL

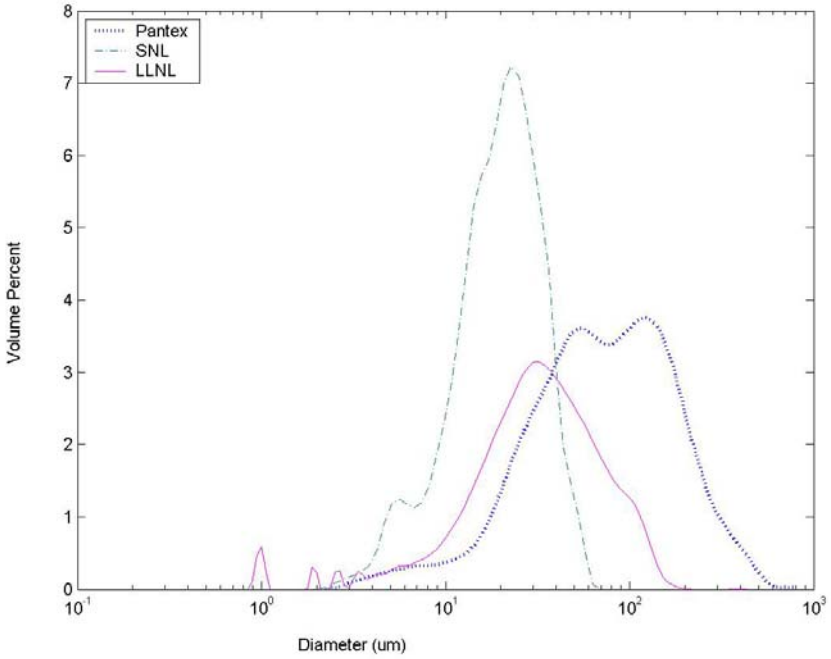

Figure 4.4.1-4 Sample B PSD for Pantex, SNL, and LLNL

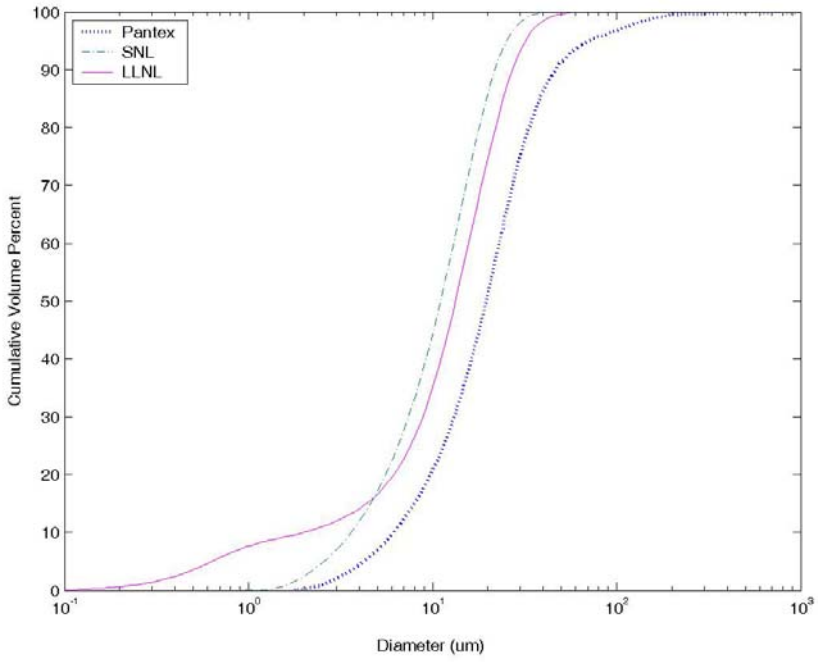

Figure 4.4.1-5 Sample C Cumulative PSD for Pantex, SNL, and LLNL

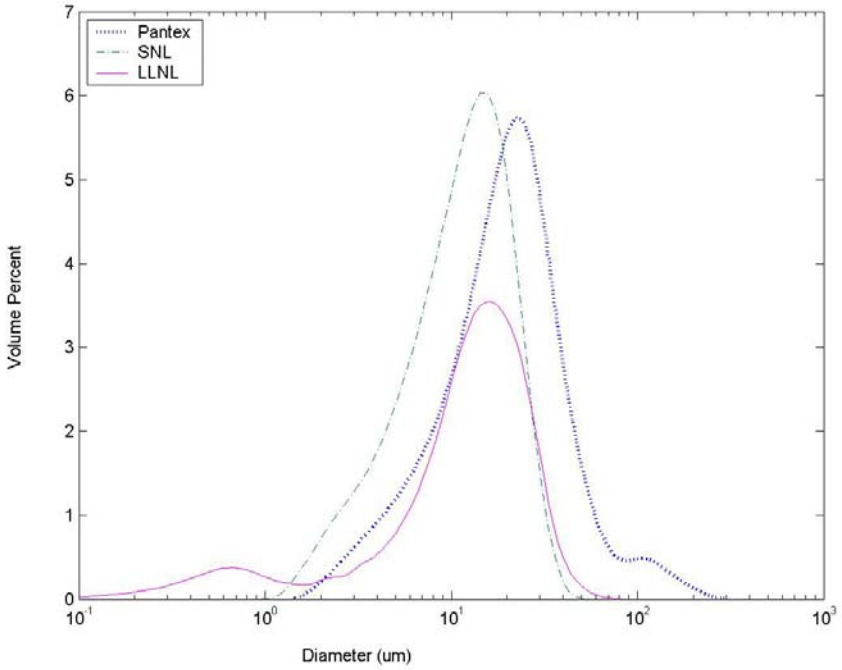

Figure 4.4.1-6 Sample C PSD for Pantex, SNL, and LLNL

submicron-sized measurements are suspect, as described previously (Section 4.3.3). Although measurement in the submicron-sized range is suspect, there is no indication that LLNL measurement in the larger sizes lacks accuracy.

4.4.2 Comparison of Subsequent SNL PSD Measurements

The mean particle size data obtained at SNL by mimicking the standard methods used at the other two laboratories was found to be much closer to the values obtained by the other labs than the original data collected using each laboratory's standard preparation methods. Plotting the original mean particle size data from the three laboratories next to the subsequent SNL data corresponding to the methods used at the other two laboratories on a bar graph gives a visual indication that the use of similar methods results in a better match of the mean particle sizes. Each lab originally measured a greater mean particle

size than SNL, except LLNL for sample C, which was lower. In every case, the mean particle sizes found using the SNL matching method were closer to the other laboratory data than the original SNL method (Figure 4.4.2-1).

To determine whether SNL was able to accurately reproduce the mean particle sizes measured by Pantex and LLNL, a two-sample t-test was applied to the data. This statistical test to determine the variance between means indicated that there was no difference between the SNL and LLNL Sample A and C means with a 95% confidence level. While SNL was able to reproduce the LLNL mean particle size measurements for Samples A and C, the sample B mean was not able to be duplicated, nor were any of the means measured by Pantex within even a 50% confidence level (Appendix E).

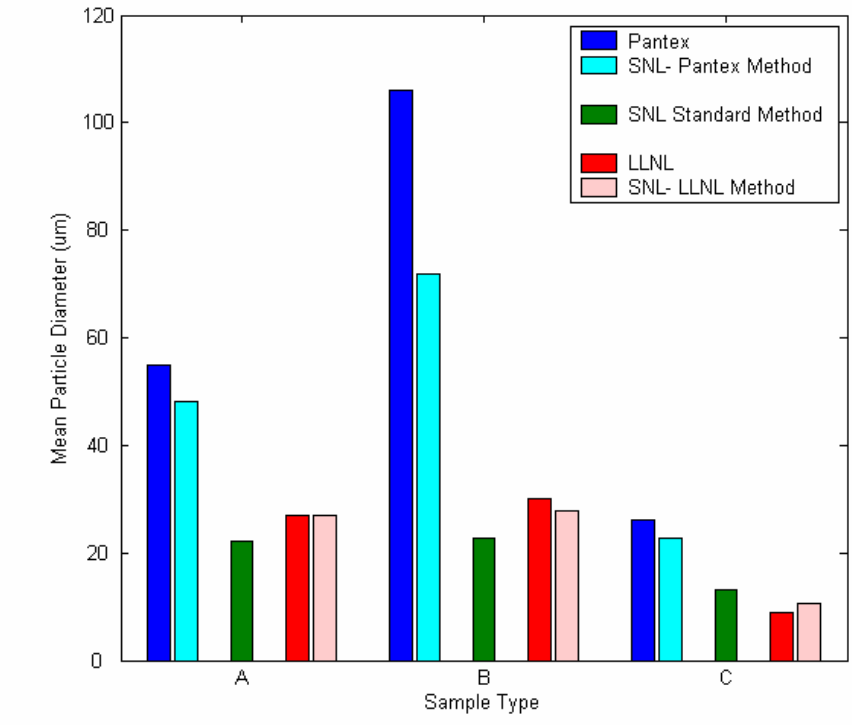

Figure 4.4.2-1 SNL Data Corresponding to Other Laboratory Methods

Once it was ascertained that most of the mean particle size values were statistically different from each other, the RPD value was used to quantify how different the values were from each other. This RPD calculation indicated that the mean particle sizes between SNL and LLNL went from as much as 20% to as close as 5% relative difference. Similarly, the SNL mean particle sizes approached those obtained by Pantex, as evidenced by the fact that RPD changed from as much as 78% difference in the original data sets to as little as 10% in the data obtained using a similar preparation method (Tables 4.4.2-1 and 4.4.2-2). This analysis demonstrates that the preparation method has a great effect on mean particle size measured and that measured mean particle sizes can be approached by mimicking the preparation method used. This suggests that although sonication may have a significant influence on mean particle size, other factors were responsible for some degree of variation in the measurements.

Table 4.4.2-1 RPD Between Initial and Subsequent SNL and LLNL Data

	Initial RPD	**Subsequent RPD**
Sample A	**13.1%**	**-5.2%**
Sample B	**20.1%**	**2.4%**
Sample C	**-17.7%**	**7.6%**

Table 4.4.2-2 RPD Between Initial and Subsequent SNL and Pantex Data

	Initial RPD	**Subsequent RPD**
Sample A	**57.55%**	**9.6%**
Sample B	**77.9%**	**31.4%**
Sample C	**55.9%**	**20.4%**

Earlier, in section 4.3.2, it was noted via the results of a DOE that carrier fluid did not have a great effect on the mean particle size. Therefore, the primary influence on SNL's ability to alter the measured mean particle size of a sample such that it approached other laboratory's mean particle sizes is sonication. Variations in sonication between laboratories include not just length of time, but also the wattage of the ultrasonic bath and physical configuration of the samples during sonication. As noted in chapter 3, LLNL used a bench top ultrasonic bath rated at 130 watts while SNL's was 180 watts.

However, the samples were configured differently inside the baths at these two laboratories. SNL placed the suspended samples in a single glass beaker in the bath, while LLNL placed them in a small polymer vial weighted down inside a larger polymer beaker that contained a small amount of water. This larger beaker was placed into the water in the bath. The effects of these wattage differences and possible attenuation from the double packaging configuration can be assessed by noticing that the LLNL data are closest to the SNL 30 second data, even though LLNL sonicated for 180 seconds (Table 4.4.2-3). This is a clear indication that the combination of the lower wattage and the use of double beakers attenuated the energy received by the samples as compared to SNL sonication.

Table 4.4.2-3 Comparison of SNL PSD Data Using Water to LLNL Data

	SNL 30 second	**SNL 60 second**	**SNL 180 second**	**LLNL 180 second**
Sample A	27	24	20	27
Sample B	28	26	23	30
Sample C	11	9	7	9

The final question raised by the results of this study was to understand what physical changes occurred to the PETN in suspension as ultrasonic energy was applied. It was seen that a dramatic change in the mean particle sizes resulted from the initial 30 second sonication of the samples. Investigations were conducted at Pantex by observing multiple types of explosives particles, including PETN in suspension after various amounts of sonication using optical microscopy techniques.

These studies indicate that increasing the sonication time and/or wattage of the ultrasonic bath used may have two effects on the PETN samples. First, sonication of Sample B PETN particles in suspension were seen to damage the crystals, causing the mean particle size to decrease with increasing sonication time. This apparent breakage of particles noted by Pantex was more pronounced for PETN particles with a prismatic crystal habit [76] (Figure 4.4.2-2 through 4.4.2-4).

Second, sonication of Sample C PETN particles in suspension was seen to disaggregate the PETN particles upon initial sonication. Continued sonication, however, appeared to cause breakage of even these less delicate particles based on the optical microscopy evidence (Figure 4.4.2-5 through 4.4.2-7). Therefore, the effects of sonication on the PETN samples varied, depending on the morphology of the particles.

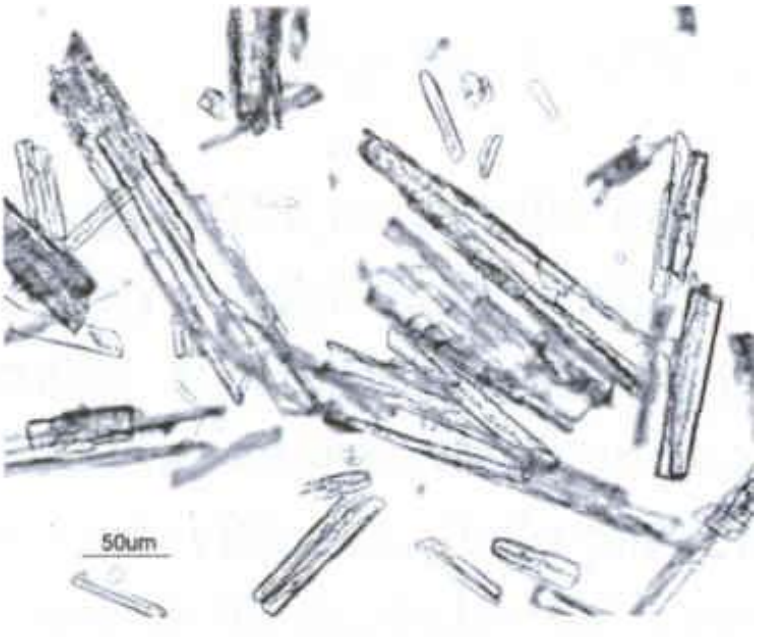

Figure 4.4.2-2 Optical Microscopy of Prismatic Sample B With No Sonication

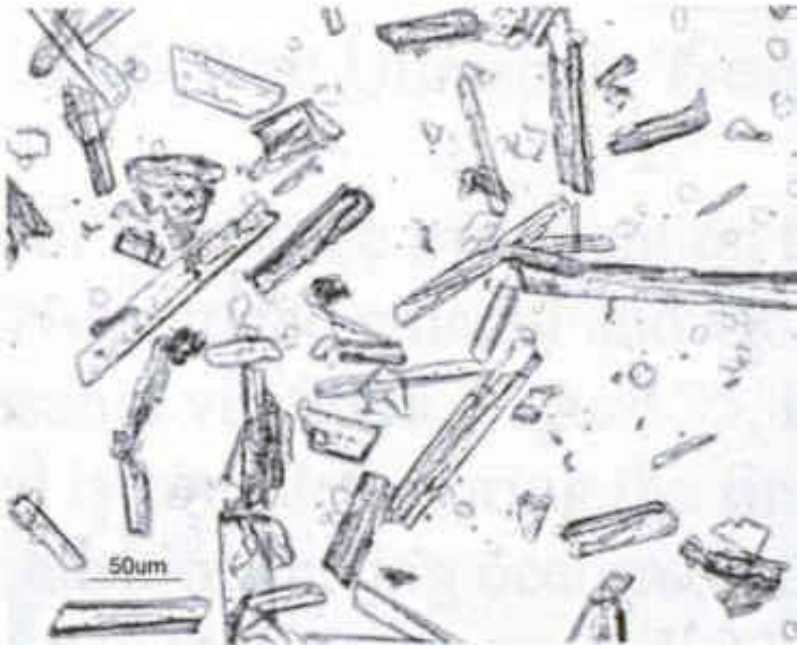

Figure 4.4.2-3 Optical Microscopy of Prismatic Sample B With 1 Minute Sonication

Figure 4.4.2-4 Optical Microscopy of Prismatic Sample B With 3 Minute Sonication

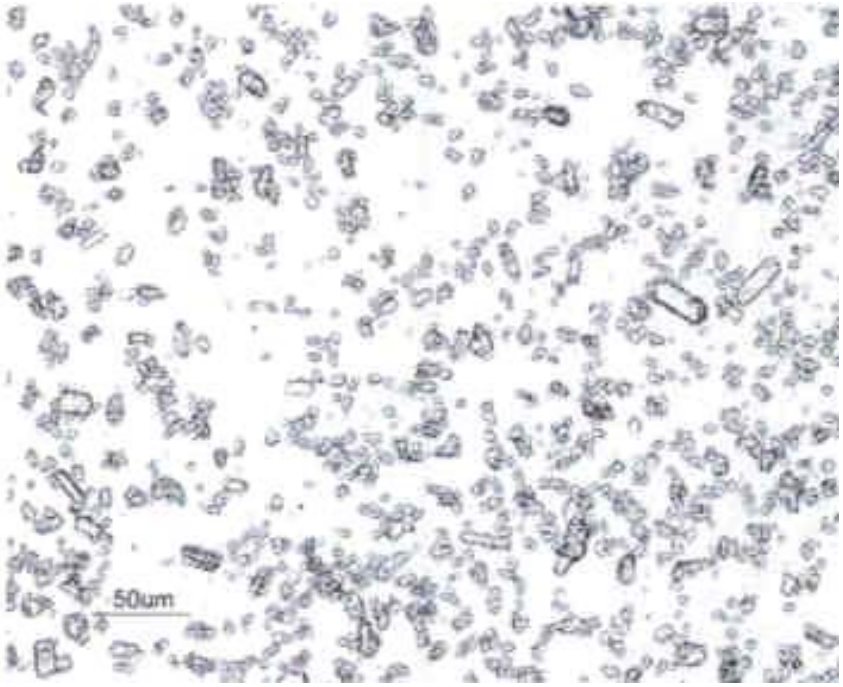

Figure 4.4.2-5 Optical Microscopy of Equant Sample C With No Sonication

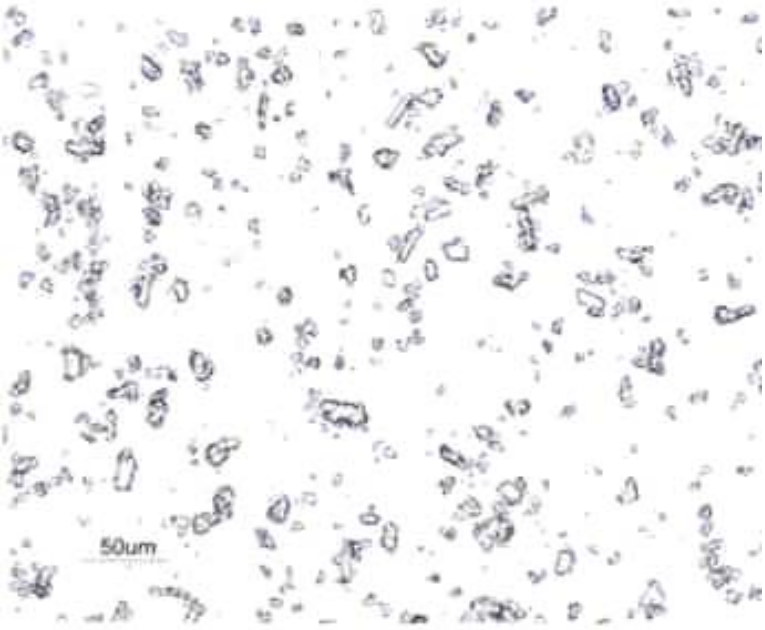

Figure 4.4.2-6 Optical Microscopy of Equant Sample C With 1 Minute Sonication

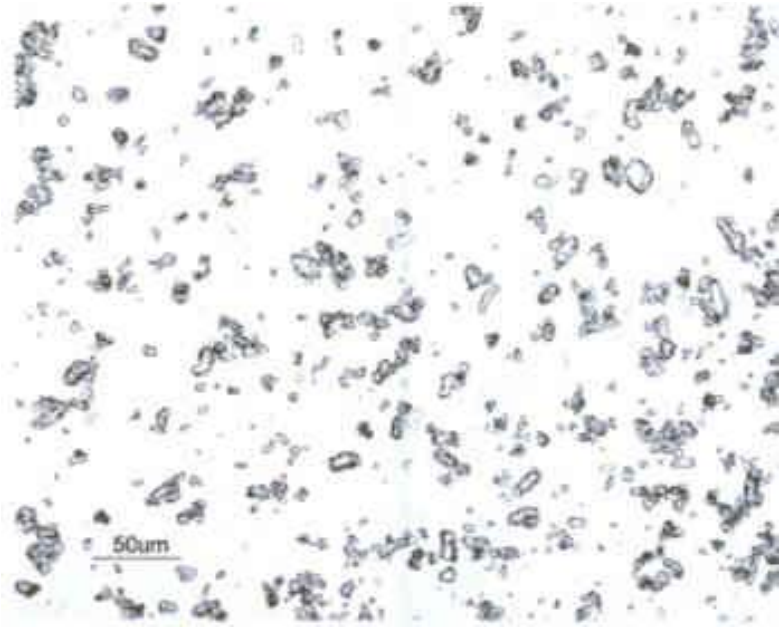

Figure 4.4.2-7 Optical Microscopy of Equant Sample C With 3 Minute Sonication

CHAPTER 5
CONCLUSIONS

- Although there is not good general agreement between laboratories regarding PETN PSDs measured by light scattering instruments, the particle sizes of three PETN powders have been measured, benchmarked against the Pantex SSA measurement, and can be approached by mimicking the standard preparation methods used at each laboratory.
- These PETN samples do not contain submicron-sized PETN particles, and submicron-sized particles are not produced with increasing sonication.
- The choice of carrier fluid has no consistent effect on the mean particle size or on the presence of submicron-sized PETN particles.
- A large change occurs in PETN particle size distributions, when samples are subjected to even a small amount of sonication.
- Sonication was seen to enhance the dispersion of equant particles but may induce breakage of other particles, especially delicate prismatic particles.
- Selecting the best method when measuring PETN particle size distributions may depend on particle morphology.

CHAPTER 6
FUTURE WORK

- Measurement of the 0.48 and 1.23 micron particle size standards by Pantex should be performed to document the instrument's measurement capability in this range using Pantex's standard sample preparation method.
- PETN suspensions that resulted in distinctive multi-modal particle size distributions should be evaluated to identify what mechanism is responsible for the unusual distributions.
- Optical microscopy of sonicated PETN particle suspensions in various carrier fluids should be performed at SNL to verify trends in dispersion and breakage noticed at Pantex and to discern what instantaneous changes occur in the PETN particles upon initial sonication.
- Image analysis on optical and SEM photomicrographs should be conducted to quantify the volume percent of submicron-sized particles in the images and to collect orthogonal length and width information about PETN particles so that this can be related to particle diameter measurements reported by light scattering instruments.
- Studies should be undertaken to understand why the BET SSA measurements of Samples A and B performed after compaction of samples in the FSSS tube decreased, rather than increased, as would be expected.

CHAPTER 7
REFERENCES

1. Rogers, J.W., and A. A. Duncan, *Effects of Particle Characteristics on Performance of RR5K PETN*, Albuquerque, NM: Sandia National Laboratories/New Mexico; 1981. SAND81-2199. Available from NTIS, Springfield, VA.

2. Dinegar, R.H., *The Effect of Heat on PETN*, Proceedings of the 3rd International Conference of Groupe de Travail de Pyrotechnie, Juan-Lespin, France, Assoc. Francaise de Pyrotechnie, Paris. 1989.

3. Cady, H.H., *The PETN-DiPEHN-Tri-PEON System*, Los Alamos, NM.: University of California; 1972. LA-4486-MS. Available from NTIS, Springfield, VA.

4. Watson, S., M.J. Gifford and J.E. Field, *The Initiation of Fine Grain Pentaerythritol Tetranitrate By Laser-driven Flyer Plates.* JAP 2000.; **88**(1):p. 65–69.

5. Gifford, M.J., P.E. Luebcke, and J.E. Field, *A Mechanism for the Deflagration-to-Detonation Transition in Ultrafine Granular Explosives*, CP505 In: M.D. Furnish, L.C. Chhabildas and R.S. Hixson, editors. *Shock Compression of Condensed Matter*. American Institute of Physics; 1999. p. 845–848.

6. Cooper, P.W., S.R. Kurowski, and B.A. Tuttle, *Introduction to the Technology of Explosives*. New York, NY: Wiley-VCH, Inc.; 1996. 204 p.

7. Duncan, A. *Previous PETN Characterization*, personal communication, BWXT Pantex, Amarillo, Texas, December 2004.

8 . Moore, Melissa, *Results of Previous Studies*, personal communication, BWXT Pantex, Amarillo, Texas, December 2004.

9 . Lewis, Pat, "*Results of PETN PSD Analysis*", personal communication, Lawrence Livermore National Laboratory, Livermore, CA, December 2004.

10. Chambers, David M., Claudia L. Brackett and O. David Sparkman, Perspectives on Pentaerythritol Tetranitrate (PETN) Decomposition. Livermore CA: Lawrence Livermore National Laboratory; 2005. URCL-ID-148956.

11. Cooper, P.W., *Explosives Engineering*. New York, NY: Wiley-VCH, Inc.; 1996. 460 p.

12 . Pacific Scientific, *A Glossary of Pyrotechnic and Explosive Terminology*. 2005. available at http://www.psemc.com/references.asp.

13. Davis, Tenney L., *The Chemistry of Powder and Explosives.* New York: Wiley. 1966. 500 p.

14. Zaoui, A. and W. Sekkal, *Molecular Dynamics Study of Mechanical and Thermodynamic Properties of Pentaerythritol Tetranitrate,* Solid State Communications, 2001. **118**: p. 345-350.

15 . Dobrats, B.M. and P.C. Crawford, *LLNL Explosives Handbook: Properties of Explosives and Explosive Simulants*. Livermore, CA.: University of California; 1985. p. 19–126.

16. Rudolph, Meyer, *Explosives.*, 2nd ed. New York: Verlag Chemic; 1981. p. 263.

17 . Amethyst Galleries, "Descriptive Crystal Habits", Amethyst Galleries, Inc. 1996. Available at: http://mineral.galleries.com/minerals/habits.htm#prismati.

18 . Duncan, A., *Recent Work at Pantex*, personal communication, BWXT Pantex, Amarillo, Texas, October 2005.

19. Tarver, Craig M, Tri D. Tran and Richard E. Whipple, *Thermal Decomposition of Pentaerythritol Tetranitrate*. Propellants, Explosives, Pyrotechnics, 2003. **28**(4): p. 189-193.

20. Windholz, M., *The Merck Index,* 10th ed. M. Windholz (ed), Merck & Co., Rahway, N.J.; 1983. p.1022.

21. Rosenblatt, D.H., E.P. Burrows, W.R. Mitchell, and D.L. Parmer, *Organic Explosives and Related Compounds*. In: Hutzinger, O., editor. *The Handbook of Environmental Chemistry, 3(G)*, Springer-Verlag, New York, NY. 1991.

22 . Cates, Monty, "*Solubility of explosives in various solvents*". personal communication, BWXT Pantex, Amarillo, TX, March 2005.

23 . Kaye, Seymour M., *Encyclopedia of Explosives and Related Items*, PATR 2700, Volume 8, Dover NJ: US Army Armament Research and Development Command, Large Caliber Weapons Systems Laboratory, 1978. p. P86-P120.

24. Jillavenkatesa, A., S.J. Dapkunas and L-S Lum, *Particle Size Characterization,* National Institute of Standards and Technology (NIST) Special Publication 960-1, U.S. Government Printing Office, Washington, D.C. 2001. 165 p.

25. American Society for Testing and Materials, *Standard Practice for Sampling Ceramic Whiteware Clays*, C322-03, ASTM International, West Conshohocken, PA; 2003.

26. American Society for Testing and Materials, *Standard Practice for Carbon Black—Sampling Bulk Shipments*, D1900-94(2002), ASTM International, West Conshohocken, PA; 2002.

27. American Society for Testing and Materials, *Standard Practice for Reducing Samples of Aggregate to Testing Size*, C702-98(2003), ASTM International, West Conshohocken, PA; 2003.

28. American Society for Testing and Materials, *Standard Practice for Sampling Metal Powders*, B215-04, ASTM International, West Conshohocken, PA; 2004.

29. American Society for Testing and Materials, *Standard Guide for Composite Sampling and Field Subsampling for Environmental Waste Management Activities*, D6051-96(2001), ASTM International, West Conshohocken, PA; 2001.

30. American Society for Testing and Materials, *Standard Guide for Laboratory Subsampling of Media Related to Waste Management Activities*, D6323-98(2003), ASTM International, West Conshohocken, PA; 2003.

31. ISO, *Sample preparation—Sampling and sample splitting of particulate materials for the characterization of particulate properties.* 2005. Available at http://www.iso.ch/iso/en/CatalogueDetailPage.CatalogueDetail?CSNUMBER=39988&scopelist=PROGRAMME.

32. Beddow, J.K., Size, Shape, and Texture Analysis, In: Provder, Theodore, editor. *Particle Size Distribution: Assessment and Characterization*, Washington, D.C.: American Chemical Society; 1987. p. 2–29.

33. Plantz, P.E., Particle Size Measurements From 0.1 to 1000 μm Based on Light Scattering and Diffraction, In: Barth, Howard G., editor. *Modern Methods of Particle Size Analysis*, New York, NY: John Wiley and Sons, Inc.; 1984. p. 173-209.

34. Gray, W.A., *The Packing of Solid Particles*. London: Chapman and Hall, Ltd.; 1968. 134 p.

35 . Fisher Scientific, FSSS Method Manual, 2005. Available at http://www.fisherlabequipment.com/sizer.htm.

36. Stanley, H., and T. Thornton, *What is "BET Surface Area" and How Does It Affect the Performance of a Battery?*. Norcross, GA: Micromeritics Instrument Corporation; 2002. pp. 93–95.

37. Horiba Lab, BET surface Area Measurement. Available at http://www.Horibalab.com/techniques/gas.html .

38. Mansell, J., *JOWOG-9 Information Exchange*, personal communication, Atomic Weapons Establishment, UK, February 9, 2005.

39 . Lowell, S. and Joan E. Shields, *Powder Surface Area and Porosity*. 2nd ed. London: Chapman and Hall; 1984. 234 p.

40. Allen, T., *Particle Size Measurement*. 3rd ed., London: Chapman and Hall, Ltd.; 1981. 678 p.

41. Davidson, D.L., *The Analysis of Particles by Electron Microscopy and Spectroscopy*. In: Beddow, John Keith, editor. *Particle Characterization in Technology, vol.1. Applications and Microanalysis*, Boca Raton, FL: CRC Press; 1984. p. 59-65.

42. Veale, C.R., *Fine Powders: Preparation, Properties and Uses,* New York, NY: John Wiley and Sons; 1972. 147 p.

43. Ferraris, Chiarra F., Vincent A. Hackley, Ana Ivelisse Aviles, and Charles E. Buchannan, Jr., *Analysis of the ASTM Round-Robin Test on Particle Size Distribution of Portland Cement: Phase I*, Washington, DC: United States Department of Commerce; 2002. NISTIT 6883.

44. Wyatt Technology Corporation, *The Ultimate Guide to Buying a Light Scattering Instrument*. Santa Barbara, CA: Wyatt Technology Corporation; 2002. 26 p.

45. Wyatt, P.J., *Light Scattering and the Solution Properties of Macromolecules.* In: Wu, Chi-san, editor. *Handbook of Size Exclusion Chromatography and Related Techniques,* 2nd ed., New York, NY: Marcel Dekker, Inc.; 2004. p. 623–655.

46. Wedd, M.W., *Determination of Particle Size Distribution Using Laser Diffraction*, Educational Resource for Particle Technology, Educ. Reso. for Part. Techn. 032Q-Wedd. 2005. Available at http://www.erpt.org/032Q/Wedd-00.htm.

47. Provder, T., *Challenges in Particle Size Distribution Measurement, Past, Present and for the 21st Century*. Progress in Organic Coatings. 1997: **32**; p.143–153.

48. Mroczka, J., *Method of Moments in Light Scattering Data Inversion in the Particle Six Distribution Function*. Optics Communications. 1993; **99**; p. 147–151.

49. Nascimento, C.A.O., R. Guardain, and M. Giulietti, *Use of Neural Networks in the Analysis of Particle Size Distributions by Laser Diffraction.* Powder Technology. 1997; **90**; pp. 89–94.

50. Bowen, P., *Particle Size Distribution Measurement from Millimeters to Nanometers and From Rods to Platelets*. J. of Dispersion Sci. and Technol. 2002; **23**(5); p. 631–662.

51. Khalili, M.A., H.T. Solimeo, and J.N. Hockman, *An Investigation for Optimizing Sample Preparation and Measurement Conditions for a TiO2 Powder for Measuring Particle Size Distribution by Beckman Coulter LS230*, unpublished.

52. Guardani, R., C.A. O. Nascimento and R.S. Onimaru, *Use of Neural Networks in the Analysis of Particle Size Distribution by Laser Diffraction: Tests With Different Particle Systems*. Powder Technology. 2002; **126**; p. 42–50.

53 . Georgia State University, *Light Scattering*, 2005., available at:. http://hyperphysics.phy-astr.gsu.edu/hbase/atmos/scattercon.html#c1

54 . Stover, John C., *Optical Scattering: Measurement and Analysis.* New York, NY: McGraw-Hill; 1990. 238 p.

55 . Chu, Benjamin, *Laser Light Scattering: Basic Principles and Practice*. 2nd ed. New York, NY: Academic Press, Inc; 1991. 343 p.

56. Frock, H.N., *Particle Size Determination Using Angular Light Scattering*. In: Provder, Theodore, editor. *Particle Size Distribution: Assessment and Characterization*. Washington, D.C.: American Chemical Society; 1987. p. 146–160.

57. Wyatt Technology Corporation, *Angular Dependence of Scattered Light and Size*. 2005. Available at http://www.lightscattering.com/theory/rayleighscattering/size.cfm.

58 . Etzler, Frank M. and Richard Deanne, *Particle Size Analysis: A Comparison of Various Methods II*. Part. Part. Syst. Charact.; 1997; **14**; p.278-282.

59 . Etzler, Frank M. and Marie S. Sanderson, *Particle Size Analysis: A Comparative Study of Different Methods*. Part. Part. Syst. Charact. , 1995; **12**; p. 217-224.

60 . Delgado, Angel and Egon Matejevic, *Particle Size Distribution of Inorganic Colloidal Dispersions: A Comparison of Different Techniques.* Part. Part. Syst. Charact. 1991; **8**; p. 128-135.

61 . Knosche, Carsten, Hannelore Friedrich, and Michael Stintz, *Determination of Particle Size Distribution and Electrokinetic Properties with the AcoustoSizer in Comparison with Other Methods*. Part. Part Syst. Charact.. 1997; 14; p. 175-180.

62 . Barber, David, Jeffery Keuter and Kasey Kravig, *A Logical Stepwise Approach to Laser Diffraction Particle Size Distribution Analysis Methods Development and Validation*. Pharmaceutical Development and Technology. , 1998; **3** (2); p. 153-161.

63 . Naito, Maiko, Osamu Hayakawa, Kenji Nakahira, Hidetoshi Mori, Junichiro Tsubaki, *Effect of Particle Shape on the Particle Size Distribution Measured with Commercial Equipment*. Powder Technology. 1998; **100**; p.52-60.

64 . Schnieder, Martine and Timothy F. McKenna. *Comparative Study of Methods for the Measurement of Particle Size and Size Distribution of Polymeric Emulsions*. Part. Part. Syst. Charact. 2002; 19; p. 28-37.

65 . Webb, Paul A., Interpretation of Particle Size Reported By Different Analytical Techniques. Norcross, GA: Micromeritics Instrument Corp. 2005.

66 . De Ridder, F., Luc Deriemaeker, Paul Coppens, nad Robert Finsy, *Shape and Size Determination by Laser Diffraction: Feasibility of Data Analysis by Physical Modeling*. Part. Part. Syst. Charact. 2000; **17**; p. 195-205.

67 . Vanderhallen, Frank, Luc Deriemaeker, Bernard Manderick and Robert Finsy, *Shape and Size Determination by Laser Diffraction: Parametric Density Estimation by Neural Networks*. Part. Part. Syst. Charact. 2002; **19**; p. 65-72.

68 . Verheijen, Peter J. T. and Henk G. Merkus, *Simulation of Light Scattering Patterns for Instrument Comparison: Proposal for Software Validation of Laser Diffraction Instruments, ISO 13320, Part 2*. Delft: Netherlands. March 1,1999.

69. Montgomery, Douglas C., "Design and Analysis of Experiments," 5th ed. New York, NY: John Wiley and Sons, Inc.; 2001. 684 p.

70 . Levine, David M., Patricia P. Ramsey and Robert K. Smidt, "Applied Statistics for Engineers and Scientists," Upper Saddle River, NJ: Prentice Hall; 2001. 671 p.

71 . Schoenbach, Victor J., Absolute (Difference) and Relative (Ratio) Measures of Disparity," Abstract #39378, 130th Annual Meeting of the American Public

Health Association, November 9-13, 2002, Philadelphia, PA, available at: http://www.acponline.org/journals/ecp/primers/janfeb00.htm

72 . Environmental Protection Agency, "Indoor Radon Decay Product Measurement Device Protocols," Office of Air and Radiation, EPA 402-R-92-004, US Government Printing Office, Washington, DC, July 1992. available at: http://www.epa.gov/docs/iaq/radon/pubs/devprot1.html

73 . United States Army Corps of Engineers, "Miscellaneous FAQs," Hazardous, Toxic and Radioactive Waste Center of Expertise, USACOE, 2004. Available at: http://www.environmental.usace.army.mil/info/technical/chem/chemfaqs/faqmisc/faqmisc.html

74. Lewis, Pat. "Standard Method for Particle Size Distribution Measurement," personal communication, Lawrence Livermore National Laboratory, Livermore, California. January, 2005.

75. Moore, M. and D. Leinen, "Standard Method for Particle Size Distribution Measurement," Personal Communication, BWXT Pantex, Amarillo, Texas. March, 2005.

76. Duncan, A., "Effects of Sonication Time and Power", Draft white paper, BWXT Pantex, Amarillo, Texas, June 2005.

APPENDIX A

Standard Reference Material Data Sheets

Spherotech Inc.
1840 Industrial Drive, Suite 270
Libertyville, Illinois 60048-9817
Tel: (847) 680 8922
Fax: (847) 680 8927

TECHNICAL DATA

PRODUCT: SPHERO™ Polystyrene Particles, 2% DVB Crosslinked, 1.0- 1.4 µm.

CAT. NO.: PPX-10-10

LOT NO.: Q01

SIZE: 10 mL

PARTICLE CONC.: 5% w/v

PRESERVATIVE: 0.02% Sodium Azide

STORAGE: Below 30° C. Refrigeration is usually not required.

CAUTION: Do not freeze.

NOTE: Before use, resuspend by vortexing. To achieve optimum particles suspension, sonicate the reagent after vortex mixing.

PARTICLE SIZE DISTRIBUTION ANALYSIS:

Mean:	1.23 µm.
Std. Dev.:	0.029
C.V.:	2.4%

*WARNING: Sodium Azide can react with Cu and Pb in plumbing to form explosive metal azides. Flush this reagent down drains with copious amounts of water.

NOTE: FOR RESEARCH APPLICATIONS ONLY. NOT FOR DIAGNOSTIC USE.

Spherotech Inc.
1840 Industrial Drive, Suite 270
Libertyville, Illinois 60048-9817
Tel: (847) 680 8922
Fax: (847) 680 8927

TECHNICAL DATA

PRODUCT: SPHERO™ Polystyrene Particles, 2% DVB Crosslinked, 0.4 - 0.6 µm.

CAT. NO.: PPX-05-10

LOT NO.: Q01

SIZE: 10 mL

PARTICLE CONC.: 5% w/v

PRESERVATIVE: 0.02% Sodium Azide

STORAGE: Below 30° C. Refrigeration is usually not required.

CAUTION: Do not freeze.

NOTE: Before use, resuspend by vortexing. To achieve optimum particles suspension, sonicate the reagent after vortex mixing.

PARTICLE SIZE DISTRIBUTION ANALYSIS:

Mean:	0.48 µm.
Std. Dev.:	0.012
C.V.:	2.5%

*WARNING: Sodium Azide can react with Cu and Pb in plumbing to form explosive metal azides. Flush this reagent down drains with copious amounts of water.

NOTE: FOR RESEARCH APPLICATIONS ONLY. NOT FOR DIAGNOSTIC USE.

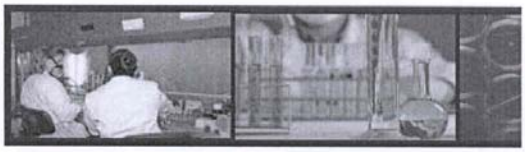

Downloadable NOTES
The following TECHNICAL INFORMATION are available for download (PDF format)

Rainbow Calibration Particles
Rainbow Fluorescent Particles
Ultra Rainbow Calibration Particles
Ultra Rainbow Fluorescent Particles
Drop Delay Calibration Particles
Fluorescent Alignment Particles
AccuCount Particles
Flow Cytometry Multiplexing Assay Particles
Flow Cytometry Compensation Particles
Flow Cytometry Data
Fluorescent Particles Info
Polystyrene Particles Info
Magnetic Particles
Magnetic Separators

SpheroTECHNICAL NOTES
The following SpheroTECHNICAL NOTES are available for download (PDF format)

STN-1: Particles Coating Procedures
STN-2: Determination of Antibody binding to particles
STN-3: Binding Capacity of Avidin Magnetic Particles
STN-4: Binding Capacity of Gt-anti-Ms-IgG Magnetic Particles
STN-5: Binding Capacity of Streptavidin Magnetic Particles
STN-6: Binding Capacity of Biotin Magnetic Particles
STN-7: Separation of Mononuclear Cells from Peripheral Blood using SPHERO Gt-ant
STN-8: Calibration and Performance Tracking of Flow Cytometer Using SPHERO Cali
STN-9: Measuring MEF with Flow Cytometer Using SPHERO Rainbow Calibration Pa
STN-10: Magnetic Particles Enzyme Immunoassay (MPEIA) using UltraMag Separator
STN-11: Magnetic Particles Coated with Pepsin, Papain and Trypsin
STN-12: Protein A Coated Magnetic Particles

CHARACTERISTICS OF POLYSTYRENE PARTICLES
Density: 1.05
Refractive Index: 1.59
Composition: Linear polystyrene
Shape: Uniform microspheres
Porosity: Nonporous
Compatibility with organic solvent: Inert to alcohol and DMSO but soluble in DMF, ace chloroform and methylene chloride.

APPENDIX B

LLNL Submicron Particle Size Data

LLNL Sample A Submicron Data Analysis

LLNLVolDiam	LLNLVolAveA	Normalized Vol. % A	Vol Diam X Norm. Vol % A
0.088989645	0		0
0.094262613	0		0
0.099848024	0		0
0.105764392	0		0
0.112031326	0		0
0.118669599	0		0
0.125701215	0		0
0.13314948	0		0
0.141039083	0		0
0.149396174	0		0
0.158248454	0		0
0.167625264	0		0
0.177557686	0		0
0.18807864	0		0
0.199223	0		0
0.211027705	0		0
0.223531883	0		0
0.236776979	0		0
0.250806897	0		0
0.26566814	0		0
0.281409967	0		0
0.298084556	0		0
0.315747177	0		0
0.334456373	0		0
0.354274159	0		0
0.375266223	0		0
0.397502144	0		0
0.421055627	0		0
0.446004742	0		0
0.472432184	0		0
0.500425551	0		0
0.530077629	0		0
0.561486703	0		0
0.594756882	0		0
0.629998443	0		0
0.667328197	0		0
0.706869879	0		0
0.748754552	0		0
0.793121049	0.14676	0.088391135	0.07010487
0.840116426	0.513845	0.309480395	0.259999563
0.889896453	0.654185	0.394004869	0.350623536
0.942626133	0.3455575	0.208123601	0.196182745
0.998480243	0	0	0
Volume % submicron	1.6603475		
Mean Diameter			0.876910714

LLNL Sample B Submicron Data Analysis

LLNLVolDiam	LLNLVolAveB	Normalized Vol. % B	Vol Diam X Norm. Vol % B
0.088989645	0		0
0.094262613	0		0
0.099848024	0		0
0.105764392	0		0
0.112031326	0		0
0.118669599	0		0
0.125701215	0		0
0.13314948	0		0
0.141039083	0		0
0.149396174	0		0
0.158248454	0		0
0.167625264	0		0
0.177557686	0		0
0.18807864	0		0
0.199223	0		0
0.211027705	0		0
0.223531883	0		0
0.236776979	0		0
0.250806897	0		0
0.26566814	0		0
0.281409967	0		0
0.298084556	0		0
0.315747177	0		0
0.334456373	0		0
0.354274159	0		0
0.375266223	0		0
0.397502144	0		0
0.421055627	0		0
0.446004742	0		0
0.472432184	0		0
0.500425551	0		0
0.530077629	0		0
0.561486703	0		0
0.594756882	0		0
0.629998443	0		0
0.667328197	0		0
0.706869879	0		0
0.748754552	0		0
0.793121049	0		0
0.840116426	0		0
0.889896453	0.08968	0.078814444	0.070136694
0.942626133	0.4644925	0.408214964	0.384794093
0.998480243	0.58369	0.512970592	0.512191001
Volume % submicron	1.1378625		
Mean Diameter			0.967121788

LLNL Sample C Submicron Data Analysis

LLNLVolDiam	LLNLVolAveC	Normalized Vol. % C	Vol Diam X Norm. Vol % C
0.074875455	0.00341	0.000438884	3.28617E-05
0.079312105	0.0068225	0.00087809	6.96432E-05
0.084011643	0.0102475	0.001318905	0.000110803
0.088989645	0.0136975	0.001762938	0.000156883
0.094262613	0.01717	0.002209866	0.000208308
0.099848024	0.020675	0.002660977	0.000265693
0.105764392	0.02423	0.003118524	0.000329829
0.112031326	0.0278375	0.003582827	0.000401389
0.118669599	0.0315475	0.004060323	0.000481837
0.125701215	0.03543	0.00456002	0.0005732
0.13314948	0.039525	0.005087067	0.00067734
0.141039083	0.0439075	0.005651117	0.000797028
0.149396174	0.048605	0.006255709	0.000934579
0.158248454	0.05371	0.006912749	0.001093932
0.167625264	0.05927	0.007628349	0.001278704
0.177557686	0.0653625	0.008412484	0.001493701
0.18807864	0.0720625	0.009274808	0.001744393
0.199223	0.0794425	0.010224651	0.002036986
0.211027705	0.08759	0.011273276	0.002378974
0.223531883	0.0965775	0.012430013	0.002778504
0.236776979	0.106475	0.013703871	0.003244761
0.250806897	0.11738	0.0151074	0.00378904
0.26566814	0.1293375	0.01664639	0.004422416
0.281409967	0.142415	0.018329531	0.005158113
0.298084556	0.1566525	0.020161969	0.006009972
0.315747177	0.1720625	0.022145314	0.00699232
0.334456373	0.1886275	0.024277313	0.008119702
0.354274159	0.206285	0.026549923	0.009405952
0.375266223	0.2249	0.028945767	0.010862369
0.397502144	0.24429	0.031441358	0.012498007
0.421055627	0.264165	0.033999371	0.014315627
0.446004742	0.2841275	0.036568646	0.01630979
0.472432184	0.30369	0.039086439	0.018465692
0.500425551	0.3222525	0.041475526	0.020755413
0.530077629	0.3391075	0.04364485	0.023135159
0.561486703	0.3534725	0.045493698	0.025544107
0.594756882	0.364525	0.046916211	0.027903739
0.629998443	0.3714625	0.047809102	0.03011966
0.667328197	0.373605	0.048084853	0.032088378
0.706869879	0.3704775	0.047682328	0.033705201
0.748754552	0.36194	0.046583508	0.034879614
0.793121049	0.3482475	0.044821214	0.035548648
0.840116426	0.3301225	0.042488435	0.035695232
0.889896453	0.30875	0.039737686	0.035362426
0.942626133	0.2856575	0.036765565	0.034656182
0.998480243	0.262555	0.033792156	0.0337408
Volume % submicron	7.7697025		
Mean Diameter			0.540572906

APPENDIX C

Garnet Calibration Check Data

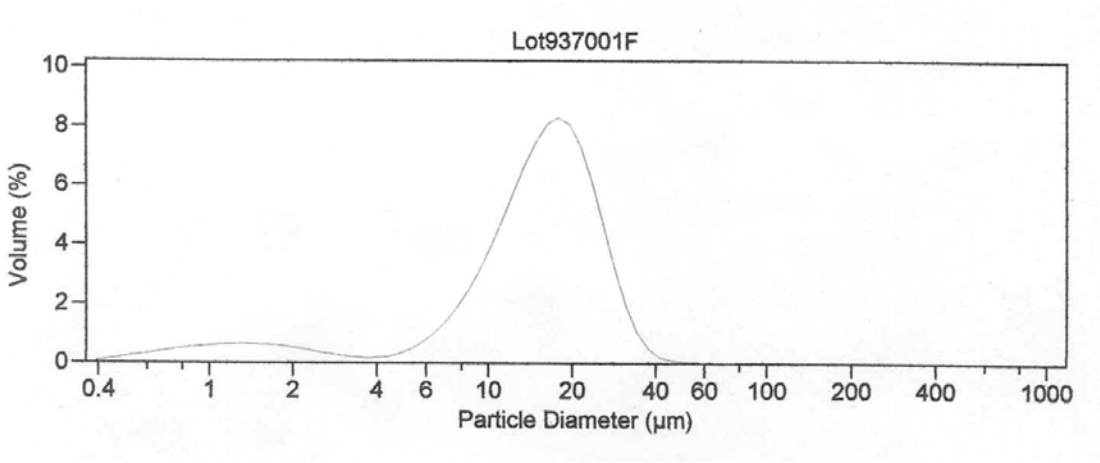

15 micron garnet analyzed March 17, 2004

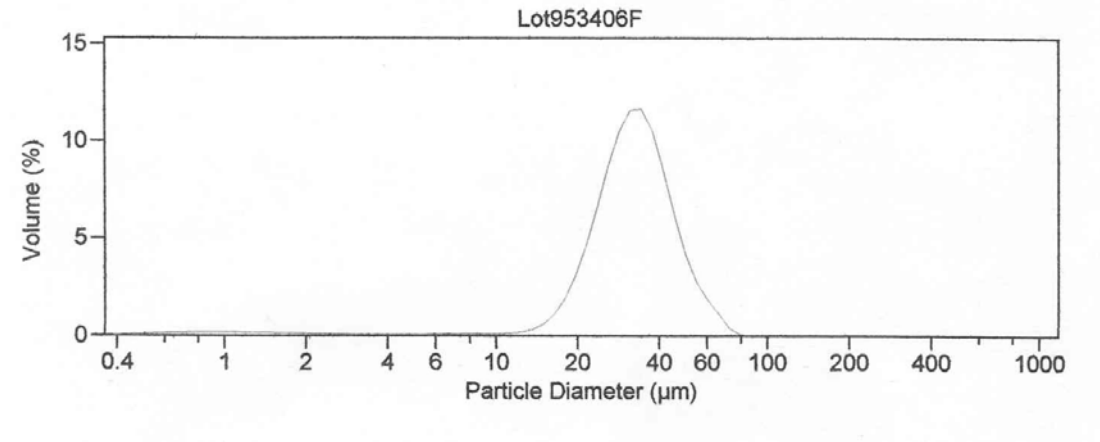

35 micron garnet analyzed March 17, 2004

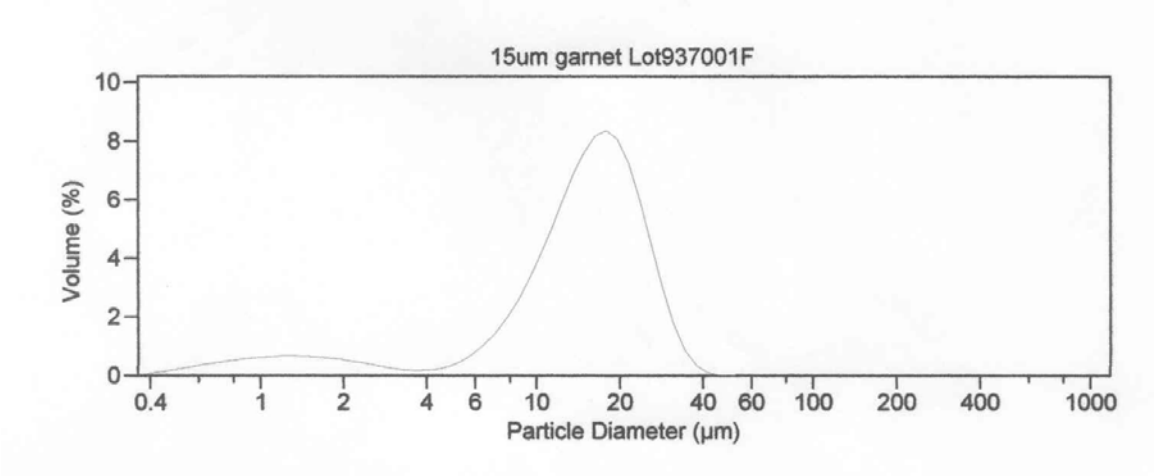

15 micron garnet analyzed July 5, 2004

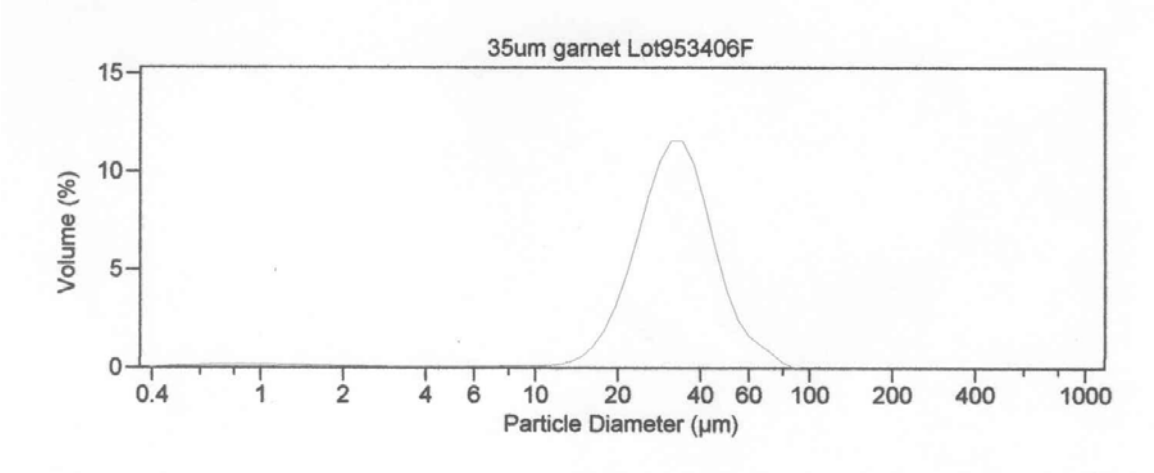

35 micron garnet analyzed July 5, 2004

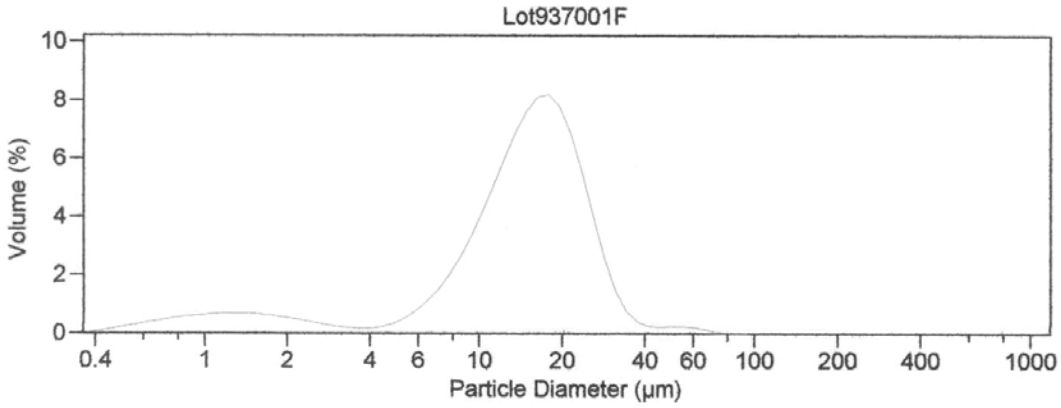

15 micron garnet analyzed July 19, 2004

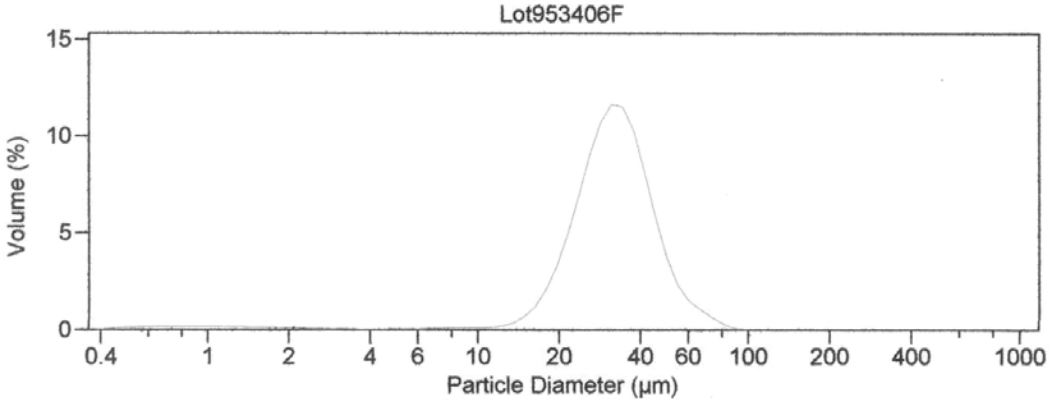

35 micron garnet analyzed July 19, 2004

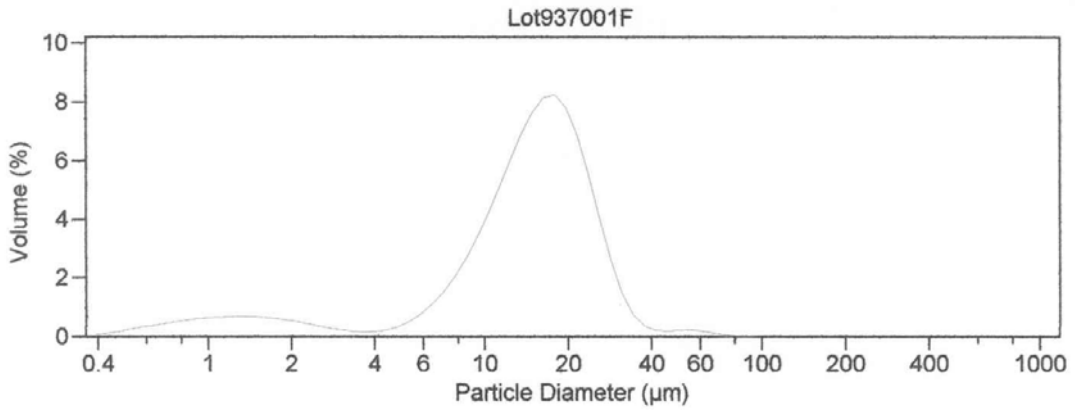

15 micron garnet analyzed August 22, 2004

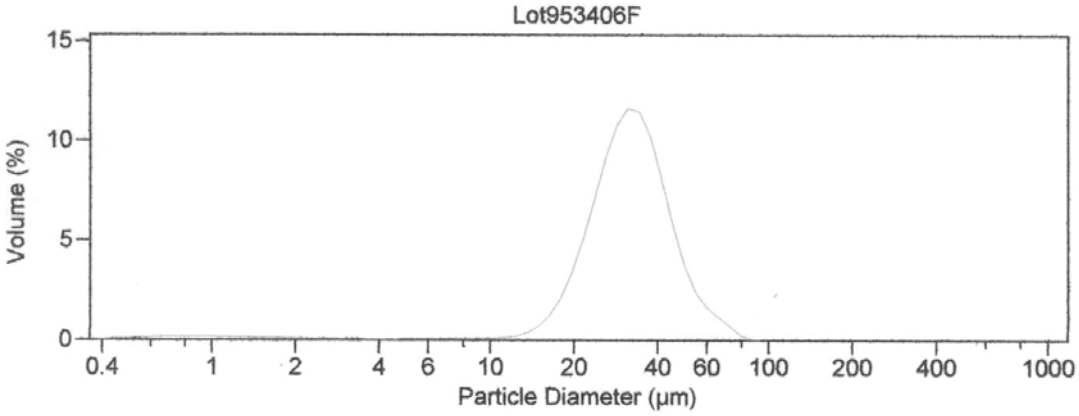

35 micron garnet analyzed August 22, 2004

APPENDIX D

SNL PSD Graphs from Subsequent Study

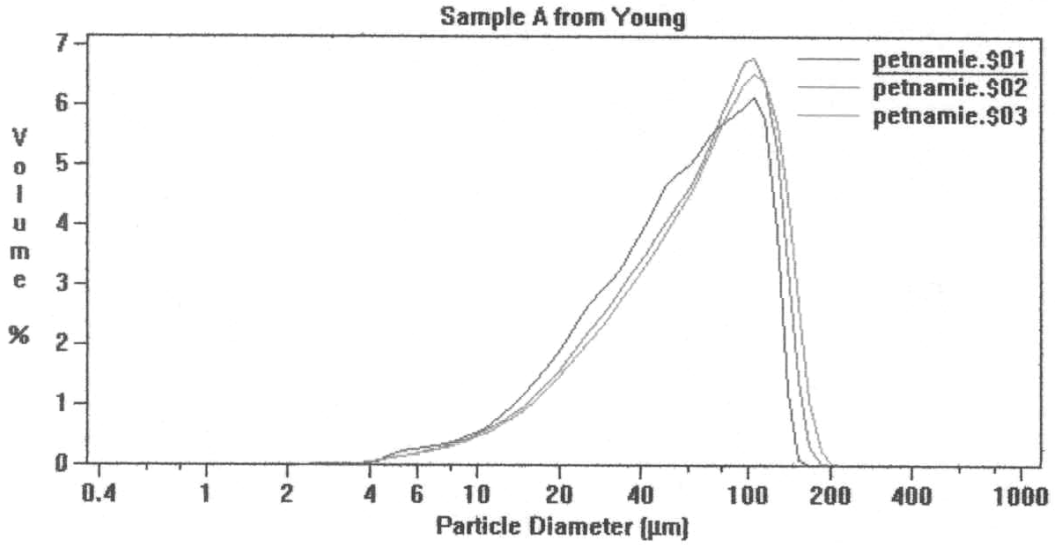

PSD for Sample A, water, 0 seconds

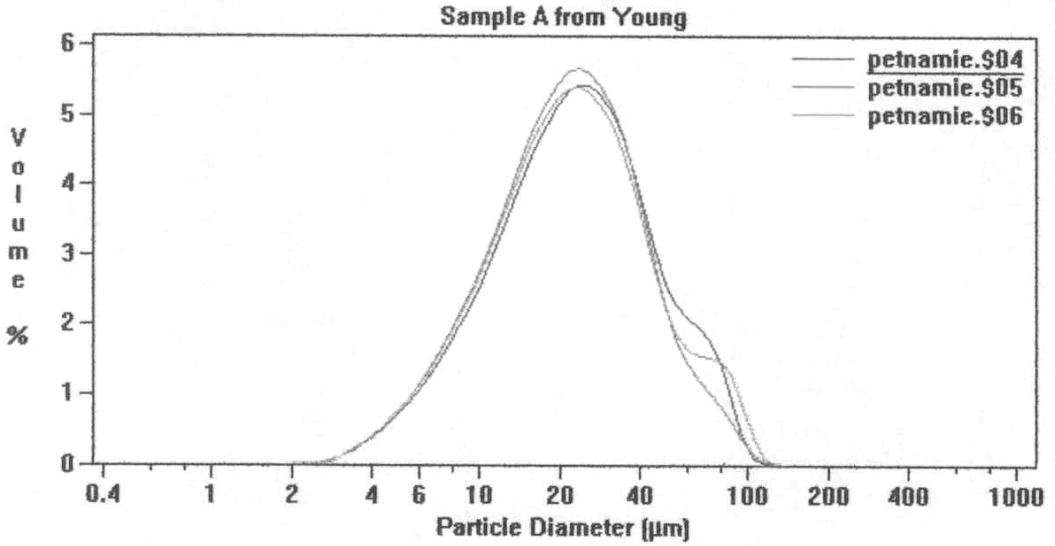

PSD for Sample A, water, 30 seconds

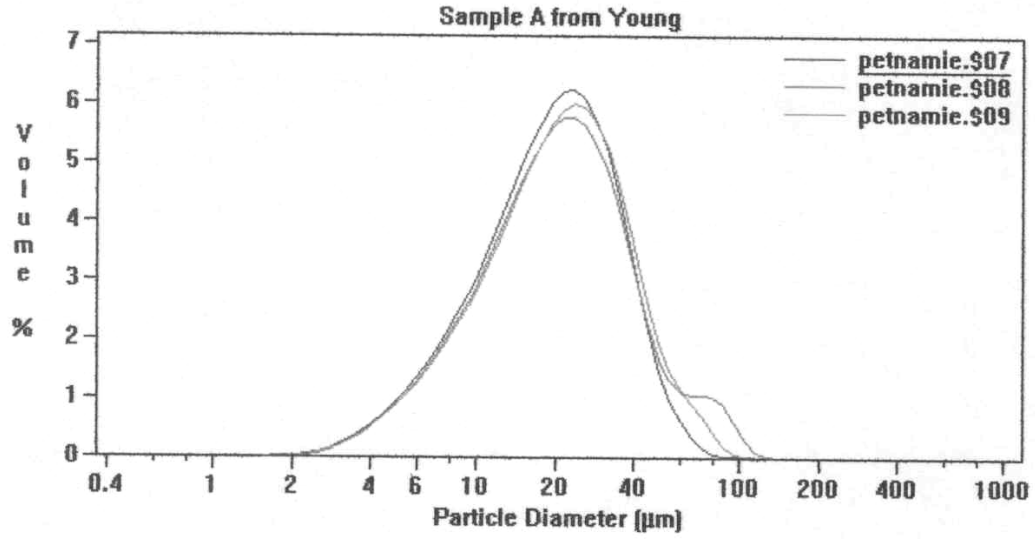

PSD for Sample A, water, 60 seconds

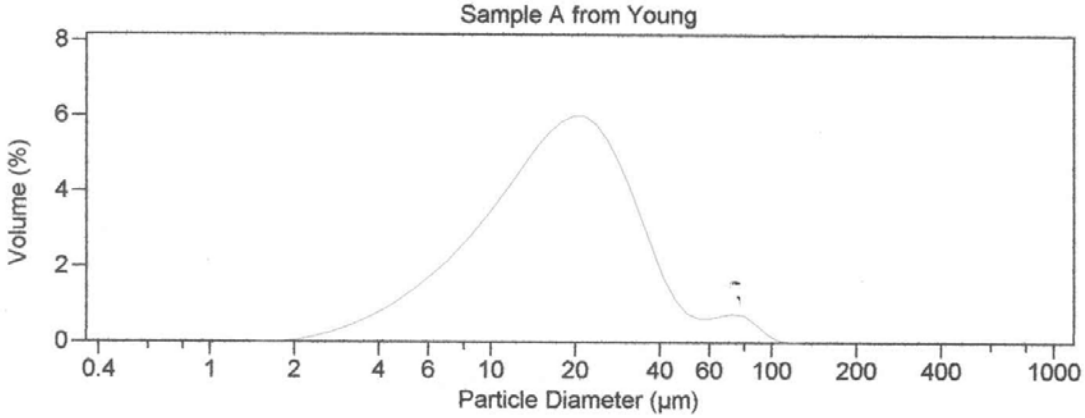

PSD for Sample A, water, 180 seconds

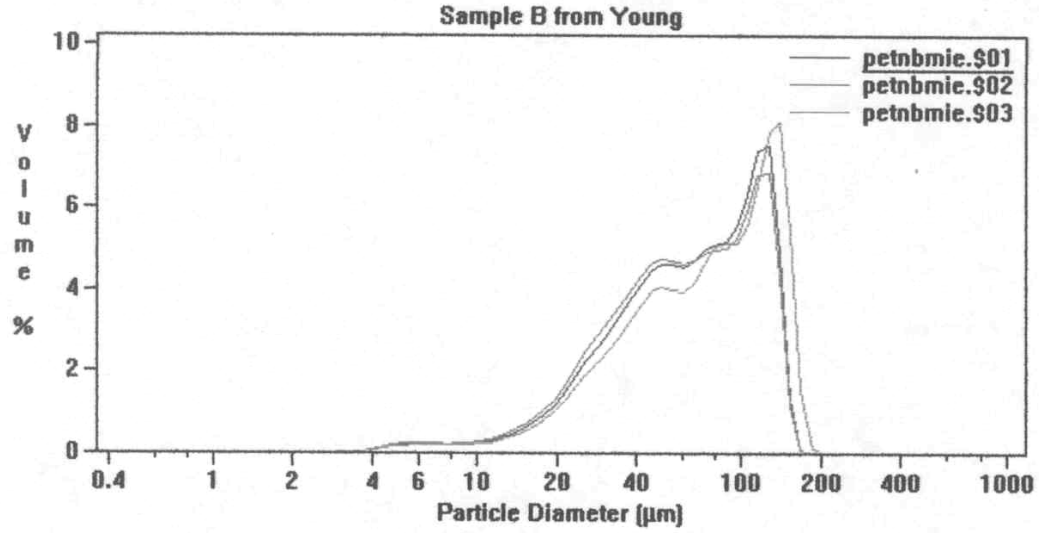

PSD for Sample B water, 0 seconds

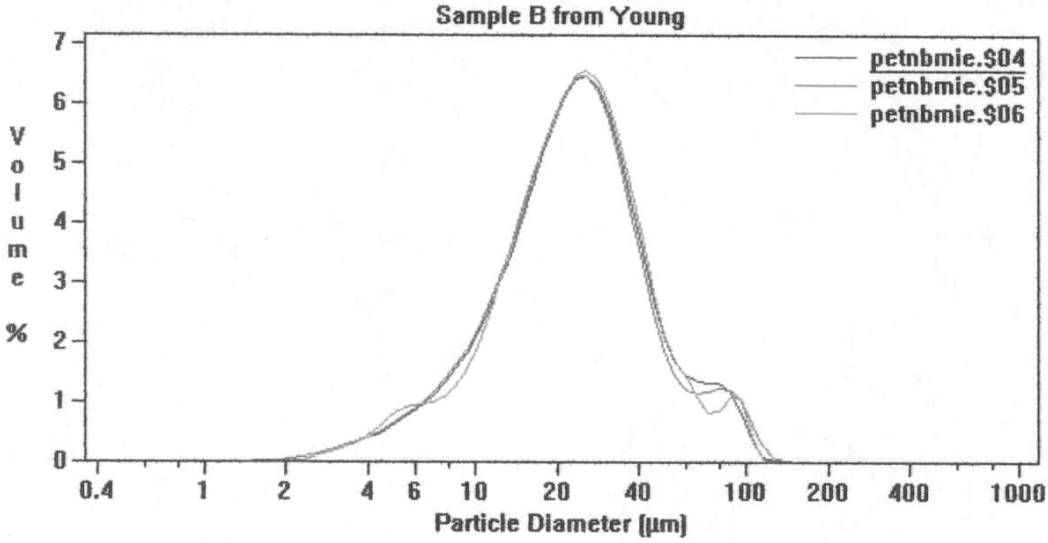

PSD for Sample B water, 30 seconds

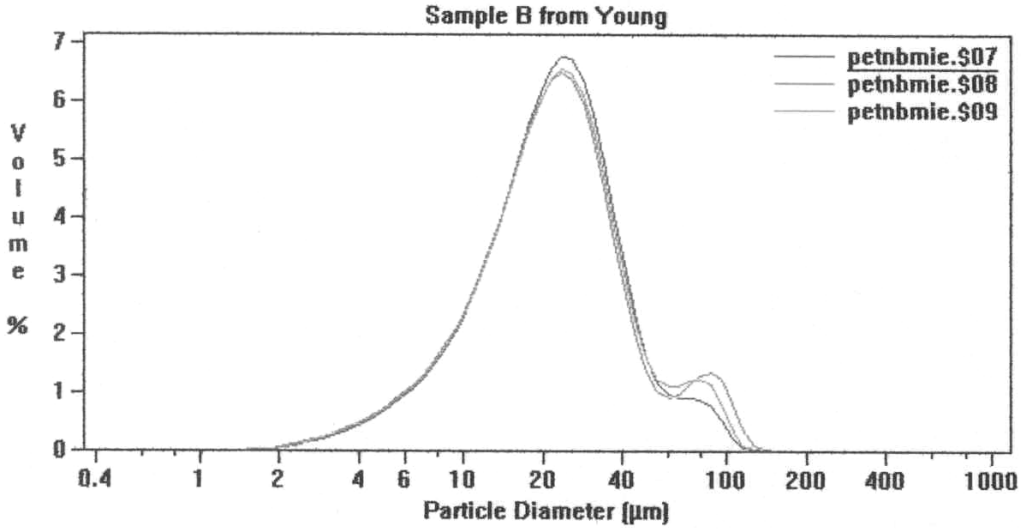

PSD for Sample B water, 60 seconds

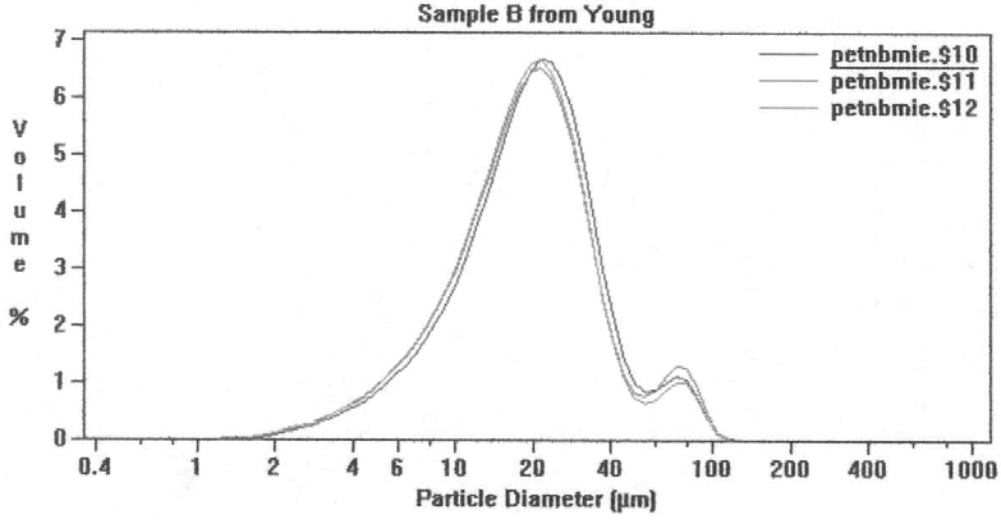

PSD for Sample B water, 180 seconds

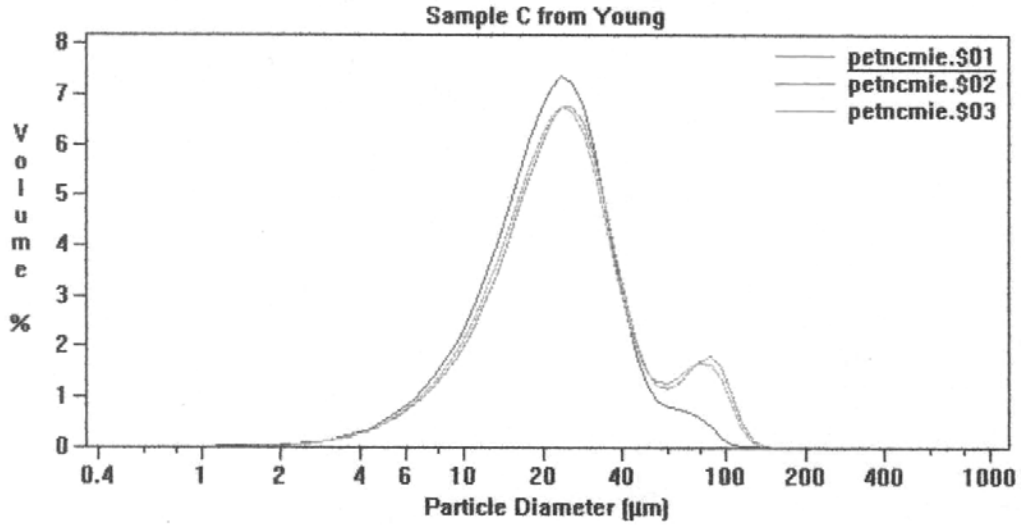

PSD for Sample C water, 0 seconds

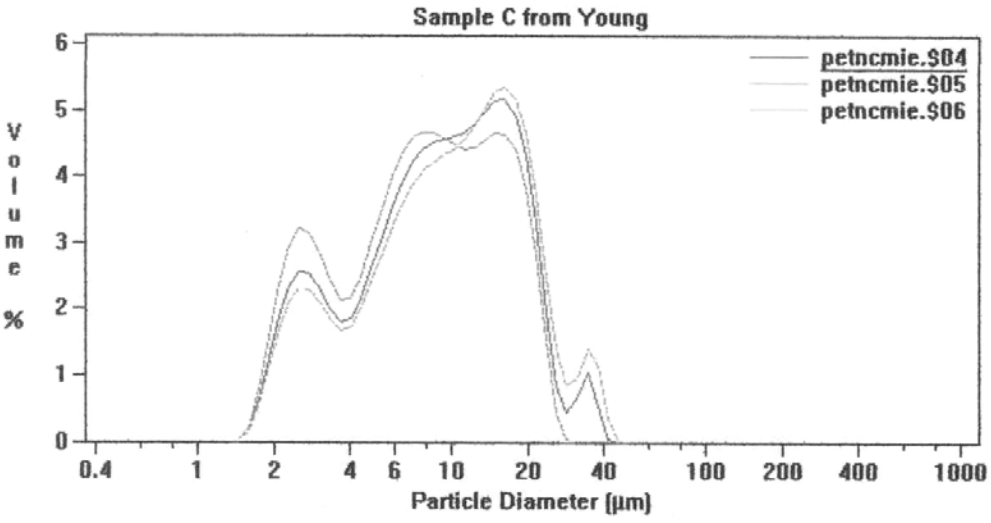

PSD for Sample C water, 30 seconds

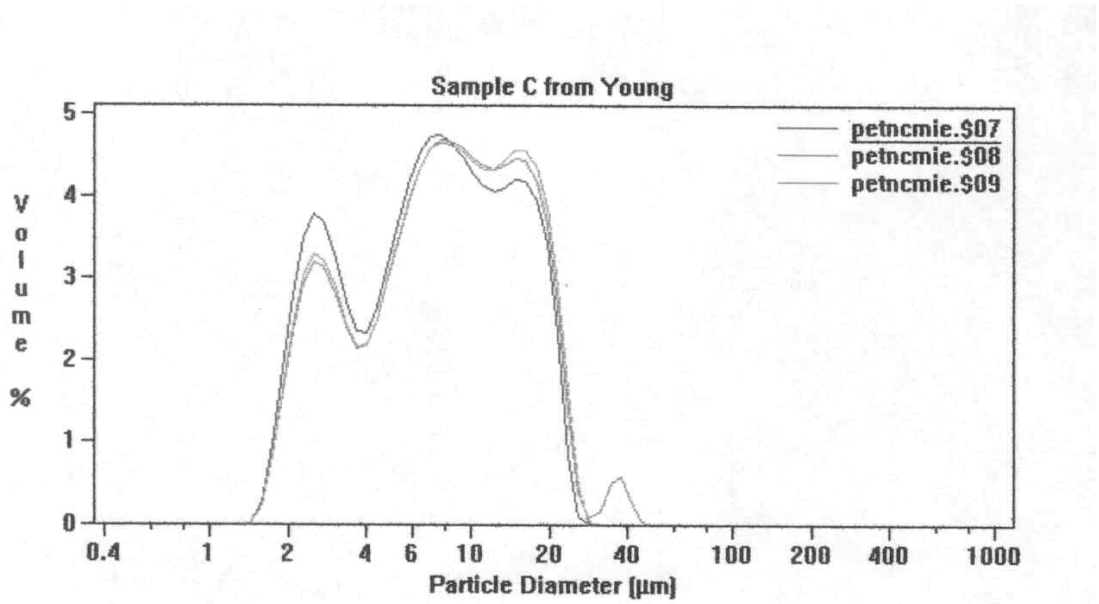

PSD for Sample C water, 60 seconds

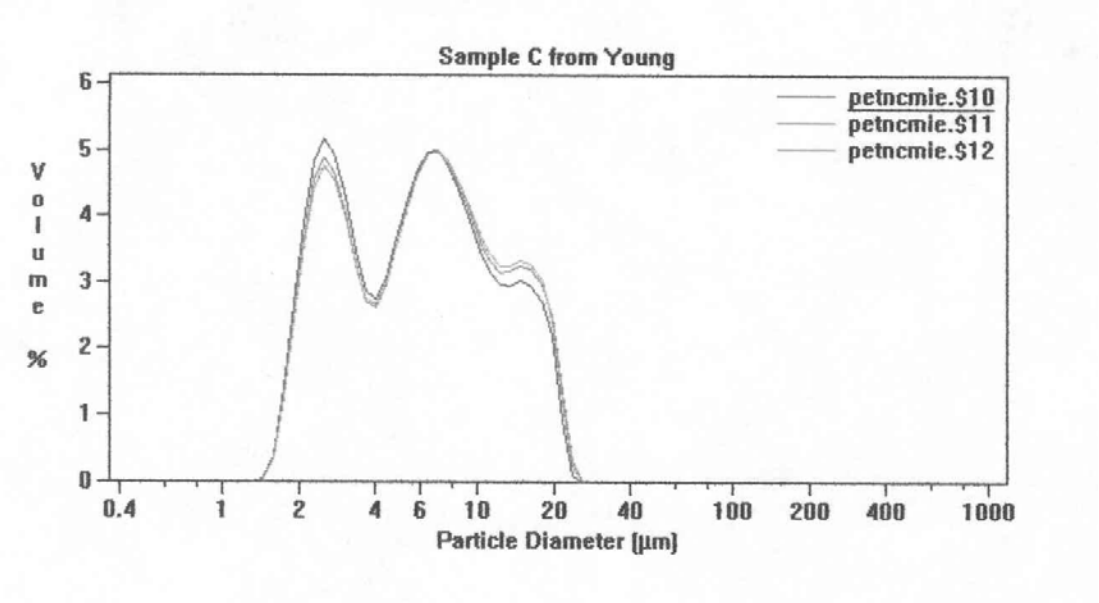

PSD for Sample C water, 180 seconds

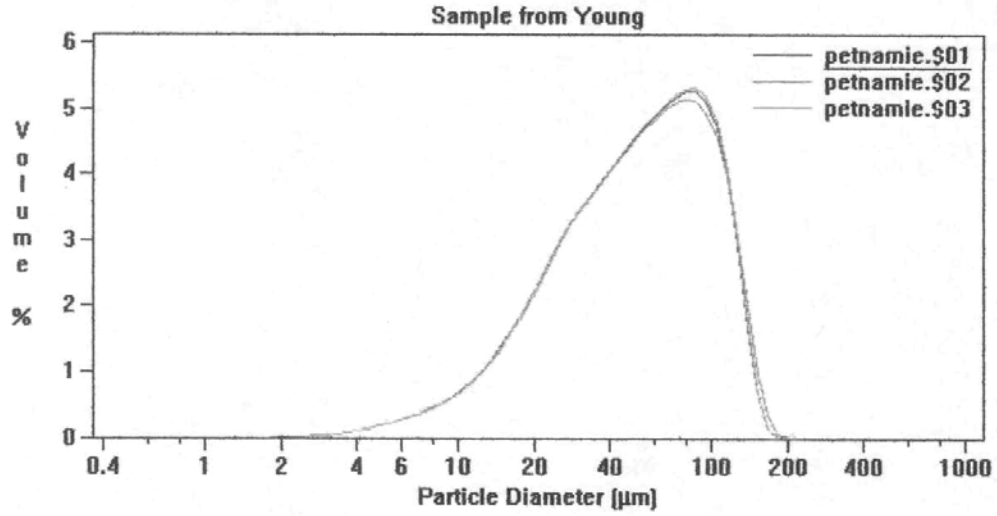

PSD for Sample A IPA/water, 0 seconds

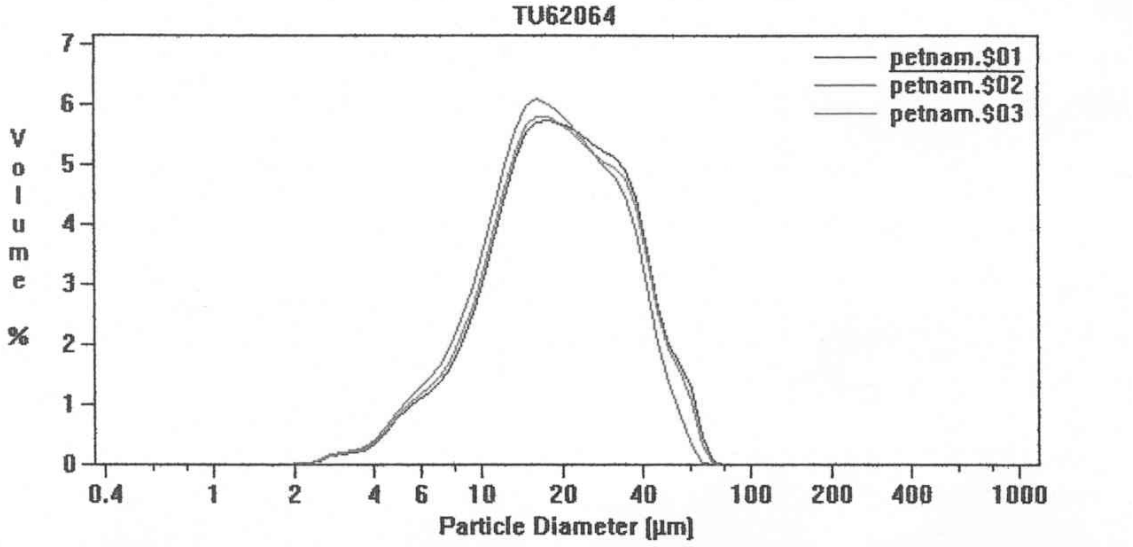

PSD for Sample A IPA/water, 30 seconds

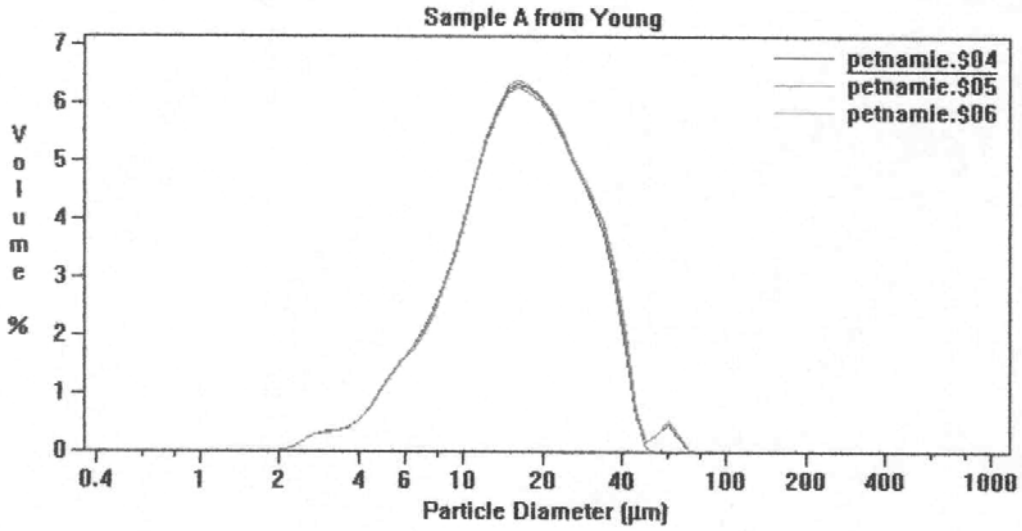

PSD for Sample A IPA/water, 60 seconds

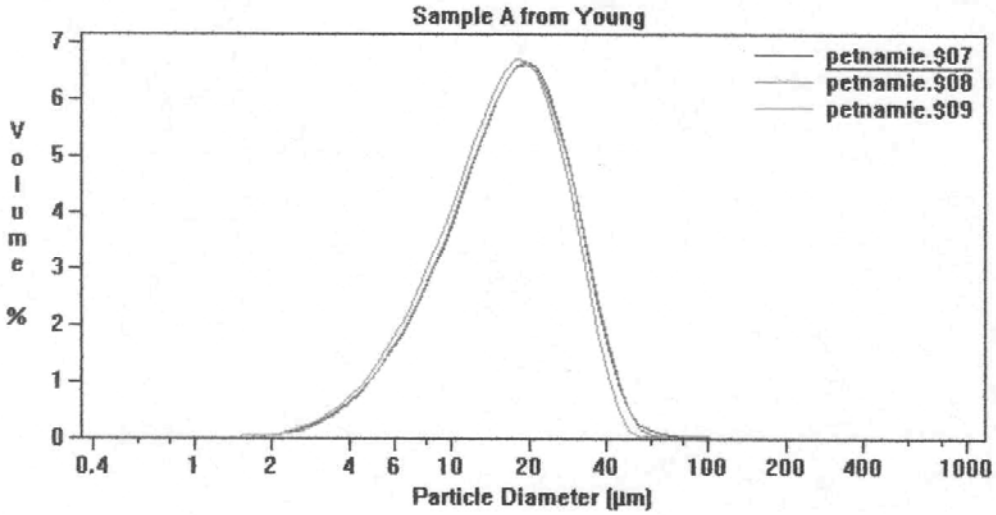

PSD for Sample A IPA/water, 180 seconds

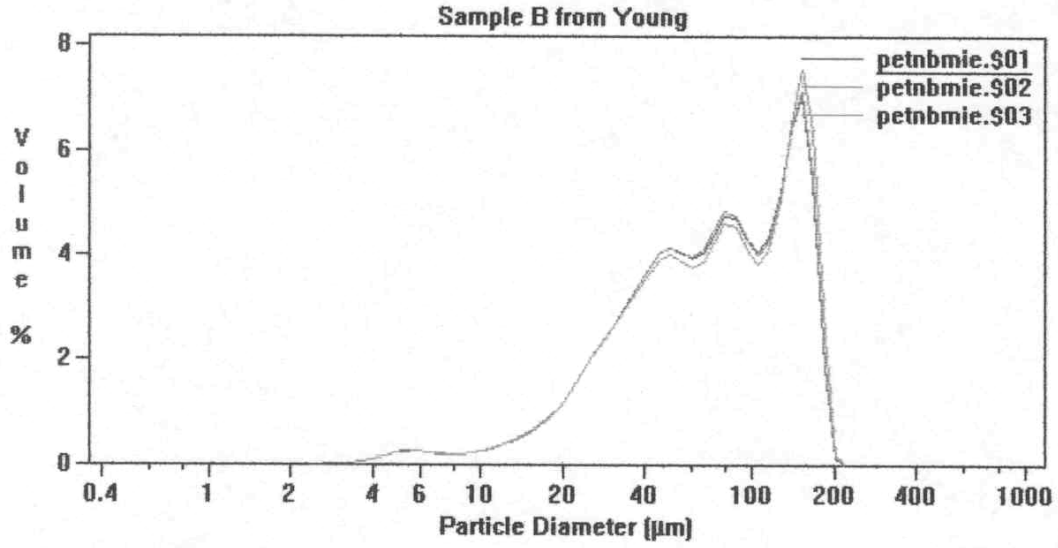

PSD for Sample B IPA/water, 0 seconds

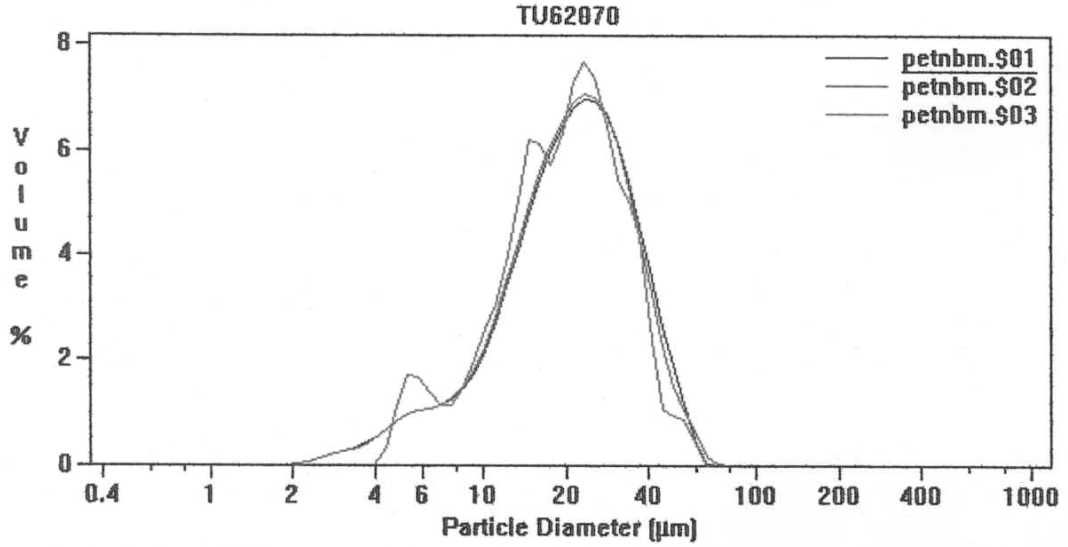

PSD for Sample B IPA/water, 30 seconds

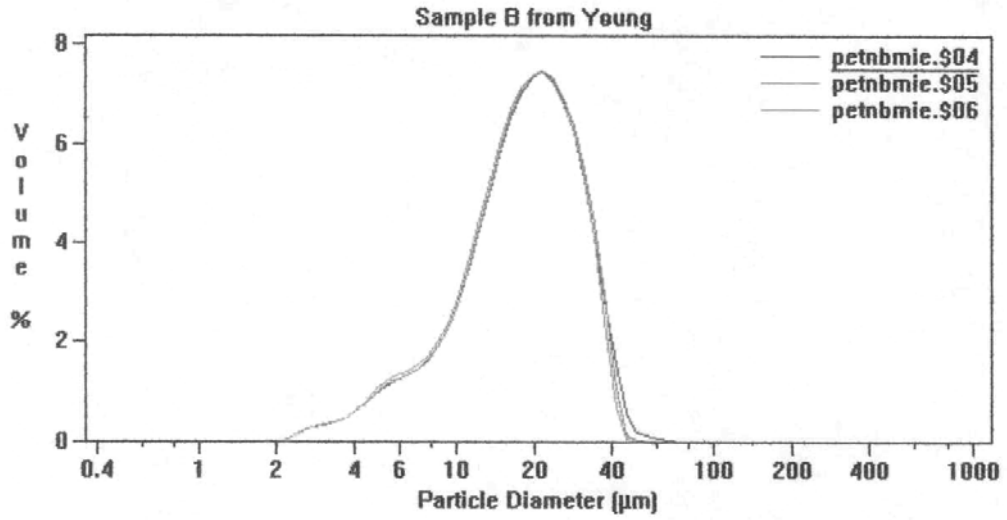

PSD for Sample B IPA/water, 60 seconds

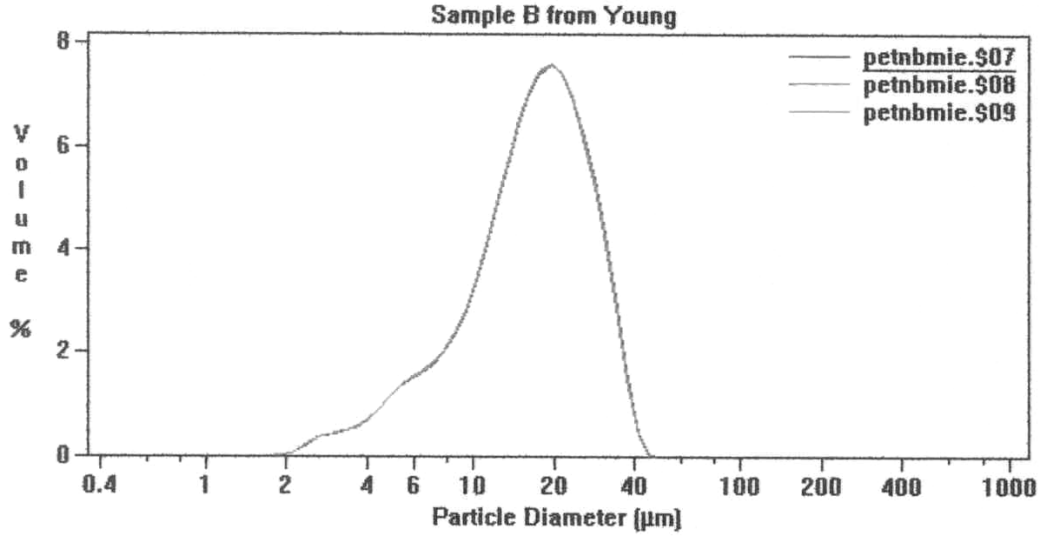

PSD for Sample B IPA/water, 180 seconds

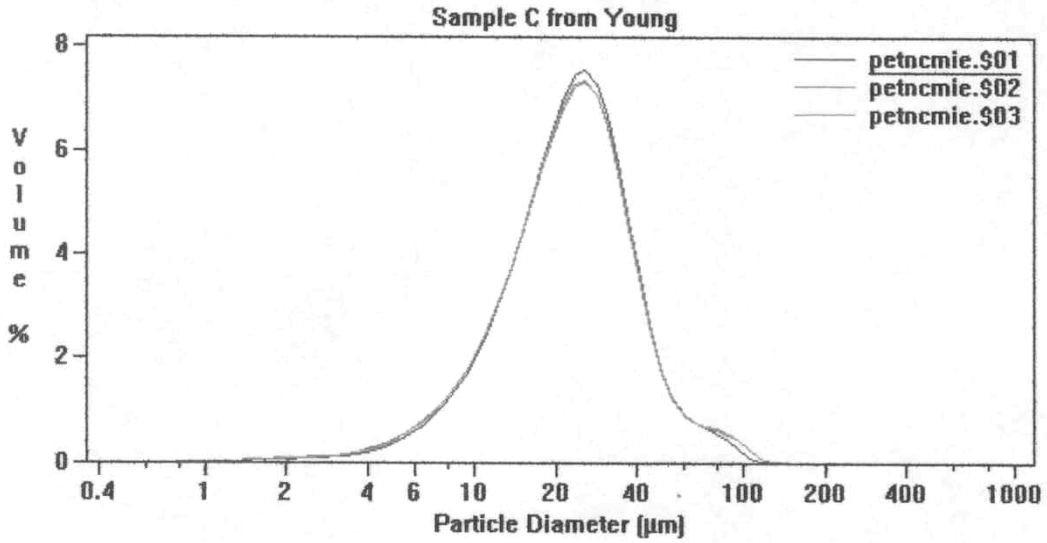

PSD for Sample C IPA/water, 0 seconds

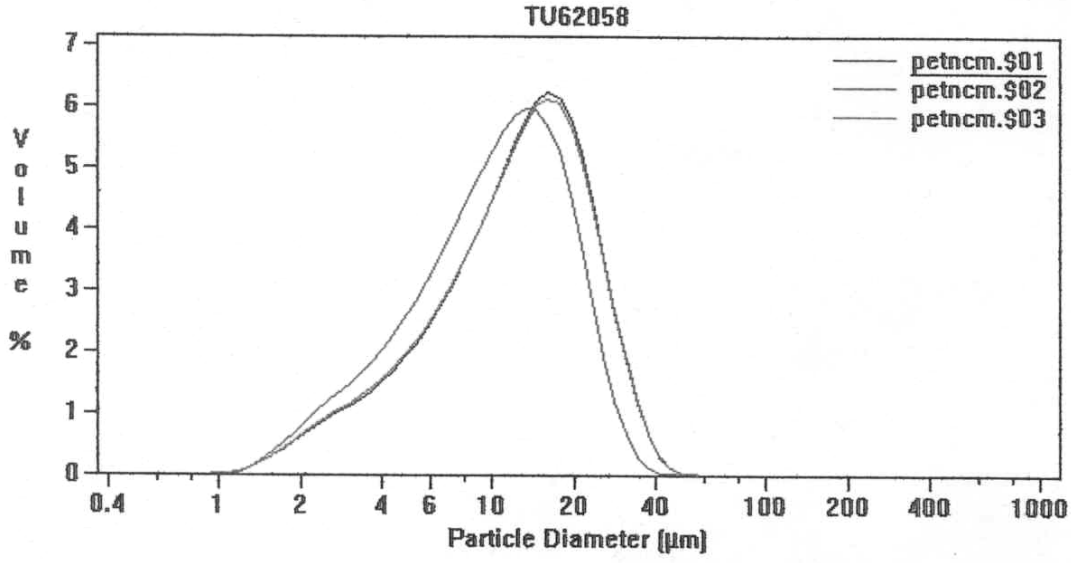

PSD for Sample C IPA/water, 30 seconds

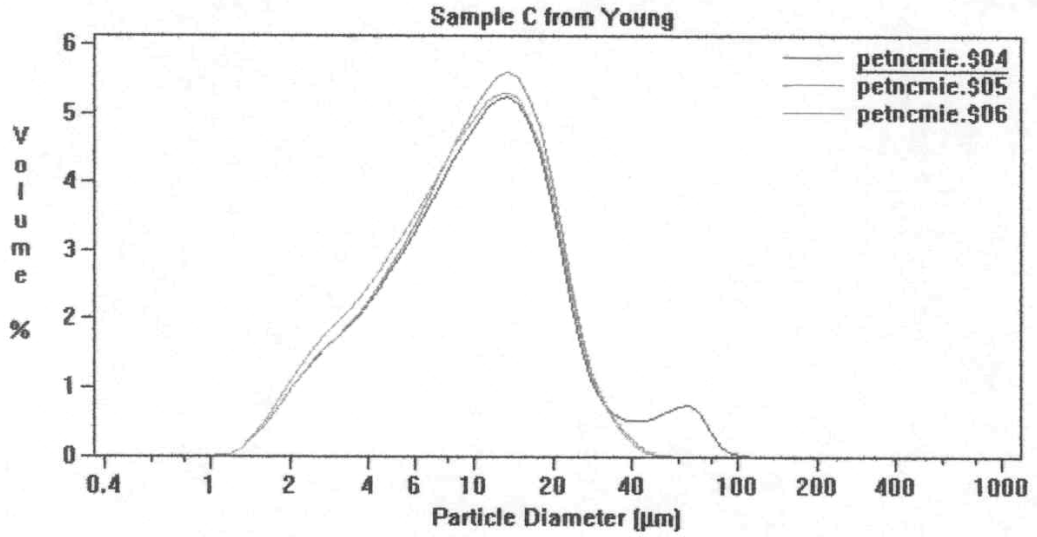

PSD for Sample C IPA/water, 60 seconds

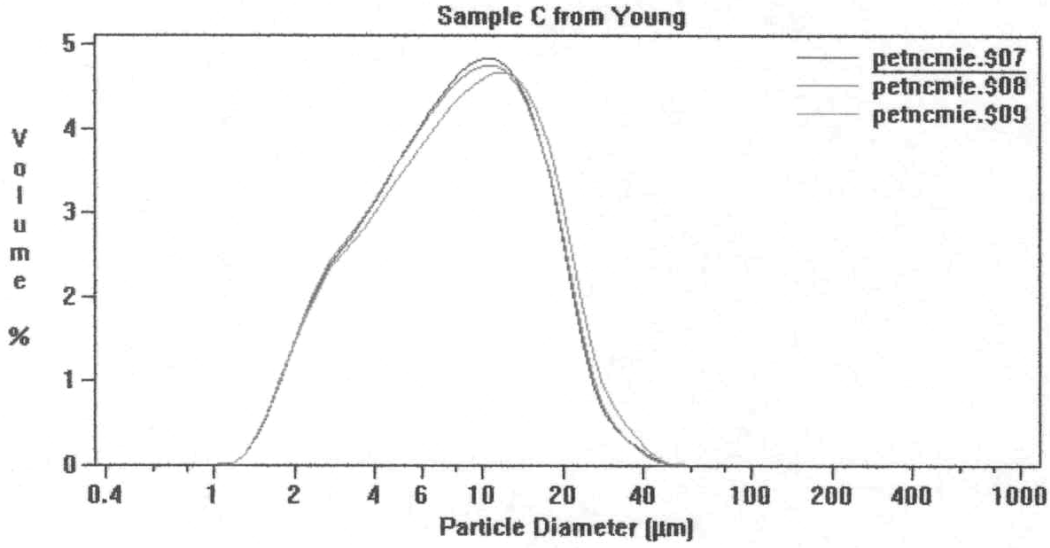

PSD for Sample C IPA/water, 180 seconds

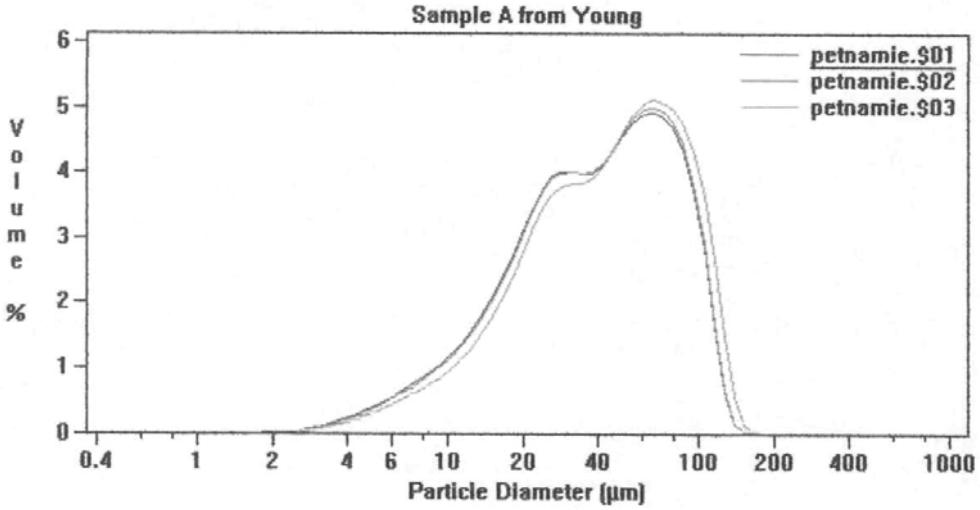

PSD for Sample A, ethanol, 0 seconds

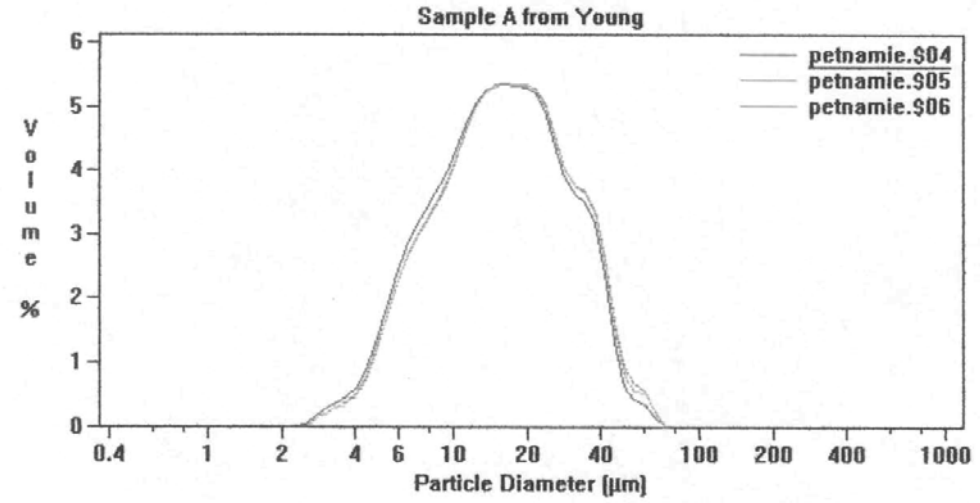

PSD for Sample A, ethanol, 30 seconds

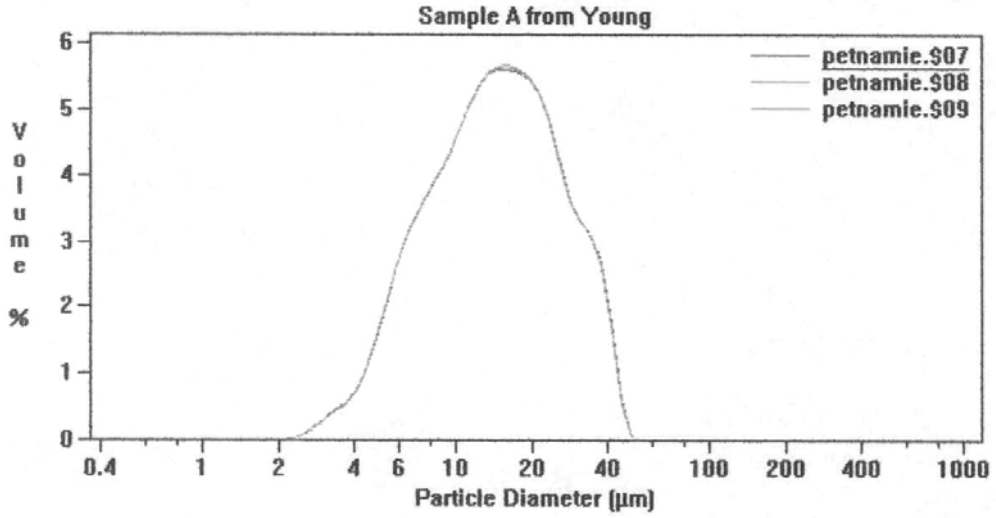

PSD for Sample A, ethanol, 60 seconds

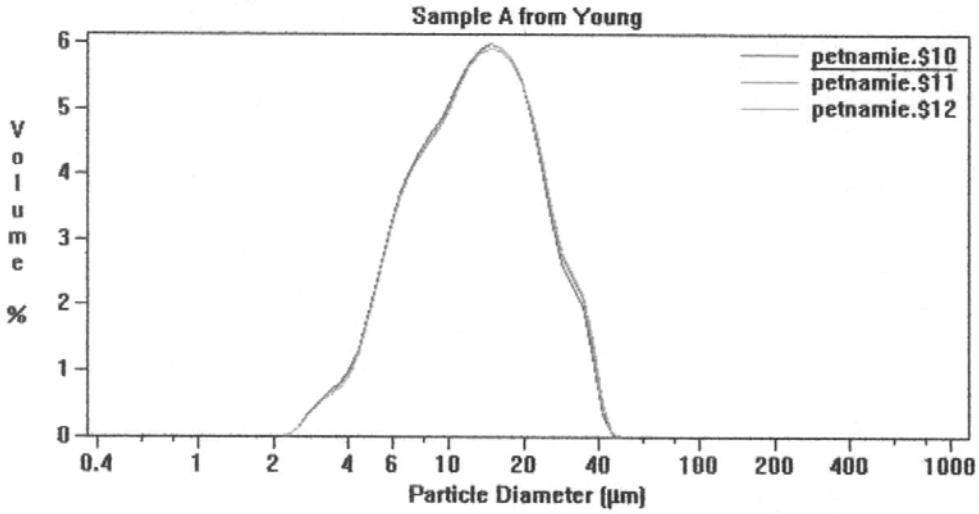

PSD for Sample A, ethanol, 180 seconds

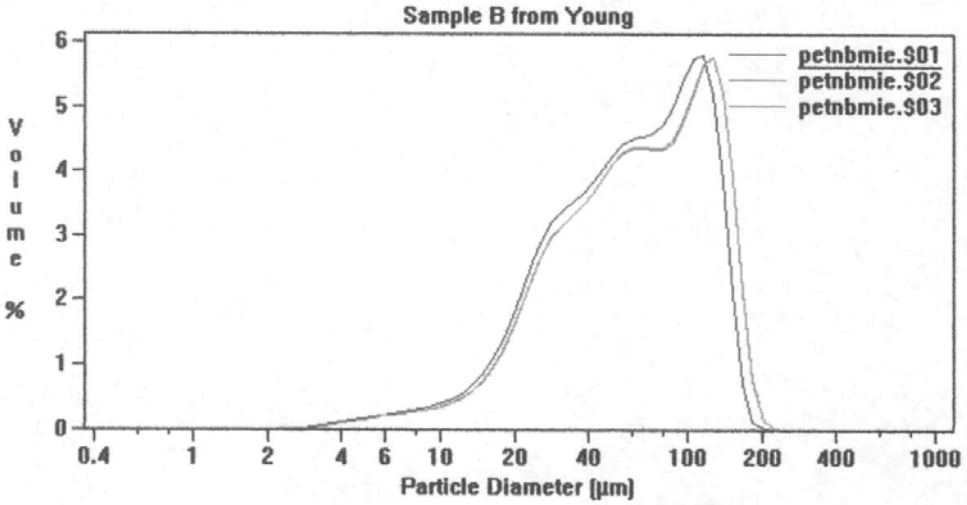

PSD for Sample B, ethanol, 0 seconds

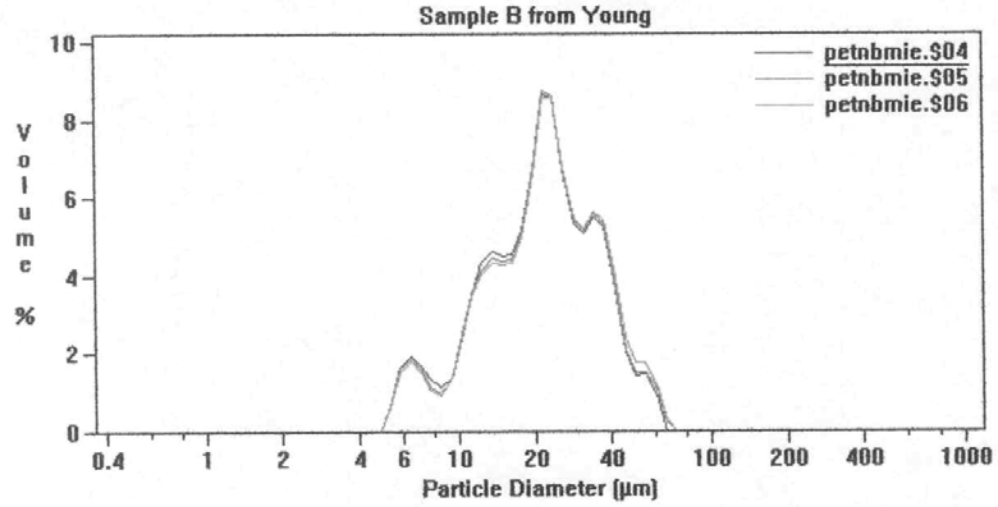

PSD for Sample B, ethanol, 30 seconds

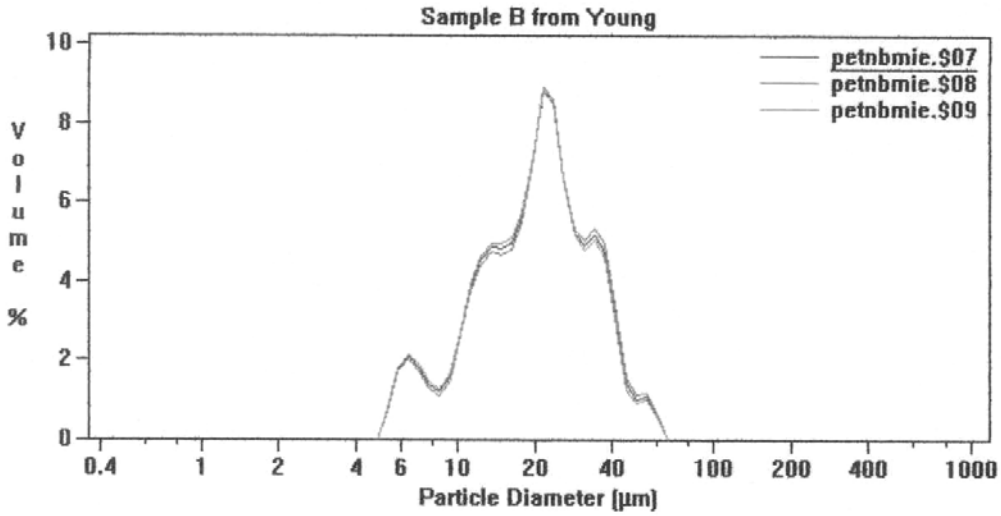

PSD for Sample B, ethanol, 60 seconds

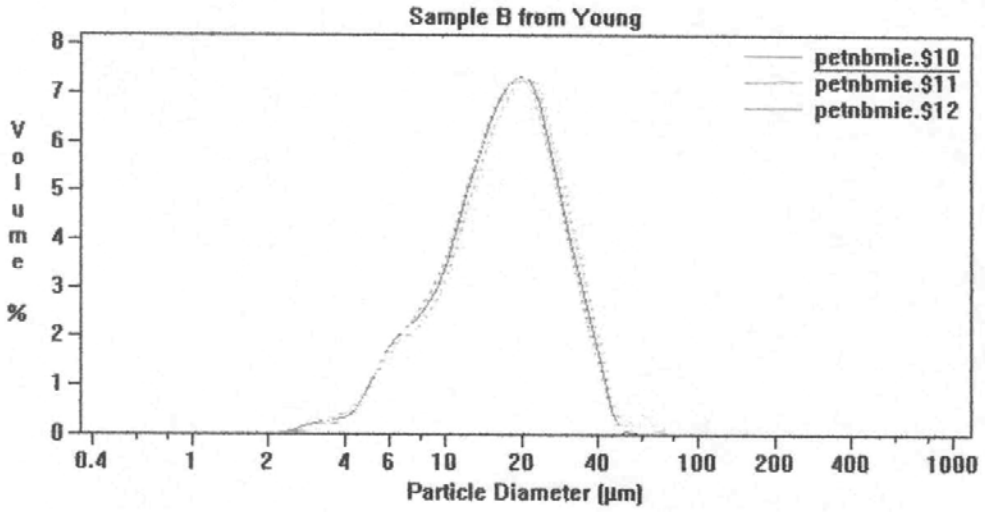

PSD for Sample B, ethanol, 180 seconds

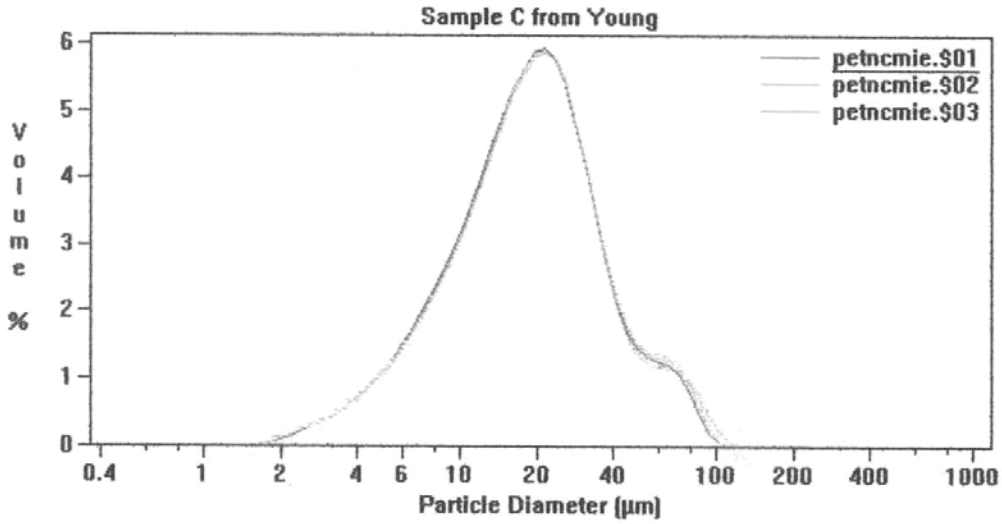

PSD for Sample C, ethanol, 0 seconds

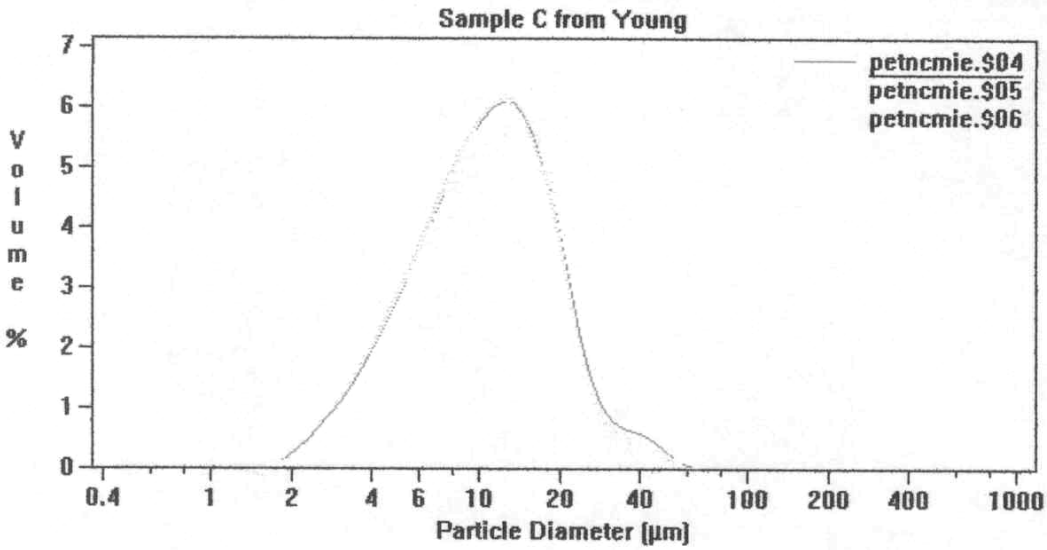

PSD for Sample C, ethanol, 30 seconds

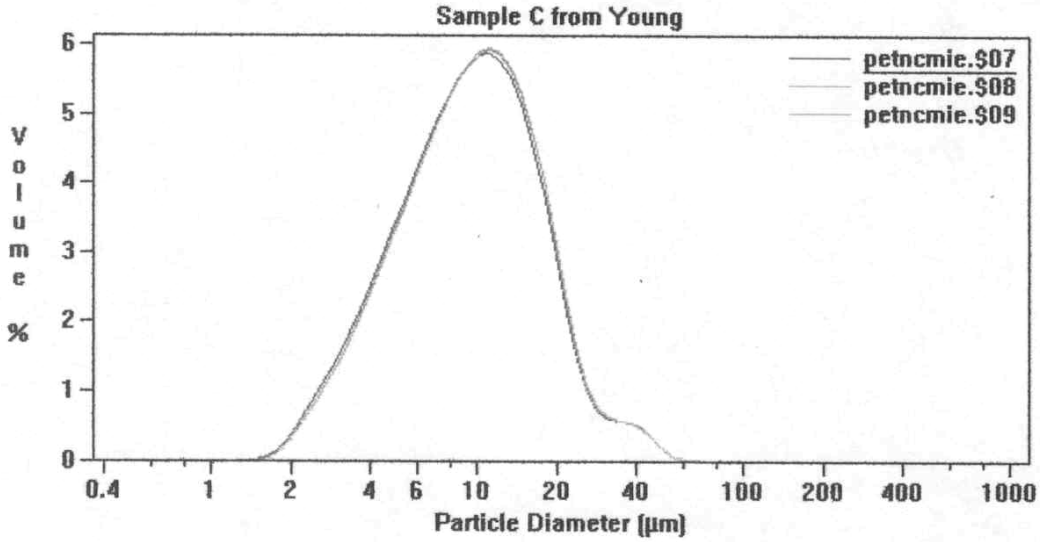

PSD for Sample C, ethanol, 60 seconds

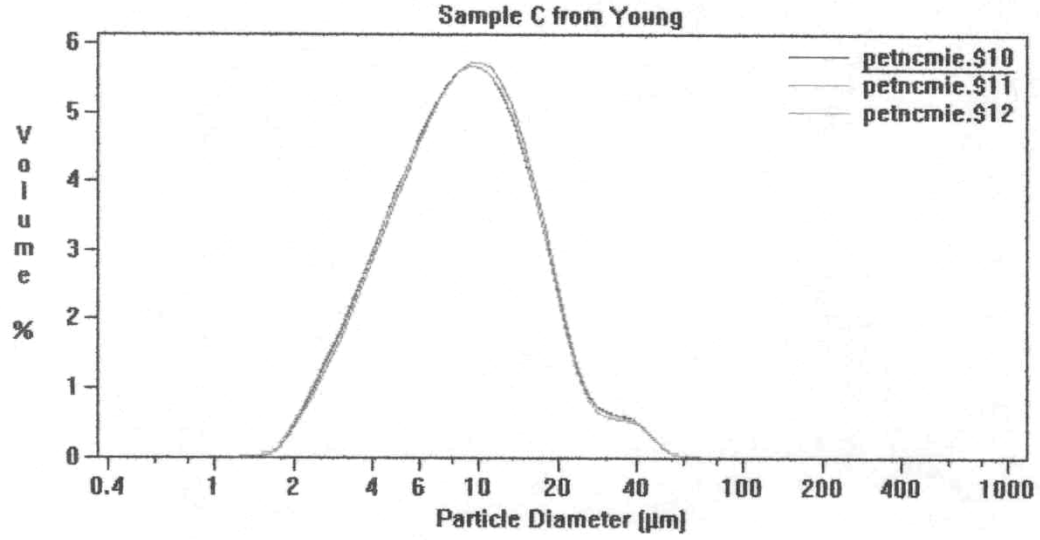

PSD for Sample C, ethanol, 180 seconds

APPENDIX E

Statistical Analysis

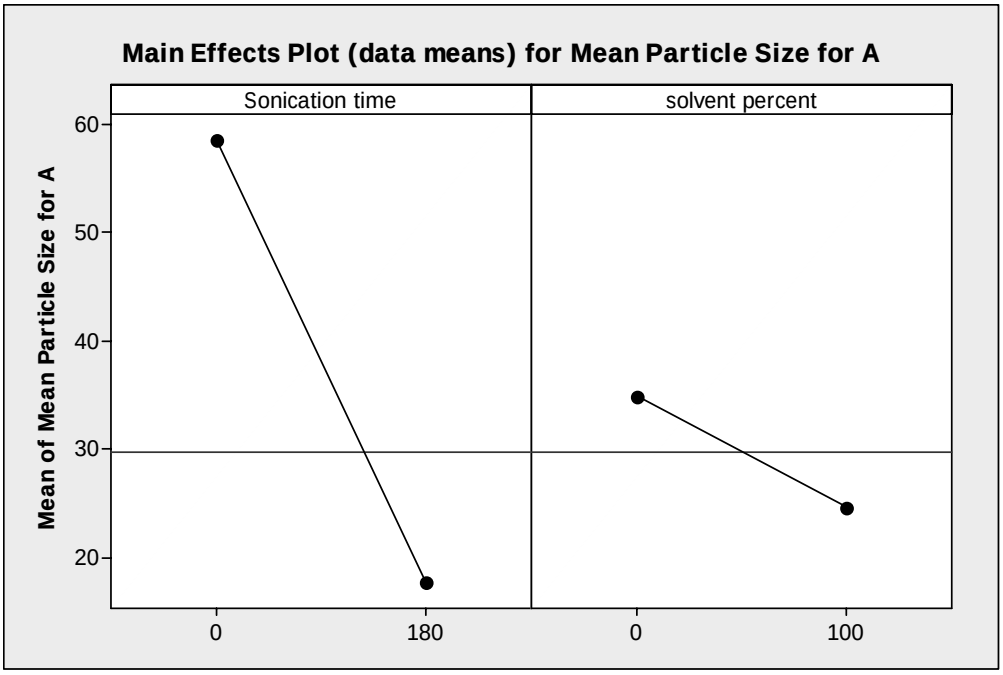

Main Effects Plot for Sample A

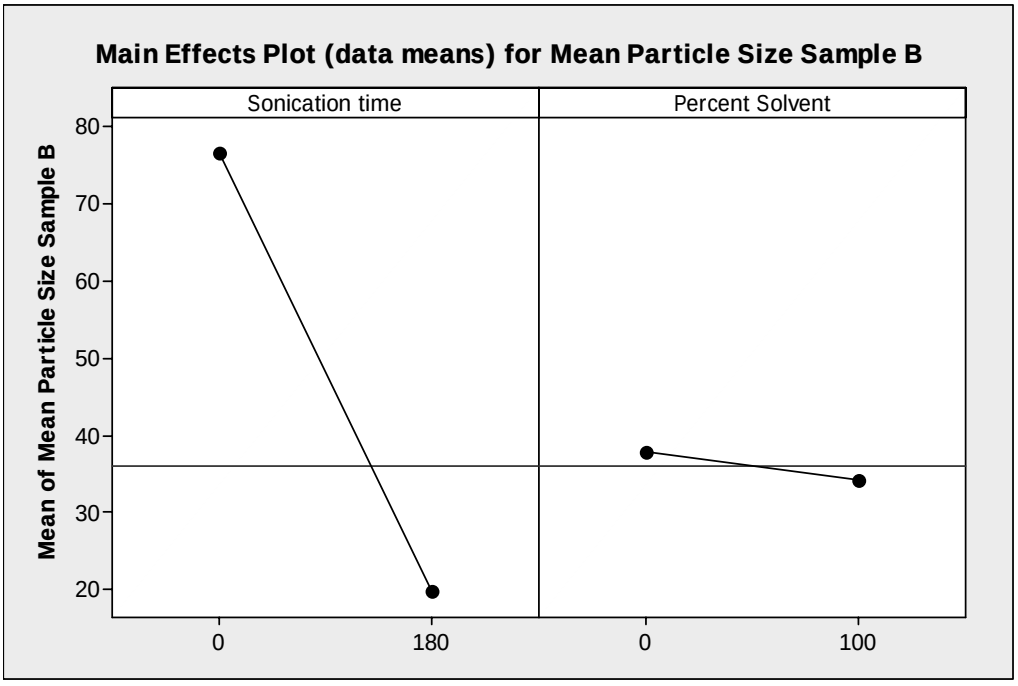

Main Effects Plot for Sample B

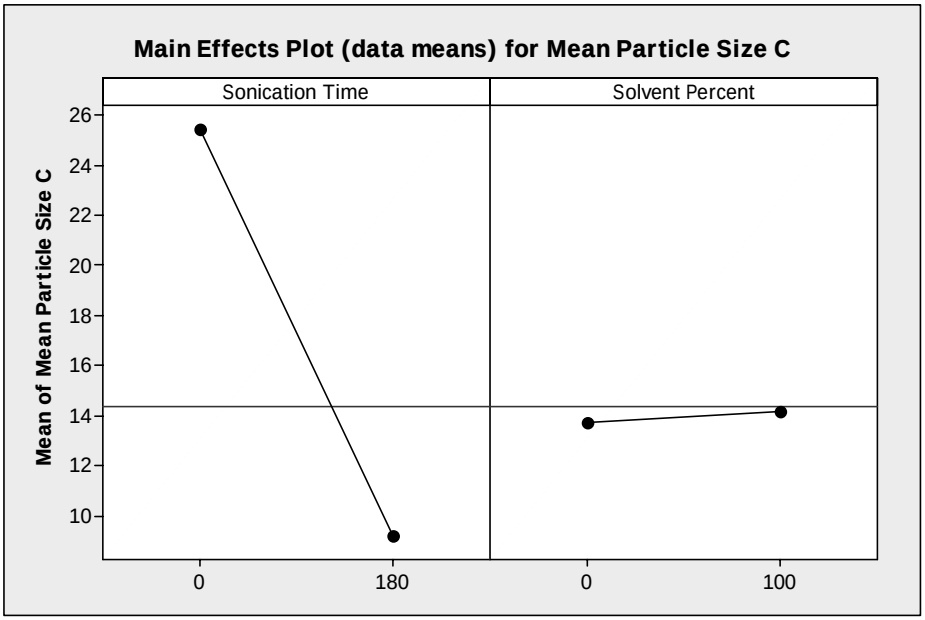

Main Effects Plot for Sample C

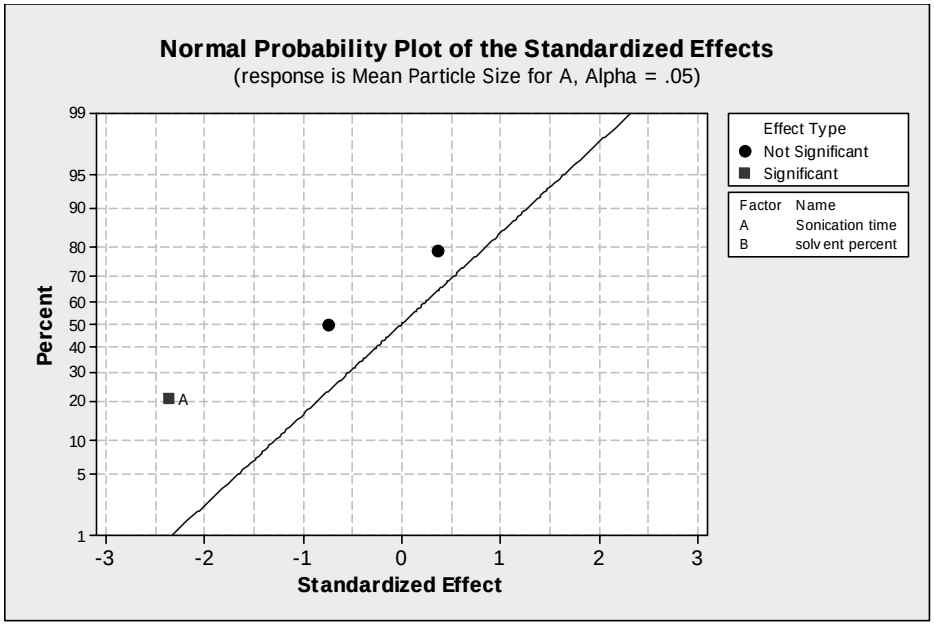

Normalized Probability Plot Showing Significant Factors Affecting Mean Particle Size for Sample A

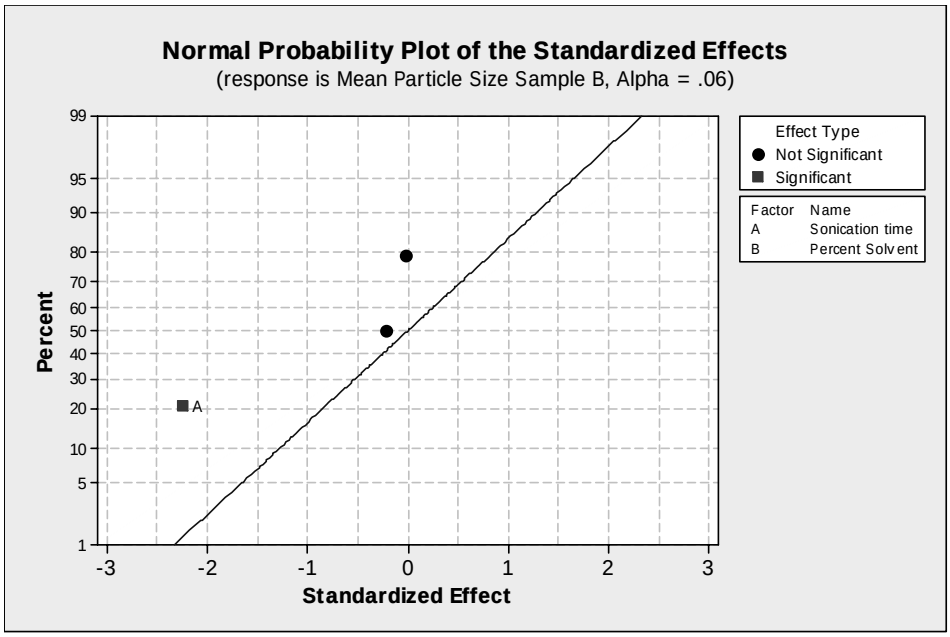

Normalized Probability Plot Showing Significant Factors Affecting Mean Particle Size for Sample B

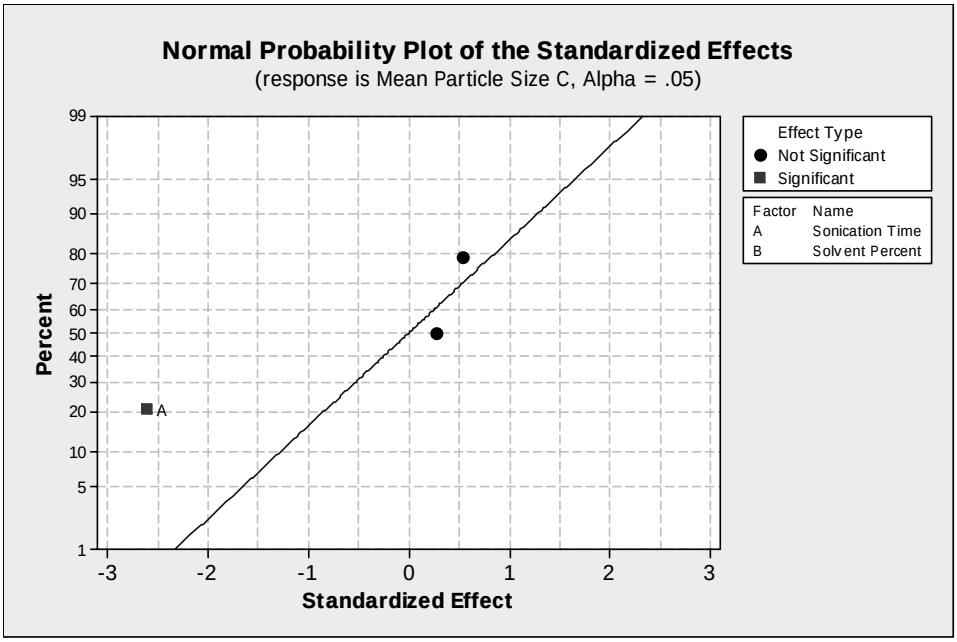

Normalized Probability Plot Showing Significant Factors Affecting Mean Particle Size for Sample C

Factorial Fit Table for Sample A

Estimated Effects and Coefficients for Mean Particle Size for A (coded units)

Term	Effect	Coef	SE Coef	T	P
Constant		26.10	4.818	5.42	0.001
Sonication time	-28.41	-14.20	6.027	-2.36	0.046
solvent percent	-8.82	-4.41	5.901	-0.75	0.476
Sonication time*solvent percent	5.33	2.66	7.382	0.36	0.728

S = 15.8518 R-Sq = 44.84% R-Sq(adj) = 24.16%

Analysis of Variance for Mean Particle Size for A (coded units)

Source	DF	Seq SS	Adj SS	Adj MS	F	P
Main Effects	2	1601.67	1535.93	767.96	3.06	0.103
2-Way Interactions	1	32.72	32.72	32.72	0.13	0.728
Residual Error	8	2010.24	2010.24	251.28		
Total	11	3644.63				

Factorial Fit Table for Sample B

Estimated Effects and Coefficients for Mean Particle Size Sample B (coded units)

Term	Effect	Coef	SE Coef	T	P
Constant		31.10	6.900	4.51	0.002
Sonication time	-38.85	-19.43	8.632	-2.25	0.055
Percent Solvent	-3.80	-1.90	8.451	-0.22	0.828
Sonication time*Percent Solvent	-0.51	-0.25	10.572	-0.02	0.981

S = 22.7024 R-Sq = 39.01% R-Sq(adj) = 16.14%

Analysis of Variance for Mean Particle Size Sample B (coded units)

Source	DF	Seq SS	Adj SS	Adj MS	F	P
Main Effects	2	2636.96	2636.04	1318.02	2.56	0.138
2-Way Interactions	1	0.30	0.30	0.30	0.00	0.981
Residual Error	8	4123.21	4123.21	515.40		
Total	11	6760.47				

Factorial Fit Table for Sample C

Estimated Effects and Coefficients for Mean Particle Size C (coded units)

Term	Effect	Coef	SE Coef	T	P
Constant		12.933	1.792	7.22	0.000
Sonication Time	-11.670	-5.835	2.242	-2.60	0.032
Solvent Percent	1.175	0.587	2.195	0.27	0.796
Sonication Time*Solvent Percent	2.899	1.449	2.746	0.53	0.612

S = 5.89692 R-Sq = 46.89% R-Sq(adj) = 26.97%

Analysis of Variance for Mean Particle Size C (coded units)

Source	DF	Seq SS	Adj SS	Adj MS	F	P
Main Effects	2	235.893	237.978	118.989	3.42	0.084
2-Way Interactions	1	9.687	9.687	9.687	0.28	0.612
Residual Error	8	278.189	278.189	34.774		
Total	11	523.769				

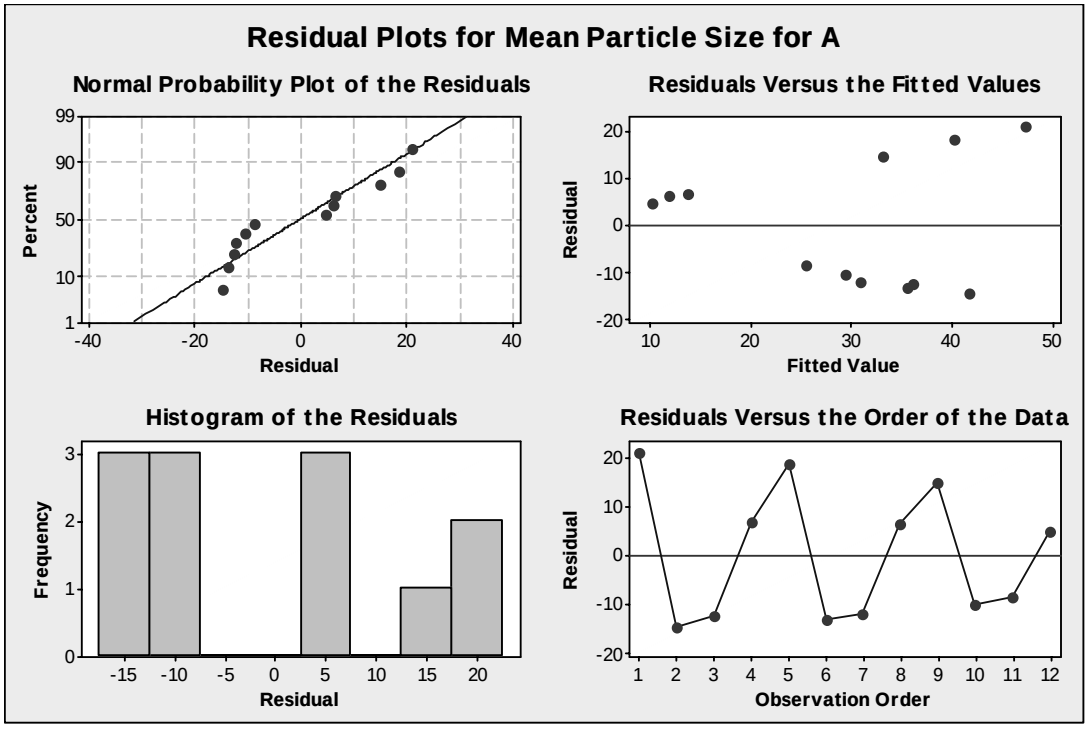

Residual Plots for Sample A

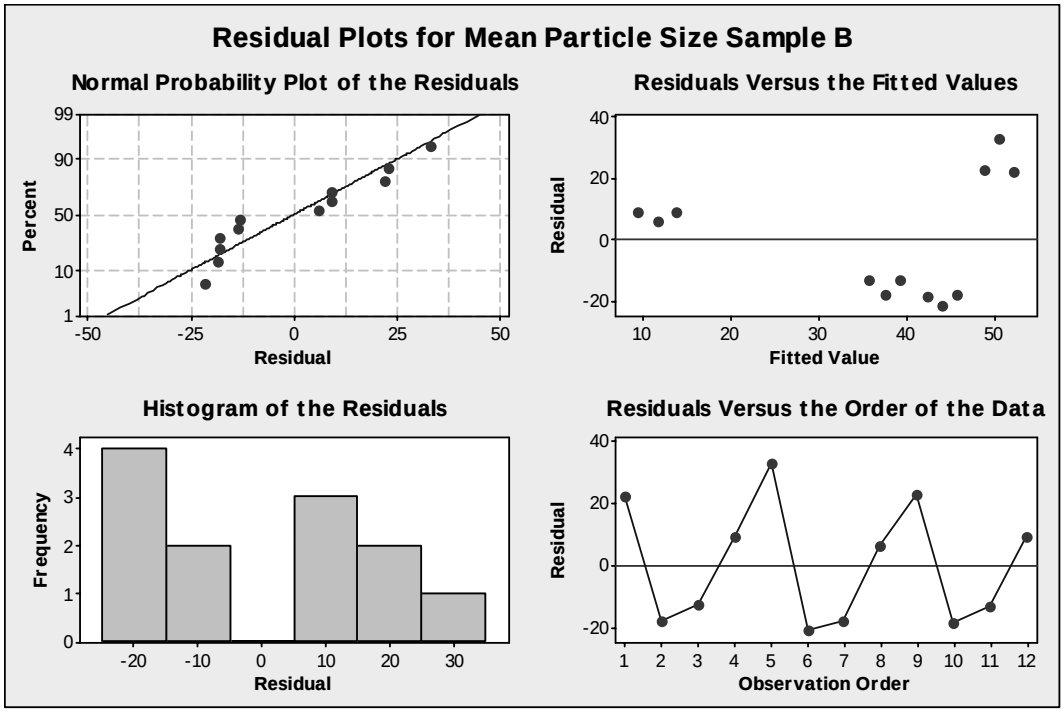

Residual Plots for Sample B

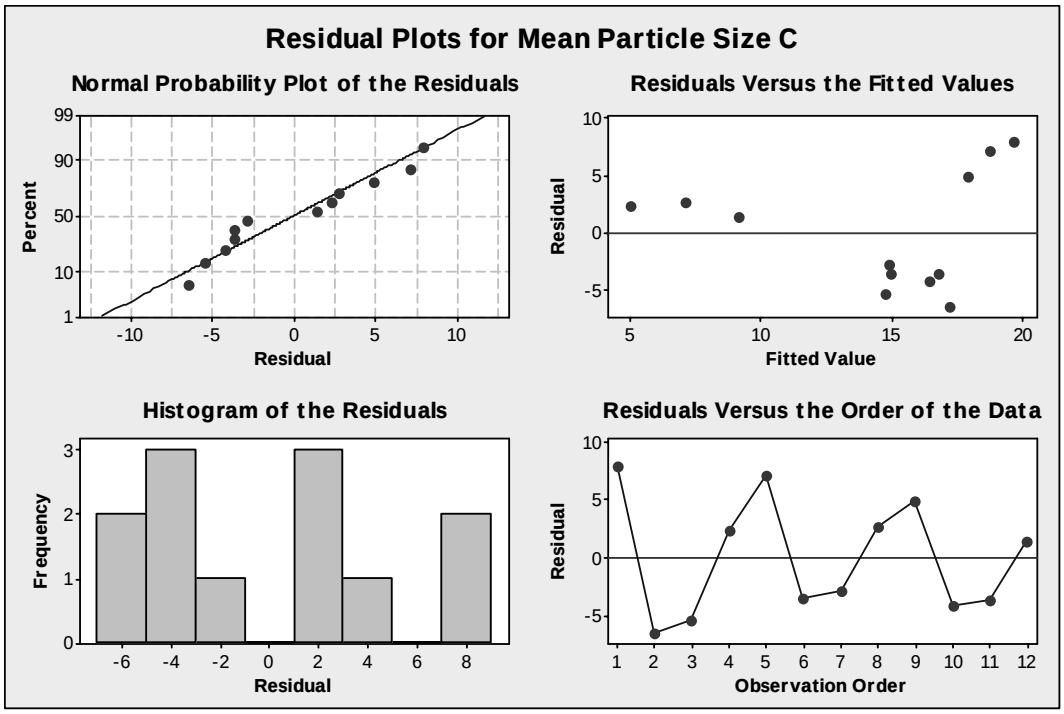

Residual Plots for Sample C

Two-Sample t-Test Results for LLNL and Matching SNL Means for Sample A

Hypothesized Difference	**0**
Level of Significance	**0.05**
Population 1 Sample	
Sample Mean	**27.1325**
Sample Size	**4**
Sample Standard Deviation	**0.443274**
Population 2 Sample	
Sample Mean	**26.95**
Sample Size	**3**
Sample Standard Deviation	**1.178148**
Population 1 Sample Degrees of Freedom	3
Population 2 Sample Degrees of Freedom	2
Total Degrees of Freedom	5
Pooled Variance	0.673108
Difference in Sample Means	0.1825
t-Test Statistic	0.291247
Two-Tailed Test	
Lower Critical Value	**-2.57058**
Upper Critical Value	**2.570582**
***p*-Value**	**0.782558**
Do not reject the null hypothesis	

Two-Sample t-Test Results for LLNL and Matching SNL Means for Sample B

Hypothesized Difference	**0**
Level of Significance	**0.05**
Population 1 Sample	
Sample Mean	**29.54**
Sample Size	**4**
Sample Standard Deviation	**0.300111**
Population 2 Sample	
Sample Mean	**27.78**
Sample Size	**3**
Sample Standard Deviation	**0.16563**
Population 1 Sample Degrees of Freedom	3
Population 2 Sample Degrees of Freedom	2
Total Degrees of Freedom	5
Pooled Variance	0.065013
Difference in Sample Means	1.76
t-Test Statistic	9.037602
Two-Tailed Test	
Lower Critical Value	**-2.57058**
Upper Critical Value	**2.570582**
***p*-Value**	**0.000277**
Reject the null hypothesis	

Two-Sample t-Test Results for LLNL and Matching SNL Means for Sample C

Hypothesized Difference	**0**
Level of Significance	**0.05**
Population 1 Sample	
Sample Mean	**9.9445**
Sample Size	**4**
Sample Standard Deviation	**0.984334**
Population 2 Sample	
Sample Mean	**10.68**
Sample Size	**3**
Sample Standard Deviation	**1.222453**
Population 1 Sample Degrees of Freedom	3
Population 2 Sample Degrees of Freedom	2
Total Degrees of Freedom	5
Pooled Variance	1.179105
Difference in Sample Means	-0.7355
t-Test Statistic	-0.88685
Two-Tailed Test	
Lower Critical Value	**-2.57058**
Upper Critical Value	**2.570582**
***p*-Value**	**0.415775**
Do not reject the null hypothesis	

Two-Sample t-Test Results for Pantex and Matching SNL Means for Sample A

Hypothesized Difference	**0**
Level of Significance	**0.5**
Population 1 Sample	
Sample Mean	**55.35**
Sample Size	**3**
Sample Standard Deviation	**1.933158**
Population 2 Sample	
Sample Mean	**48.17**
Sample Size	**3**
Sample Standard Deviation	**2.543167**
Population 1 Sample Degrees of Freedom	2
Population 2 Sample Degrees of Freedom	2
Total Degrees of Freedom	4
Pooled Variance	5.102399
Difference in Sample Means	7.18
t-Test Statistic	3.892986
Two-Tailed Test	
Lower Critical Value	**-0.7407**
Upper Critical Value	**0.740697**
***p*-Value**	**0.017646**
Reject the null hypothesis	

Two-Sample t-Test Results for Pantex and Matching SNL Means for Sample B

Hypothesized Difference	**0**
Level of Significance	**0.5**
Population 1 Sample	
Sample Mean	**106.33**
Sample Size	**3**
Sample Standard Deviation	**1.27738**
Population 2 Sample	
Sample Mean	**71.8**
Sample Size	**3**
Sample Standard Deviation	**3.467425**
Population 1 Sample Degrees of Freedom	2
Population 2 Sample Degrees of Freedom	2
Total Degrees of Freedom	4
Pooled Variance	6.827368
Difference in Sample Means	34.53
t-Test Statistic	16.18511
Two-Tailed Test	
Lower Critical Value	**-0.7407**
Upper Critical Value	**0.740697**
***p*-Value**	**8.53E-05**
Reject the null hypothesis	

Two-Sample t-Test Results for Pantex and Matching SNL Means for Sample C

Hypothesized Difference	**0**
Level of Significance	**0.5**
Population 1 Sample	
Sample Mean	**25.51**
Sample Size	**3**
Sample Standard Deviation	**1.27738**
Population 2 Sample	
Sample Mean	**22.83**
Sample Size	**3**
Sample Standard Deviation	**0.3005**
Population 1 Sample Degrees of Freedom	2
Population 2 Sample Degrees of Freedom	2
Total Degrees of Freedom	4
Pooled Variance	0.861
Difference in Sample Means	2.68
t-Test Statistic	3.537357

Two-Tailed Test	
Lower Critical Value	**-0.7407**
Upper Critical Value	**0.740697**
***p*-Value**	**0.024071**
Reject the null hypothesis	

DISTRIBUTION:

3	MS0435	S. Young, 2122
1	MS0633	T. Sterk, 2952
1	MS0889	J. Braithwaite, 1825
1	MS1452	E. S. Hafenrichter, 2552
1	MS1455	B. Andrzejewski, 2555
1	MS 1455	R. Carlson, 2555
1	MS1455	C. Gresham, 2555
2	MS1455	S. A. Klassen, 2555
1	MS1455	V. Loyola, 2555
1	MS1455	T. Massis, 2555
1	MS1455	L.Minier, 2555
1	MS1455	R. Patton, 2555
1	Dierdre Monroe Los Alamos National Laboratory P.O. box 1663, MSP950 Los Alamos, NM 87545	
1	Alan Burnham Lawrence Livermore National Laboratory P.O. Box 808 Livermore, CA 94551	
2	MS9018	Central Technical Files, 8944
2	MS0899	Technical Library, 4536